SMHI

REPORT OCEANOGRAPHY (RO) No. 48, 2013

BaltiX V 1.1 : A 3D Ocean Modelling Configuration for Baltic & North Sea Exchange Analysis

Front: The Baltic Sea, seen from Askö Island

ISSN: 0283-1112

BaltiX

A 3D Ocean Modelling Configuration for Baltic & North Sea Exchange Analysis

V 1.1 : February 2013

R. Hordoir, B. W. An, J. Haapala, C. Dieterich,
S. Schimanke, A. Höglund and H.E.M. Meier

February 8, 2013

Contents

1 Introduction **3**

2 Configuration description **4**
2.1 Description of the Configuration 4
2.1.1 Domain 4
2.1.2 Open Boundary Conditions 5
2.1.3 Surface Boundary 5
2.2 Advection, Diffusion and Numerical Aspects 5
2.3 Forcing Dataset 5
2.3.1 Atmospheric Forcing 5

3 Barotropic Analysis **6**
3.1 Sea Surface Height Analysis 6
3.1.1 Tidally Driven SSH 6
3.1.2 Wind Driven SSH 7

4 Thermo-Haline Behaviour of the BaltiX Configuration **20**
4.1 Vertical Mixing Testing 20
4.2 Tuning of the Bathymetry in the Danish Straights 20
4.2.1 Tuning of the flow at Öresund 21
4.3 Salinity & Temperature Behaviour 21
4.3.1 SST & SSS at the SHARK Measurement Stations 21
4.3.2 Surface Temperatures and Salininity Maps for the Period 1980-1990 23
4.3.3 Deep Baltic Salinity Trend 53

5 Coupling with LIM3 the framework of MyOcean: Validation and new developments **54**
5.1 Model-Satellite SST comparison 54
5.2 Ice conditions in the Baltic Sea 55
5.3 Description of the LIM3 model 55
5.4 Experimental design for the hindcast 55
5.5 Results:Basin mean features 55
5.6 Model to Model comparison 58
5.7 Model to observed data comparison 58

6 Conclusion **58**

7 Appendix: A Technical Introduction to BaltiX **61**
7.1 Preprocessing Keys (CPP Keys) 61
7.2 Code Changes And Additions 62
7.2.1 Changes under ***key_baltix*** 62
7.2.2 Changes under ***key_ldfsma*** 64

8 Subversion Server **65**

1 Introduction

There is a need for having a reliable numerical representation of the exchanges between the Baltic Sea and the North Sea from many points of view. First, the North Sea is the salt provider of the Baltic Sea, but also the oxygen provider of the lowermost layers of the Baltic Sea. This means that any numerical analysis which has for goal to study the long term changes in this exchange can not rely on a model of the Baltic Sea that has an open boundary condition at the entrance of the Baltic Sea (i.e. : the Kattegat area). In order to represent the long term changes in the exchanges between the North Sea and the Baltic Sea, one needs to consider the coupling between these two basins which have a very different dynamical behaviour which means one needs to consider them as a whole. This means that any regional model should have its open boundary condition further away from the entrance of the Baltic Sea, that is in a place that is remote enough to allow a buffer large enough in the North Sea, so that the SSH variability at the entrance of the Baltic Sea is well represented [7].
Second, the Baltic Sea outflow has a great influence on the Norwegian Coastal Current (NCC hereafter) which is also interesting to study, and which can only be well represented if the wind effect over the Baltic Sea is taken into account [9].
Many models were successfully applied to the Baltic Sea or/and to the North Sea/Baltic Sea area. On can cite the Rossby Centre Ocean model RCO [15], which successfully represents the thermo-haline as well as the ice structures and variability of the Baltic Sea. One can also cite HIROMB [6], which is a North & Baltic Seas numerical representation used in operational oceanography.

However, all these modelling structures lack in at least one of the following points :

- They include only the Baltic Sea area, which makes impossible the study of the exchanges with the North Sea.
- They were mostly used for operational purpose, and do not have stability properties in terms of Baltic salt content which does not make them suitable for long term studies.
- They do not follow anymore the framework of a community model, and therefore do not benefit of the recent scientific or technical developments implemented in most ocean modelling platform.
- A Baltic & North Sea setup is also necessary for long term coupled simulations.

There was therefore a need to build a new Baltic & North Sea configuration, based on a community modelling framework, and designed to follow this framework eventually.

BaltiX is a Baltic & North Sea configuration based on the NEMO [14] ocean engine. Its development was started in 2011 at SMHI (Swedish Meteorological & Hydrological Institute, Norrköping, Sweden). It follows closely the development of the NEMO ocean engine, and BaltiX is updated each time an update is done in it.
In the present report, Section 2 describes the configuration and explains the choices that have been made to build it. Based on a simulation done for the period 1961-2007, we then present several results. Section 3 presents a barotropic analysis of the results provided by the configuration, and Section 4 presents results in terms of salinity and temperature variability. Section 5 has been specifically written to present the sea-ice model coupled to BaltiX and its effects in terms of sea-ice variability. A last part provides a short conclusion to the present report.

2 Configuration description

2.1 Description of the Configuration

2.1.1 Domain

The computational domain covers the entire Baltic Sea, the English Channel and the North Sea, with open boundary conditions between Cornwall and Brittany (meridional), and between Hebride Islands and Norway (zonal). Figure 1 shows the bathymetry for the entire domain.

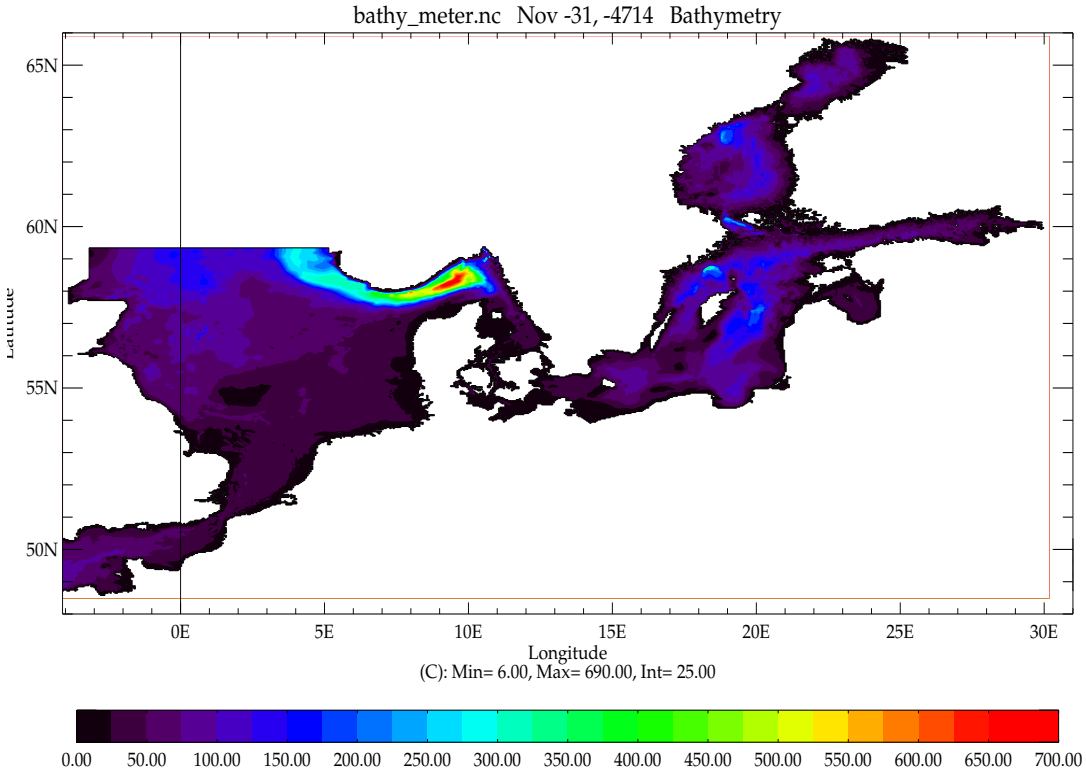

Figure 1: Bathymetry of the BaltiX configuration (in meters). The deepest point in the domain is the Norwegian trench (700 m), and the minimum depth is artificialy set to 6m.

Considering the mean depth of the North Sea (approx. 100 m), one can compute a mean Rossby radius for the North Sea of around 320 km which locates the entrance of the Baltic Sea further away enough from the open boundaries to consider that the representation of the North Sea provides a buffer large enough to ensure that most of the wind driven SSH variability at the entrance of the Baltic Sea is indeed driven by the wind forcing over the configuration. However a storm surge model is also built-in in order to provide realistic SSHs in the North Sea and close to observations SSH variability at the entrance of the Baltic Sea. This storm surge model, called BZH, is another configuration than BaltiX but build on the exact same code. The reference bathymetry of BaltiX comes from the HIROMB [6] model, except for the Danish Straights where the IOW bathymetry is used and is either averaged over each grid cell, or taken as the maximum value. This specific and critical area can also be used as a tuning parameter, as later described in the present report. The domain is therefore the same as that

of the HIROMB configuration, has a resolution of approximately 2 nautical miles (3700 m), and a basic vertical resolution of 3 m close to the surface, decreasing to 22 m at the bottom of the deepest part of the domain, that is the Norwegian trench. The vertical grid has a total of 56 levels and uses VVL coordinates [1] with an explicit free surface. Partial steps are used in order to reach a good consistency between the input bathymetry and that indeed used by the numerical model configuration.

2.1.2 Open Boundary Conditions

From a barotropic point of view, open boundary conditions are defined using the Oregon State University Tidal Inversion Model [4, 5] with 13 tidal harmonics defined both SSH and velocities. From a baroclinic point of view, Levitus [13] is used for temperature and salinity with a sponge layer, and simple radiation conditions are used for baroclinic velocities.

2.1.3 Surface Boundary

The surface boundary condition uses a bulk formulation based on [11]. The LIM3 ice model [20] is used with a fixed ice salinity equal to 10^{-3} PSU. A climatological runoff is used based on different databases for the Baltic and the North Seas, and the salinity of runoff is also set to 10^{-3} PSU which is enough to avoid any negative salinity issue close to river mouths even when the runoff is rejected on a single grid cell, as it is the case in this configuration. In addition to the TVD scheme mentioned later in the present article, the version of the NEMO Ocean Engine that is used (version 3.3.1) allows rejecting runoff as a lateral boundary condition, which produces an estuarine like baroclinic circulation close to river mouths, bringing enough salt to ensure a stable positive salinity even in the very low saline areas of the domain, such as the Gulf of Finland or the Bothnian Bay.
A quadratic friction is applied at the bottom, and the drag coefficient is computed for each bottom grid cell based on a classical law-of-the-wall, with a constant bottom roughness of 3 cm.

2.2 Advection, Diffusion and Numerical Aspects

A time splitting method is used, and a modified leapfrog method is implemented in order to ensure conservation [12]. A TVD scheme is used for tracer advection. A Laplacian diffusion scheme is used, and a Smagorinsky method [19] has been implemented in order to lower as much as possible the value of the diffusion coefficient into the two very different dynamical systems that are the North Sea and the Baltic Sea.
A $k - \epsilon$ vertical turbulence model is used, and a parameterisation of the bottom boundary layer [2, 3] is included both from an advective and a diffusive point of view. The advective part is included to help dense water flows cross over the Danish straights, which is mostly a high frequency wind driven circulation process driven both by barotropic and baroclinic currents [7]. In addition, it is important for dense water inflows to be able to reach the centre of the Baltic proper, which is a lower frequency process [15] and requires several weeks or months during which it is important that bottom dense water flows follow the bathymetry, that the z system coordinates do not induce artificial mixing.

2.3 Forcing Dataset

2.3.1 Atmospheric Forcing

The atmospheric forcing comes a downscalled run of ERA40 (used at the open boundaries) using RCA [17] for the period 1961-2007. The resolution of the atmospheric model is 25 km but depends

in terms of variability to the one degree horizontal resolution ERA40 re-analysis run that is applied at the open boundaries.

3 Barotropic Analysis

3.1 Sea Surface Height Analysis

3.1.1 Tidally Driven SSH

Validation is done by comparing simulated SSH with measurements from tidal gauges from the BODC (British Oceanographic Data Centre) for a short random time period in a place highly influenced by tides, that is the English channel. The stations chosen are Jersey (British Islands) and Newhaven on the southern coast of England.

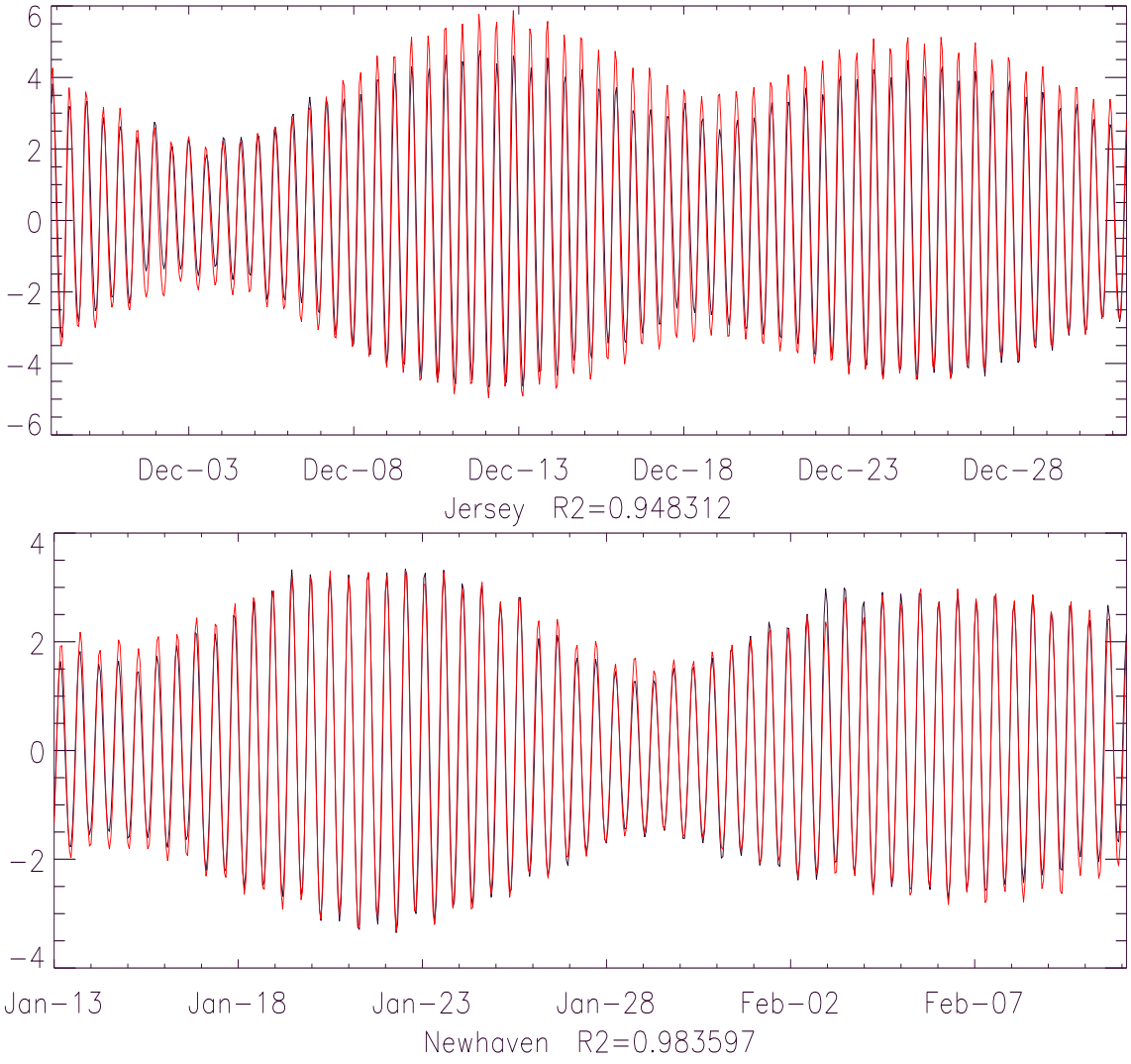

Figure 2: Measured SSH (in meters) with a frequency of one hour (black curve) and simulated ones (red curve)

These plots show that the tidal SSH is very well represented, with obviously a good representation of the neap and spring tides. However, some overshoots at high tides can be observed which suggests a tuning of the bottom drag must be done. This point is extremely critical to tune if one wants to observe the right residual flow at main straights (Straight of Dover) as specified by [16].

3.1.2 Wind Driven SSH

A comparison between simulated and measured SSH data is shown for the year 2005 for several measurements stations located in Sweden and in Finland. The correlation coefficient is also computed as well as the standard deviation of the observations and that of the . A distinction can be made between the stations located on the Swedish west coast (for example Smögen) and the ones located in the Baltic Sea. One can notice that the quality of the results is usually much better in terms of correlation within the Baltic Sea. The correlation appears to be very poor in a place like Smögen for example. The results shown come from a simulation that started in 1961. In a different simulation, for which a climatological data set was used as an initial condition, the results for the SSH at Smögen appeared to be a lot higher both in terms of correlation and RMS. This highly suggests that baroclinicity has an important effect on SSH variability. In a place like the Swedish west coast, which is highly influenced by strong Kelvin wave dynamics, the prediction of temperature and salinity appears to have an important influence of the SSH variability, and this prediction with a model that does not do any data assimilation and runs on long time periods, appears to be difficult. However, the rates of correlation obtained in the Baltic Sea in measuring stations like Stockholm or Landsort show that the SSH variability can and is well reproduced by the model, although no tuning of the bottom friction has been done, and the atmospheric forcing that is used does not do any data assimilation within its domain but just relies on assimilated at its boundaries. One can notice that the standard deviation of the modeled SSH is always less than the measured one. The ordered data allows to see that the differences are usually for the negative values of SSH for which BaltiX tends to underestimate such values.

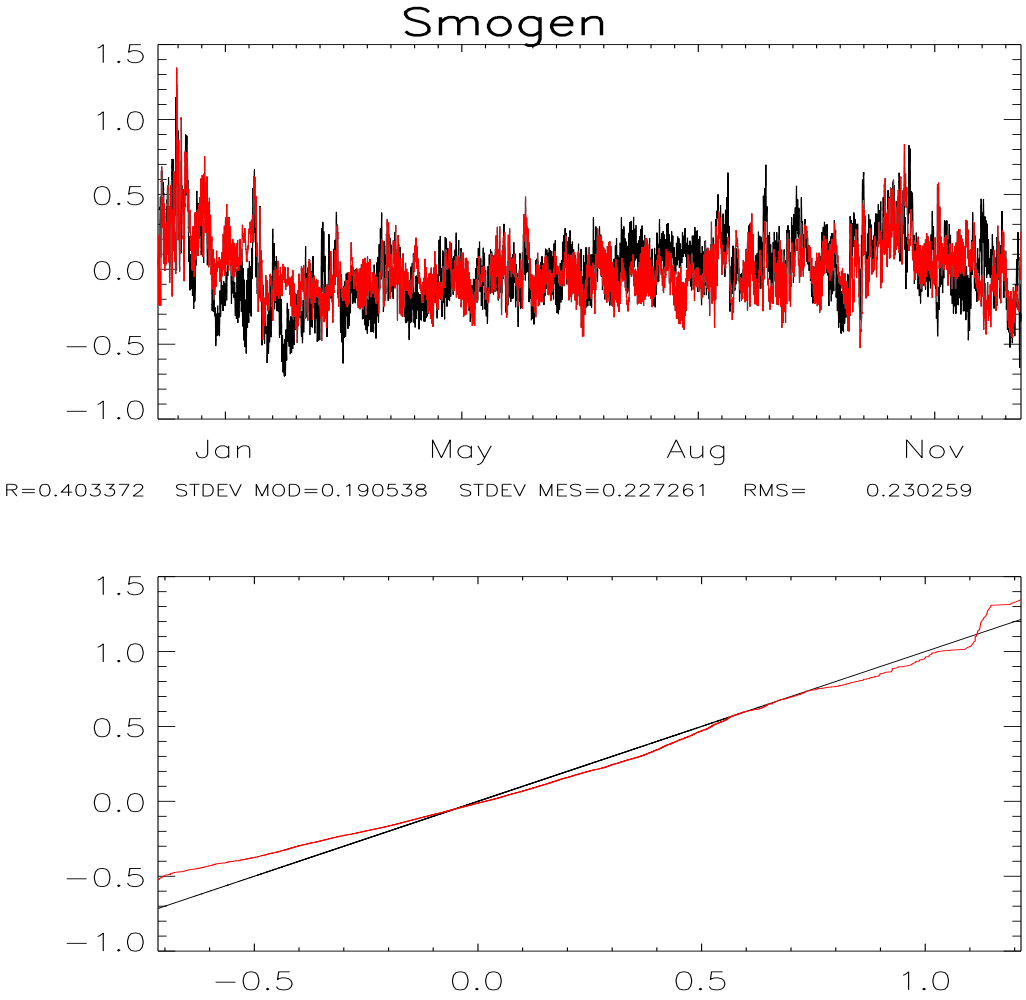

Figure 3: Top : Measured SSH (black curve) and simulated SSH (red curve), in meters, in the BaltiX configuration for year 2005. Bottom : Comparison of ordered data (in meters) for the same time period. The x-axis represents the observed dataset whereas the y-axis represents the BaltiX dataset.

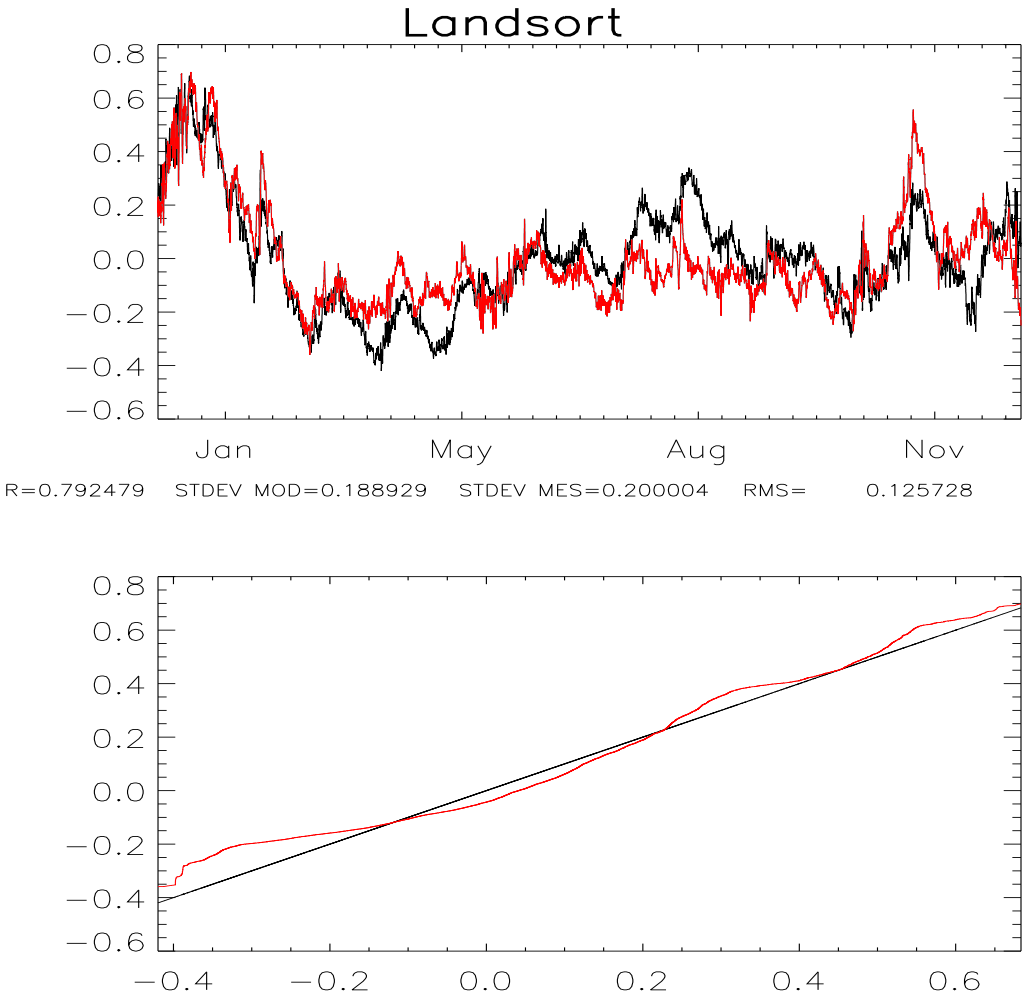

Figure 4: Top : Measured SSH (black curve) and simulated SSH (red curve), in meters, in the BaltiX configuration for year 2005. Bottom : Comparison of ordered data (in meters) for the same time period. The x-axis represents the observed dataset whereas the y-axis represents the BaltiX dataset.

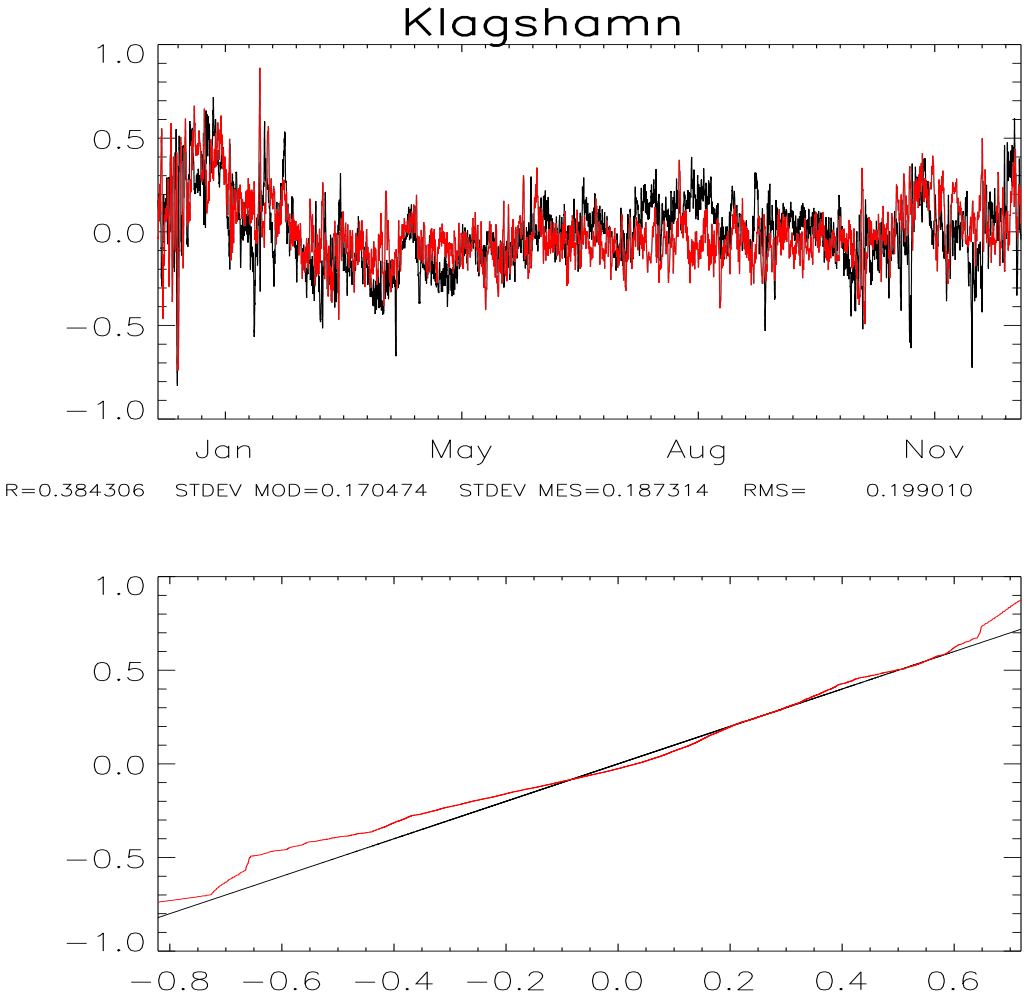

Figure 5: Top : Measured SSH (black curve) and simulated SSH (red curve), in meters, in the BaltiX configuration for year 2005. Bottom : Comparison of ordered data (in meters) for the same time period. The x-axis represents the observed dataset whereas the y-axis represents the BaltiX dataset.

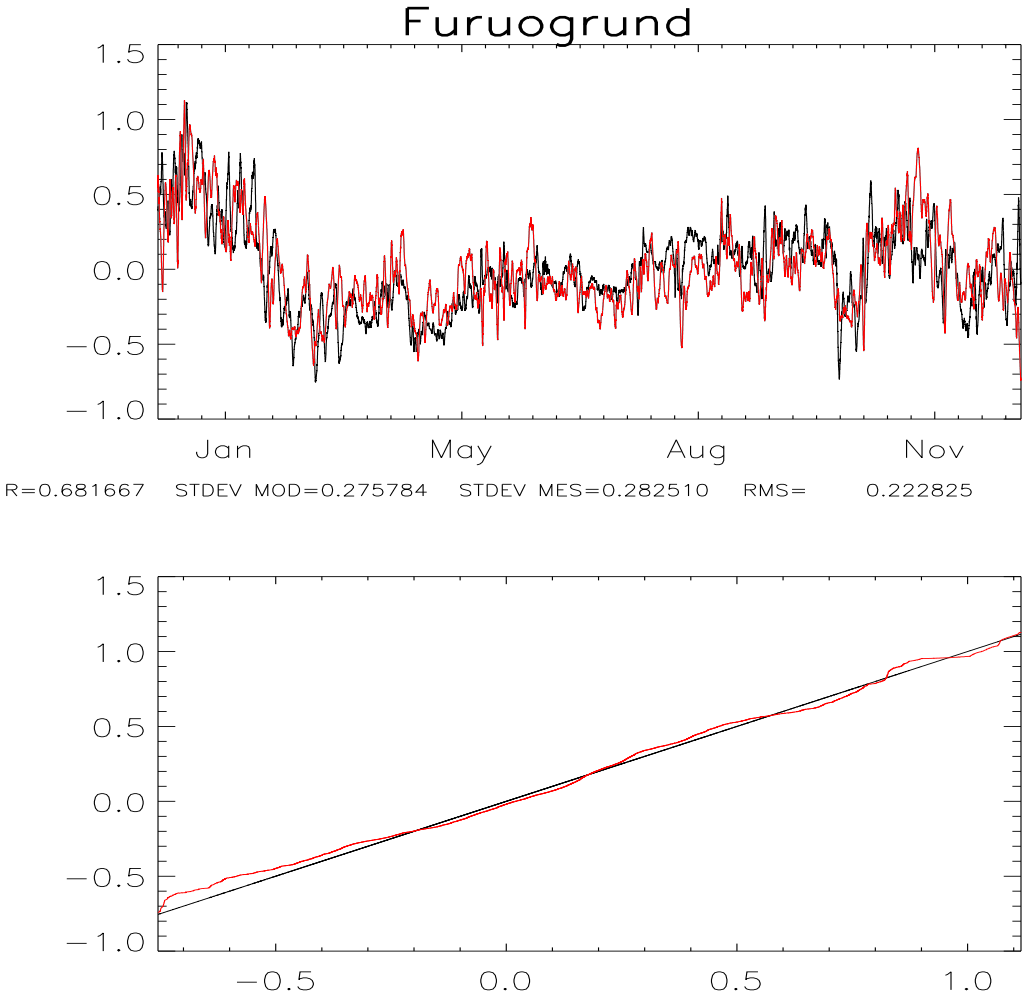

Figure 6: Top : Measured SSH (black curve) and simulated SSH (red curve), in meters, in the BaltiX configuration for year 2005. Bottom : Comparison of ordered data (in meters) for the same time period. The x-axis represents the observed dataset whereas the y-axis represents the BaltiX dataset.

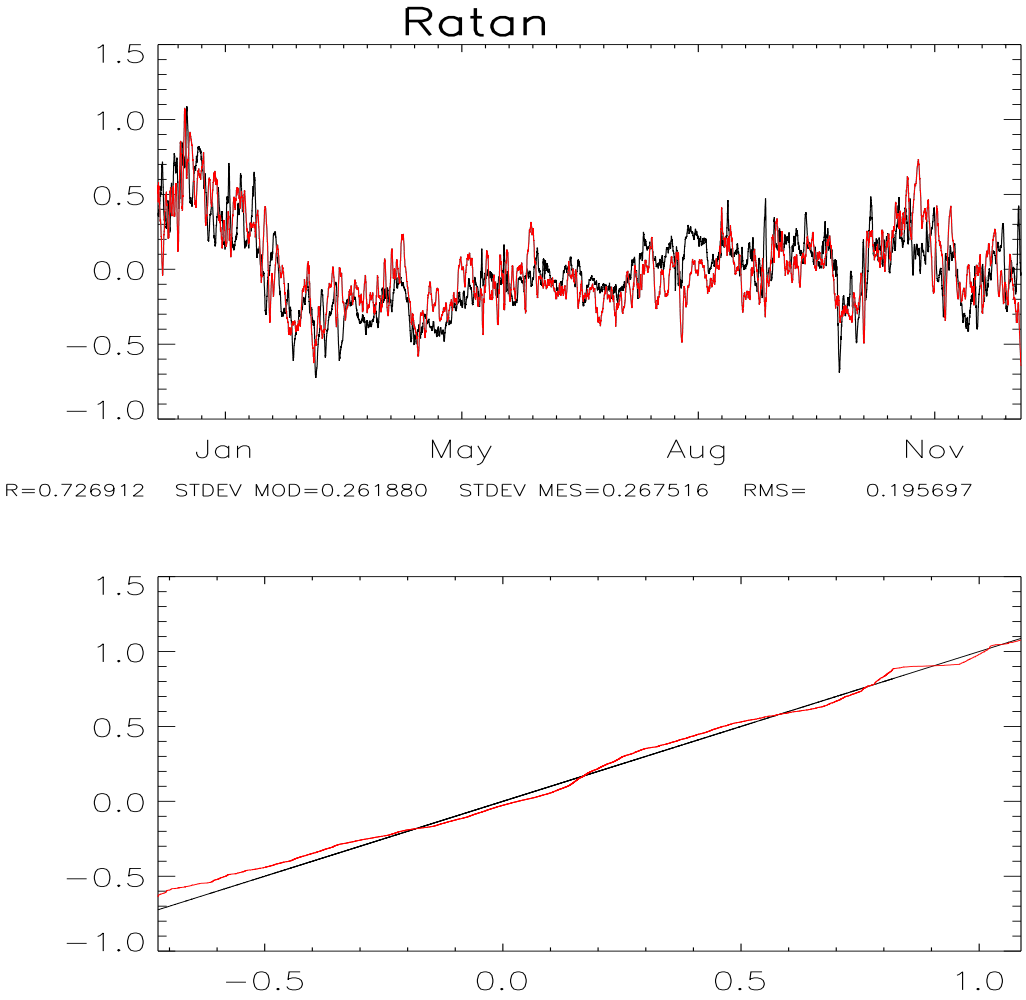

Figure 7: Top : Measured SSH (black curve) and simulated SSH (red curve), in meters, in the BaltiX configuration for year 2005. Bottom : Comparison of ordered data (in meters) for the same time period. The x-axis represents the observed dataset whereas the y-axis represents the BaltiX dataset.

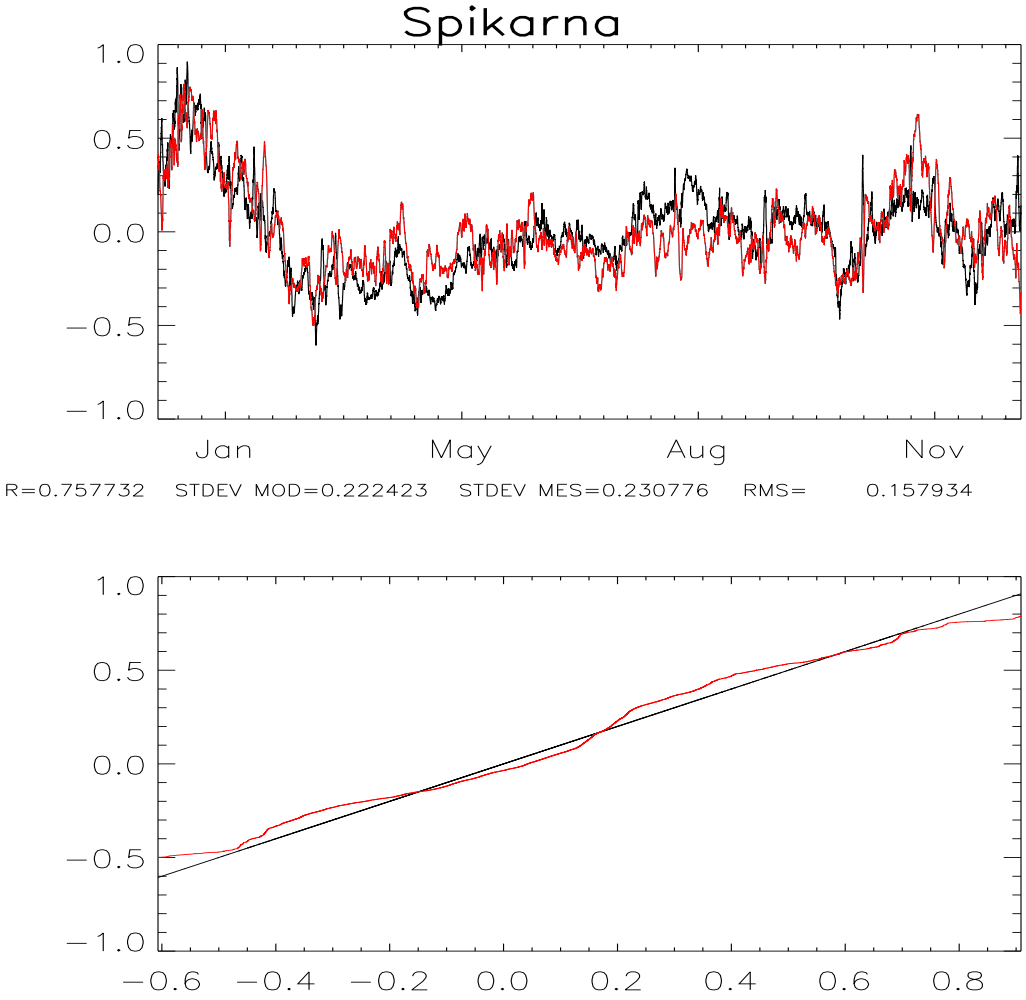

Figure 8: Top : Measured SSH (black curve) and simulated SSH (red curve), in meters, in the BaltiX configuration for year 2005. Bottom : Comparison of ordered data (in meters) for the same time period. The x-axis represents the observed dataset whereas the y-axis represents the BaltiX dataset.

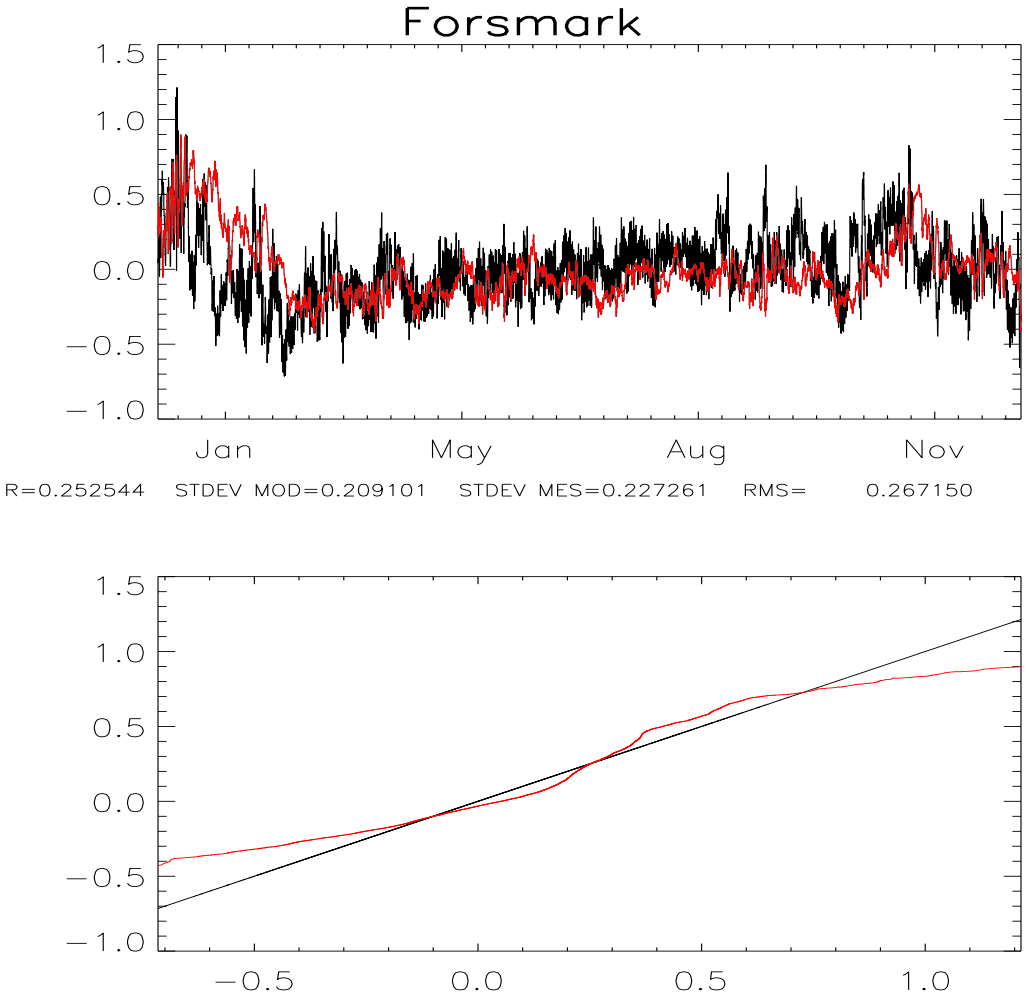

Figure 9: Top : Measured SSH (black curve) and simulated SSH (red curve), in meters, in the BaltiX configuration for year 2005. Bottom : Comparison of ordered data (in meters) for the same time period. The x-axis represents the observed dataset whereas the y-axis represents the BaltiX dataset.

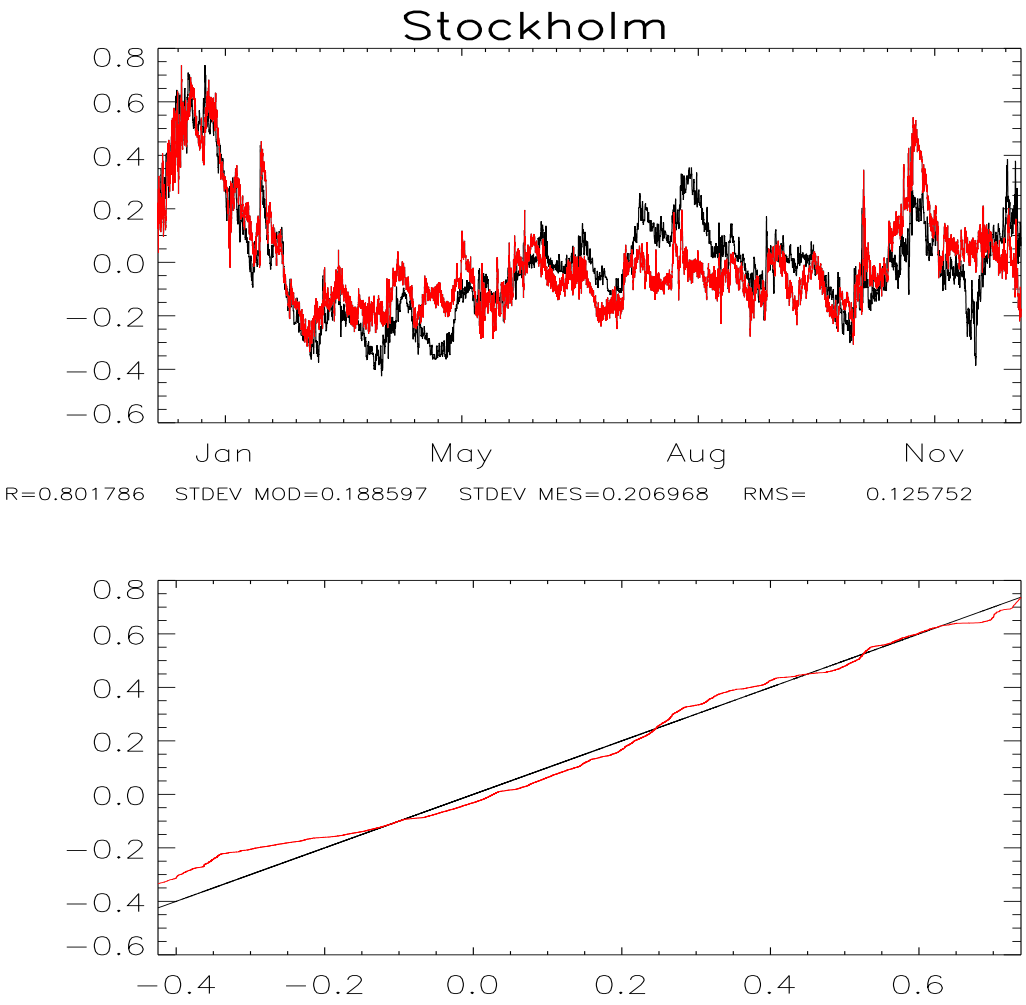

Figure 10: Top : Measured SSH (black curve) and simulated SSH (red curve), in meters, in the BaltiX configuration for year 2005. Bottom : Comparison of ordered data (in meters) for the same time period. The x-axis represents the observed dataset whereas the y-axis represents the BaltiX dataset.

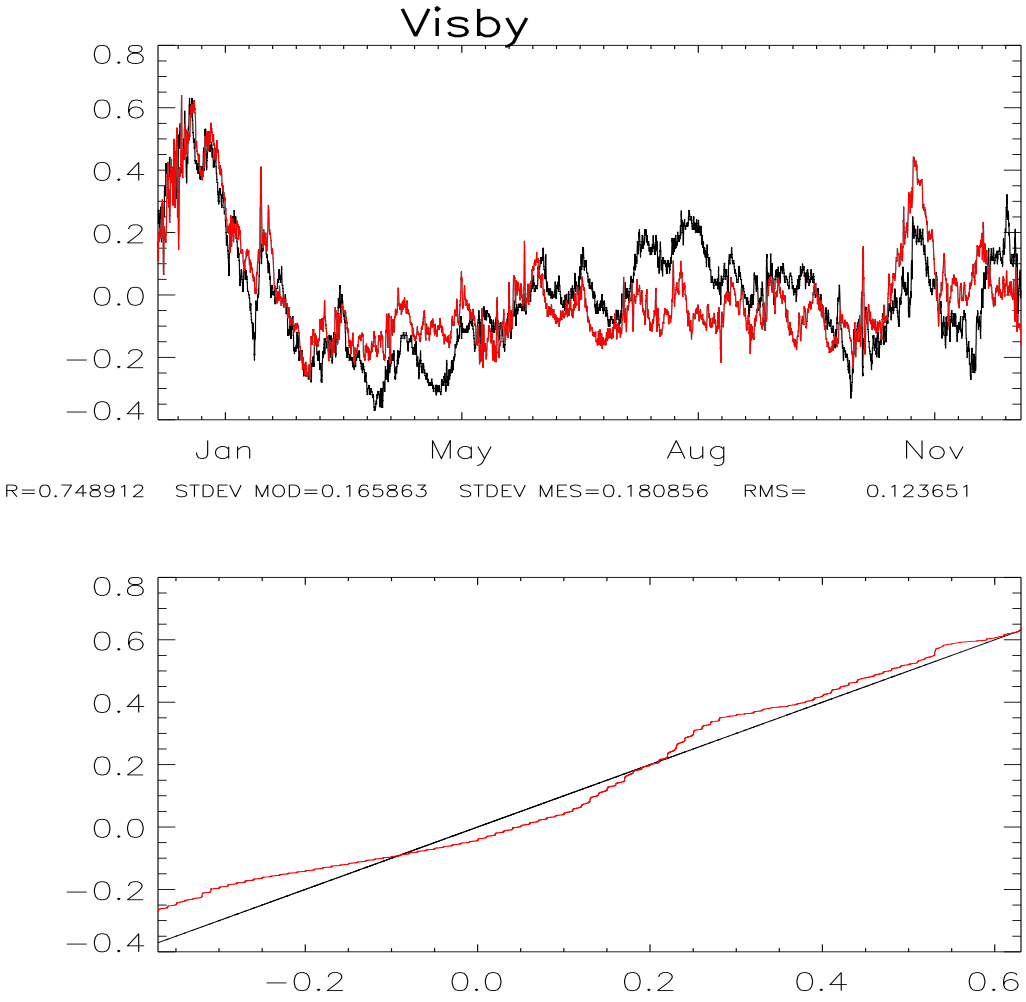

Figure 11: Top : Measured SSH (black curve) and simulated SSH (red curve), in meters, in the BaltiX configuration for year 2005. Bottom : Comparison of ordered data (in meters) for the same time period. The x-axis represents the observed dataset whereas the y-axis represents the BaltiX dataset.

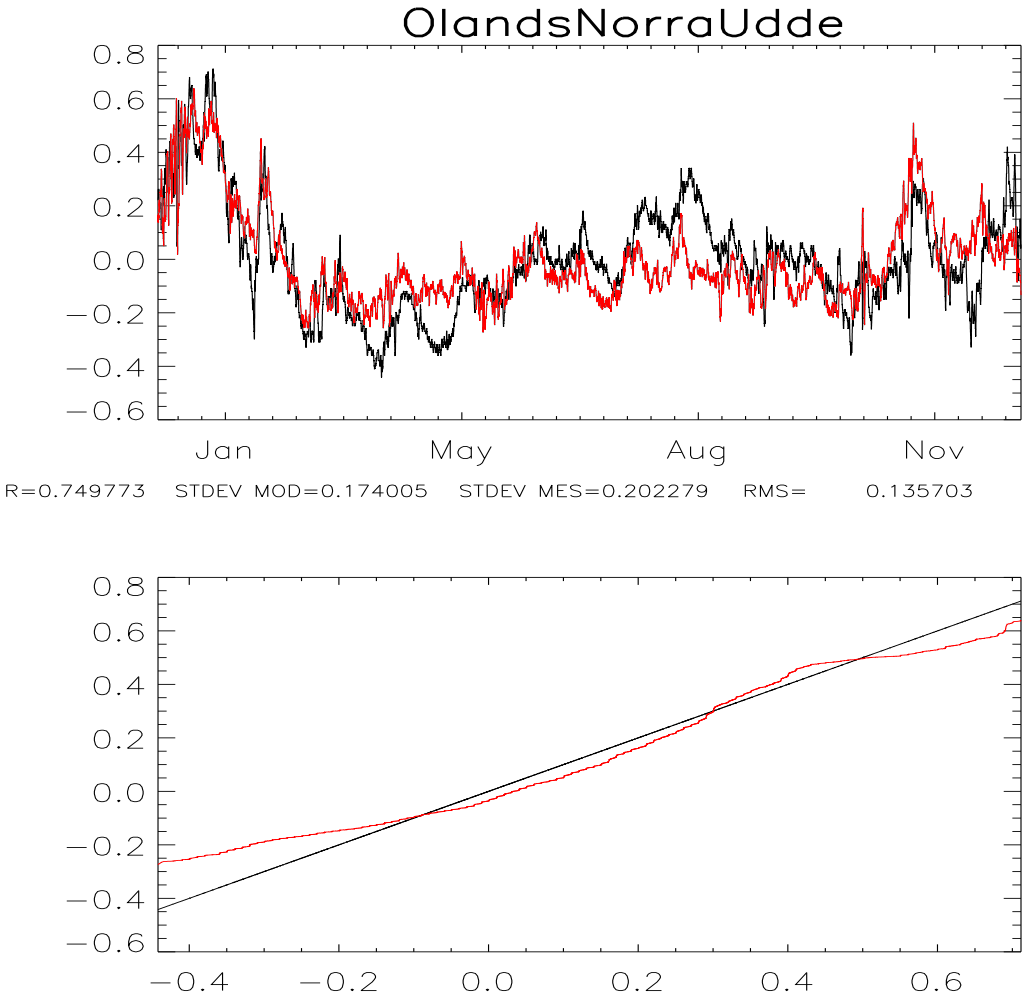

Figure 12: Top : Measured SSH (black curve) and simulated SSH (red curve), in meters, in the BaltiX configuration for year 2005. Bottom : Comparison of ordered data (in meters) for the same time period. The x-axis represents the observed dataset whereas the y-axis represents the BaltiX dataset.

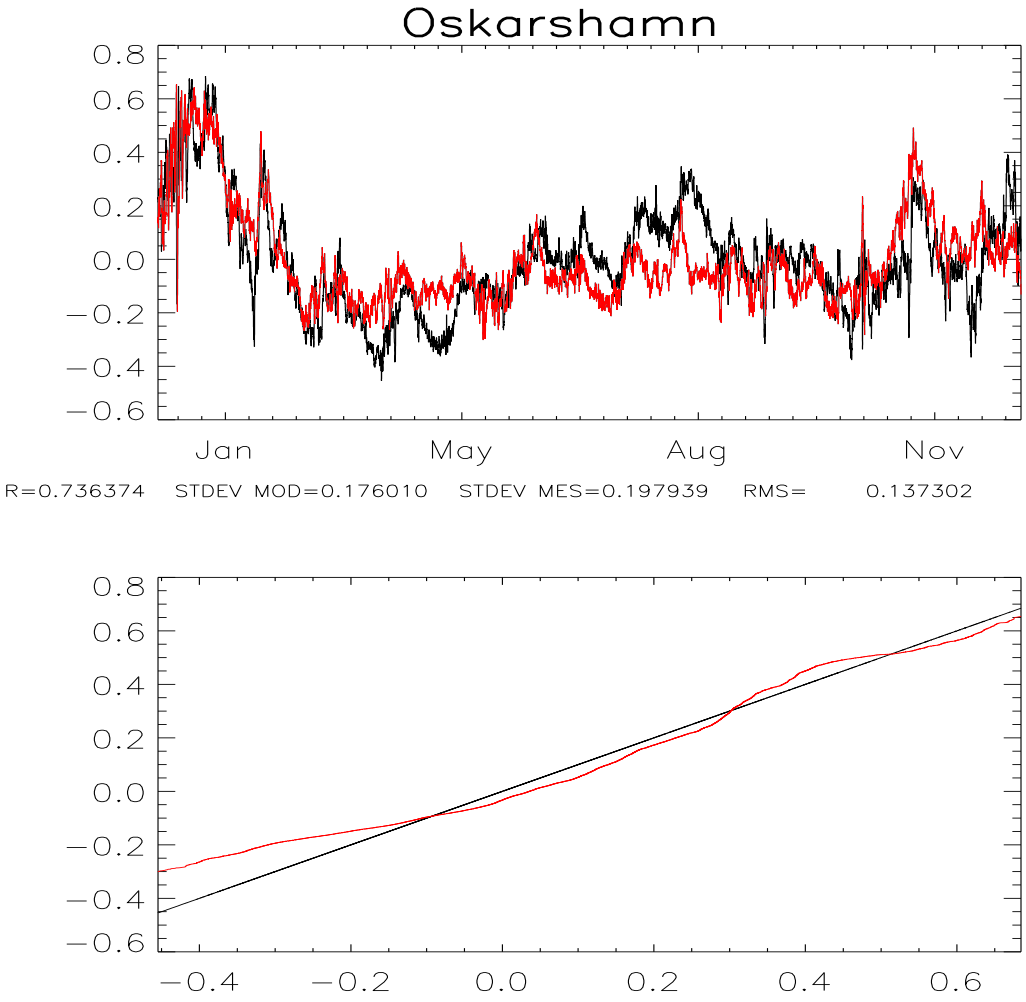

Figure 13: Top : Measured SSH (black curve) and simulated SSH (red curve), in meters, in the BaltiX configuration for year 2005. Bottom : Comparison of ordered data (in meters) for the same time period. The x-axis represents the observed dataset whereas the y-axis represents the BaltiX dataset.

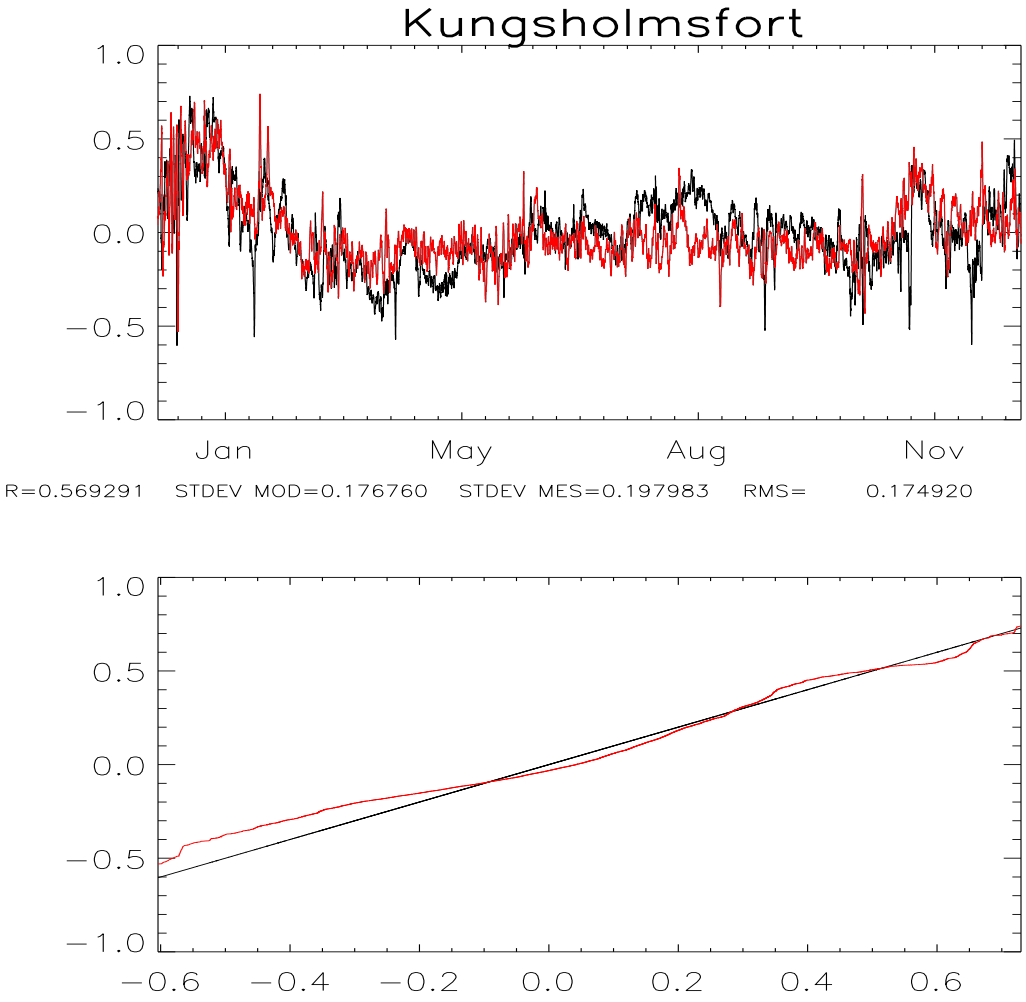

Figure 14: Top : Measured SSH (black curve) and simulated SSH (red curve), in meters, in the BaltiX configuration for year 2005. Bottom : Comparison of ordered data (in meters) for the same time period. The x-axis represents the observed dataset whereas the y-axis represents the BaltiX dataset.

4 Thermo-Haline Behaviour of the BaltiX Configuration

4.1 Vertical Mixing Testing

The $k-\epsilon$ scheme chosen to represent vertical mixing has been tested using a 1D version of the BaltiX configuration set at Gotland Deep (BY15). The testing has been done with and without atmospheric forcing, and using or not a background molecular diffusion or a background turbulent kinetic energy. All tests proved that the level of numerical diffusion within the vertical mixing model is non-existant. In the presence of Atmospheric forcing, it was shown that the pycnocline is erodated from above, but that the deep salinity changes are almost impossible to distinguish.
The conclusion of this series of test is that the tuning made on the turbulence model allows a very good preservation of the deep parts of the Baltic Sea, and insures a de-coupling between the deep parts and the surface on the time scales that were studied. This means that any deep salinity related issue has to be mostly investigated from the angle of the lateral ventilation. At the time this report is written, this issue is not yet fully adressed as it seems there is still a too high ventilation of the layers around 70m in comparison with [10], but several tunings are experimented in order to improve this problem and are presented in this report.

4.2 Tuning of the Bathymetry in the Danish Straights

The resolution of the BaltiX configuration does not permit to have a proper description of the bathymetry of the Danish straights. Many critical cross-sections like that located in Öresund can not be described by a two nautical mile grid as the error made by any representation using this grid is of more than 50% (the width of the cross-section is more than one grid cell, but less than two). Simulations performed with BaltiX have shown that the deep salinity of the Baltic Sea is extremely sensitive to the representation of this bathymetry and choices had to be made not to faithfully represent this bathymetry, but rather to represent the behaviour of the Danish straights for a given forcing dataset, and thus in order to reproduce the deep salinity of the Baltic Sea, without producing too much ventilation of the upper layers.
One useful milestone to get this tuning right, is to rely on the volumic flow at Öresund which can be very well described by a simple hydraulic model [8] The method of tuning can be detailed as follows :

- A rectange area of the Danish straights is chosen in order for the tuning to be performed. This area includes only the shallowest parts and has edges as soon as shelf break is observed on its Northern or Eastern boundary.
- In the selected rectangle, the IOW Baltic Sea Bathymetry [18] is used to computed for any grid cell of the original HIROMB bathymetry [6] the maximum depth (the HIROMB bathymetry being closer to the mean depth), and this depth is taken instead.
- All the critical cross-sections have been then checked, from a numerical perspective in order to adjust them to the same value as that of the observed cross-sections. This representation of the Danish straights proves to produce an immediate decrease of deep Baltic Salinity, and thus although the representation of the SSH is correct outside like inside the Baltic Sea.
- In the selected area, an additional depth is added and the minimum depth is also bounded to 8m. A smoothing algorithm permits to establish a proper junction at the Northern and Eastern boundaries of the selected area (Figure 15).

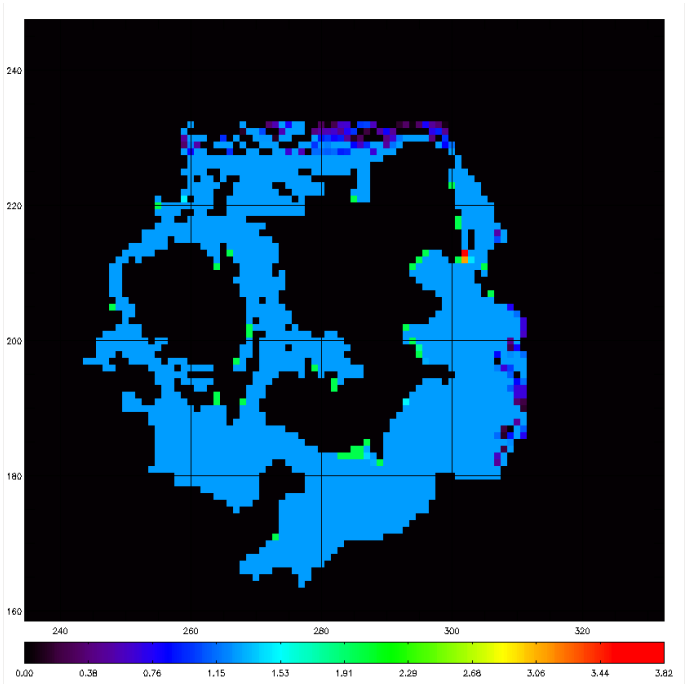

Figure 15: Tuning area for the bathymetry ofthe Danish straights. The non-black squares show where the bathymetry is increased and by how much. Units are meters.

4.2.1 Tuning of the flow at Öresund

Based on the hydraulic model of [8], the volumic flow at Öresund is computed. The flow at the cross-sections proves to have a variability that is too small if no correction on the cross-sections is made. In the meantime, increasing the Danish straights bathymetry to a point that allows the same standard deviation results in an un-realistic salinity increase of the Baltic Sea, both in its deep and shallow parts. Figure 16 shows the flow at Oresund simulated by the model and according to [8] for year 1979. The difference of result between the two simulations is not obvious on the plot. However, the simulation with increased Danish straights has a variability which is closer to the one from [8] : 34266 $m^3.s^{-1}$ for the [8] model, 30442 $m^3.s^{-1}$ for BaltiX with critical cross-sections and 31728 $m^3.s^{-1}$. The correlation reaches only 0.2 once the tidal signal is filtered, which is rather low but not surprising considering that the SSH outside of the Baltic Sea is not imposed but predicted. The spectral analysis shows that the high frequencies have the same amplitude and the M2 tide flow is clearly identified (at $10^{-0.3}$ days, which correspond to approximately half-a-day. However the low frequencies are under represended in lengthes of more than a month.

4.3 Salinity & Temperature Behaviour

4.3.1 SST & SSS at the SHARK Measurement Stations

The following figures show temperature, salinity time series and profiles for the decade 1980-1990 for all the available SHARK database measurement stations (Swedish National Oceanographic Data Centre). These figures show basically that the model reproduces temperature and salinity variability. However, the profiles show the most important bias of the configuration, yet to be solved : the pycnocline is most of the time too high, and this is especially true in deep areas. This results in a temperature profile which exhibits a too high temperature related stratification at the bottom of the mixed layer. In areas close to the North Sea, the profiles are usually well reproduced although the lack of precision both from spatial and temporal perspectives does not permit to exhibit very close

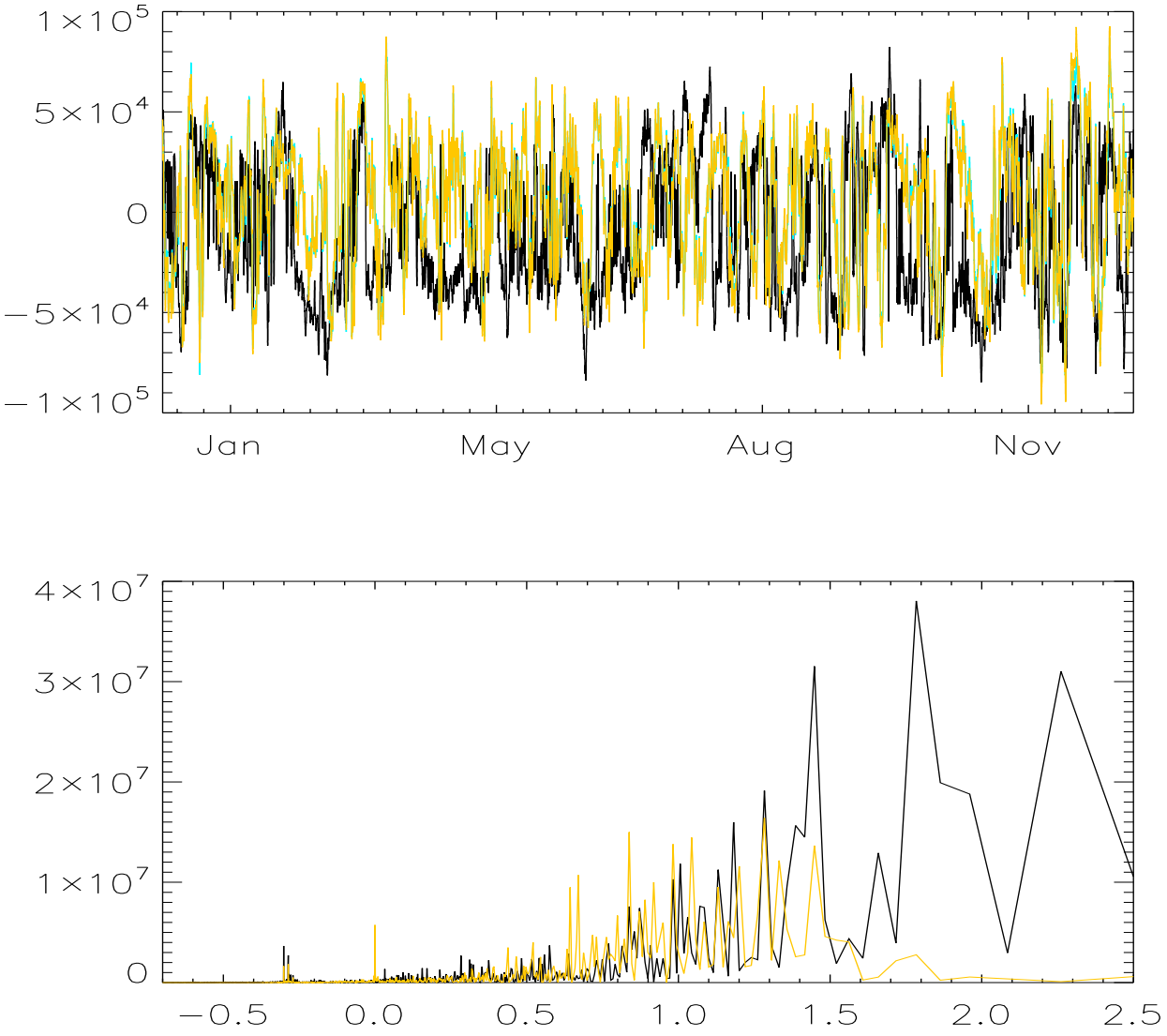

Figure 16: Year 1979 Flow at Oresund (in $m^3.s^{-1}$), according to [8] (black line) againts the same flow measured in BaltiX for the orginal critical cross-sections (yellow line) and increased by 1.25m (yellow line. Time serie on the left, spectral analysis on the right. The log-unit of the spectral analysis is days.)

to surface stratification (or lack of it) in an area with high salinity and temperature variability related with strong baroclinic and barotropic dynamics.

4.3.2 Surface Temperatures and Salininity Maps for the Period 1980-1990

We present hereafter climatological surface temperature and salinity maps for the period 1980-1990, for the months of January, April, July and October, both for the Baltic Sea area and for the Kattegat/Skagerrak and Norwegian coasts areas. These figures show that the spacial gradient of salinity in the Baltic Sea is well reproduced, however the surface salinity is too high, which is related with the too high ventilation of the pycnoclyne.

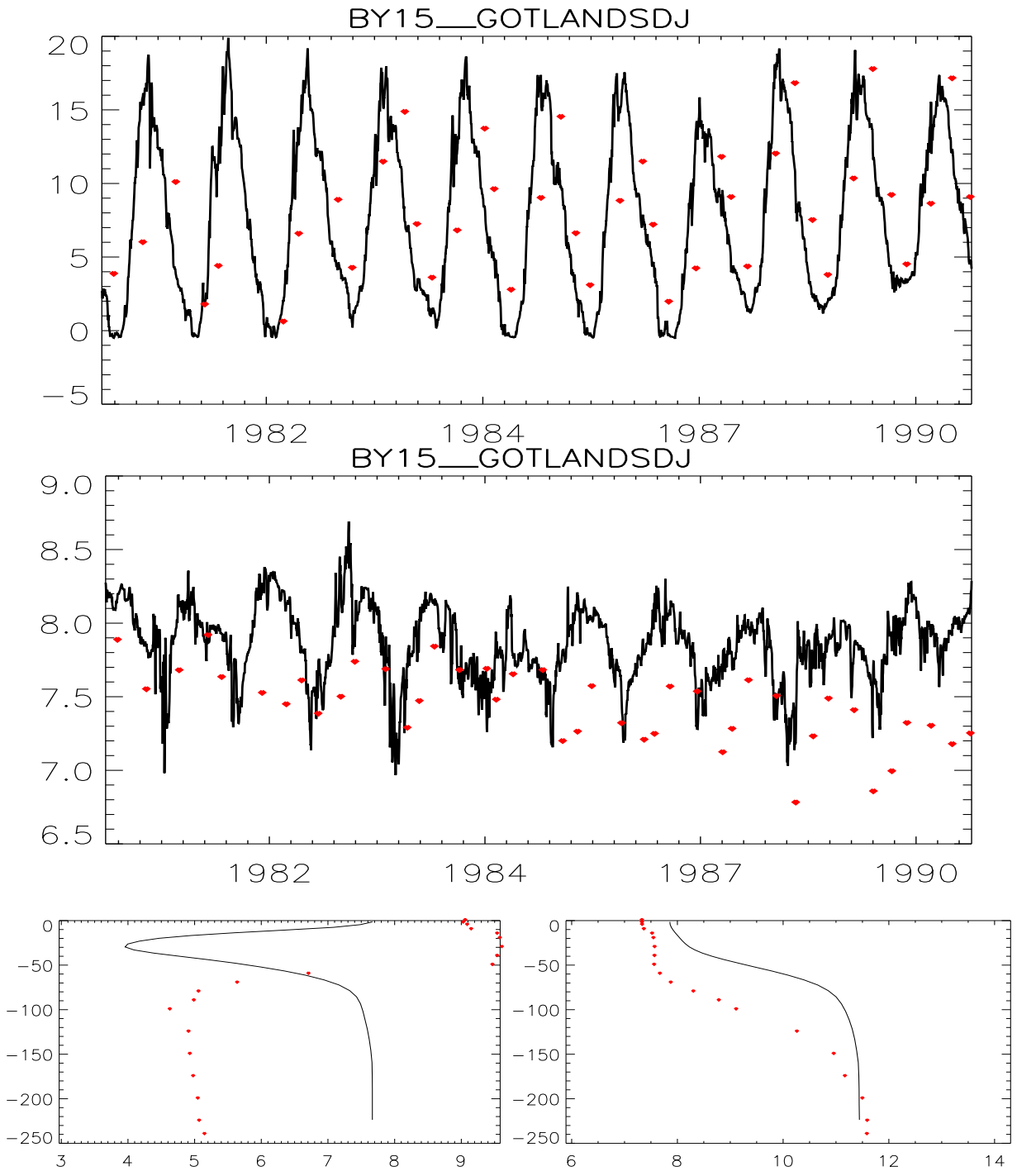

Figure 17: 1980-1990 Decade. Top two figures : Simulated SST & SSS (black), against measurement (red dots), Bottom figures: Simulated temperature and salinity profiles (black), against measurements (red dots). Temperature are measured in Celsius degrees and salinities in PSU.

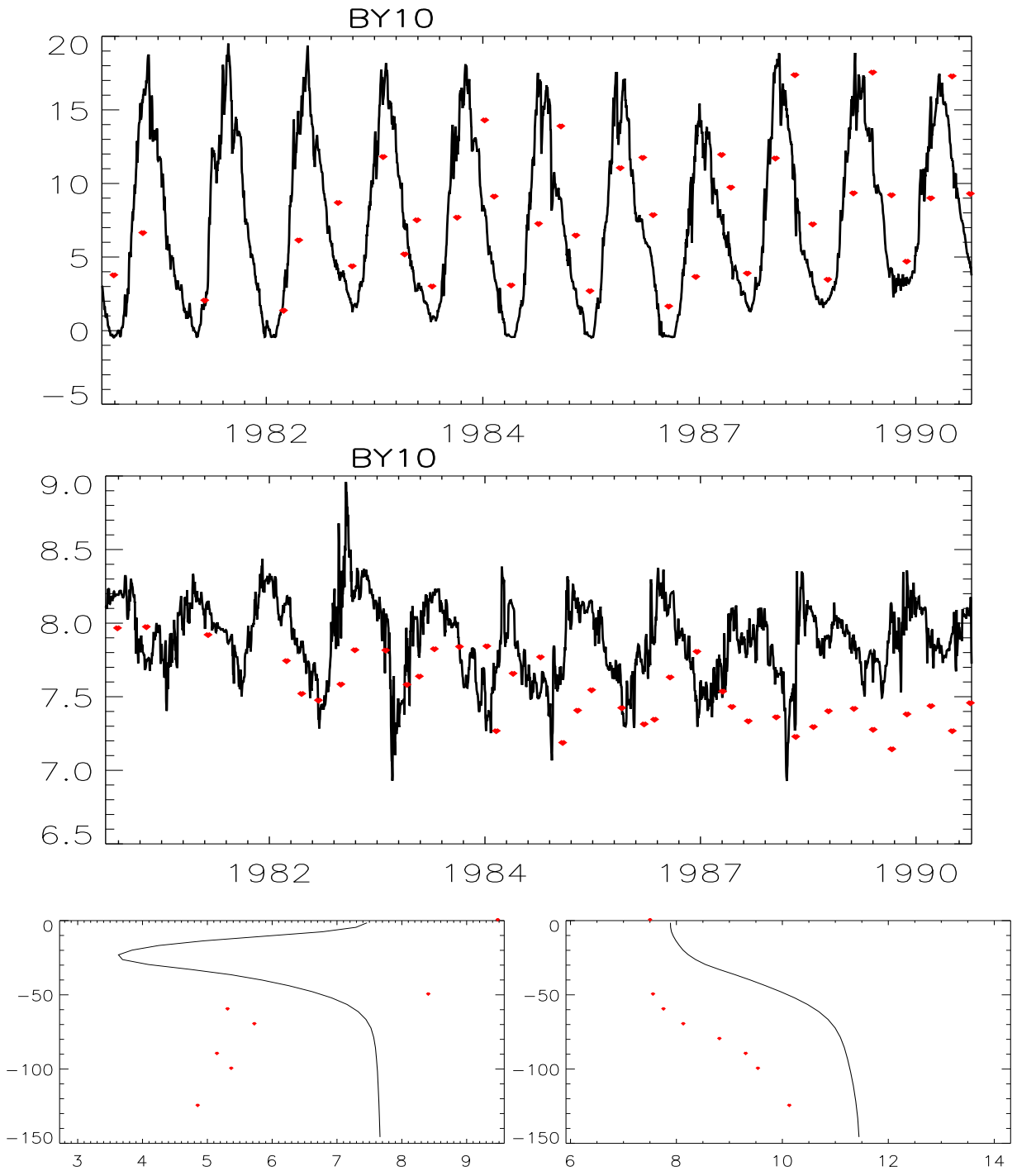

Figure 18: 1980-1990 Decade. Top two figures : Simulated SST & SSS (black), against measurement (red dots), Bottom figures: Simulated temperature and salinity profiles (black), against measurements (red dots). Temperature are measured in Celsius degrees and salinities in PSU.

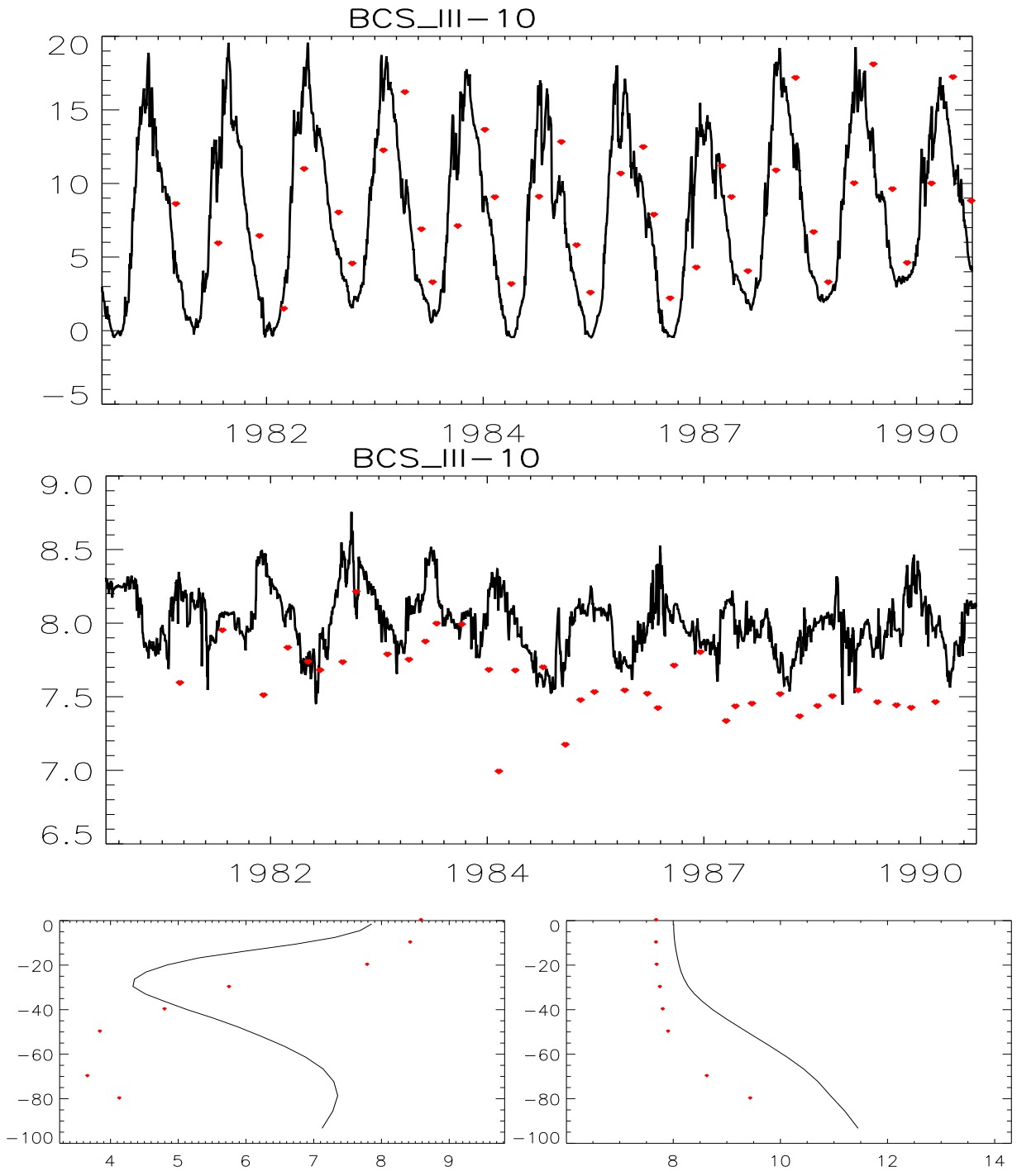

Figure 19: 1980-1990 Decade. Top two figures : Simulated SST & SSS (black), against measurement (red dots), Bottom figures: Simulated temperature and salinity profiles (black), against measurements (red dots). Temperature are measured in Celsius degrees and salinities in PSU.

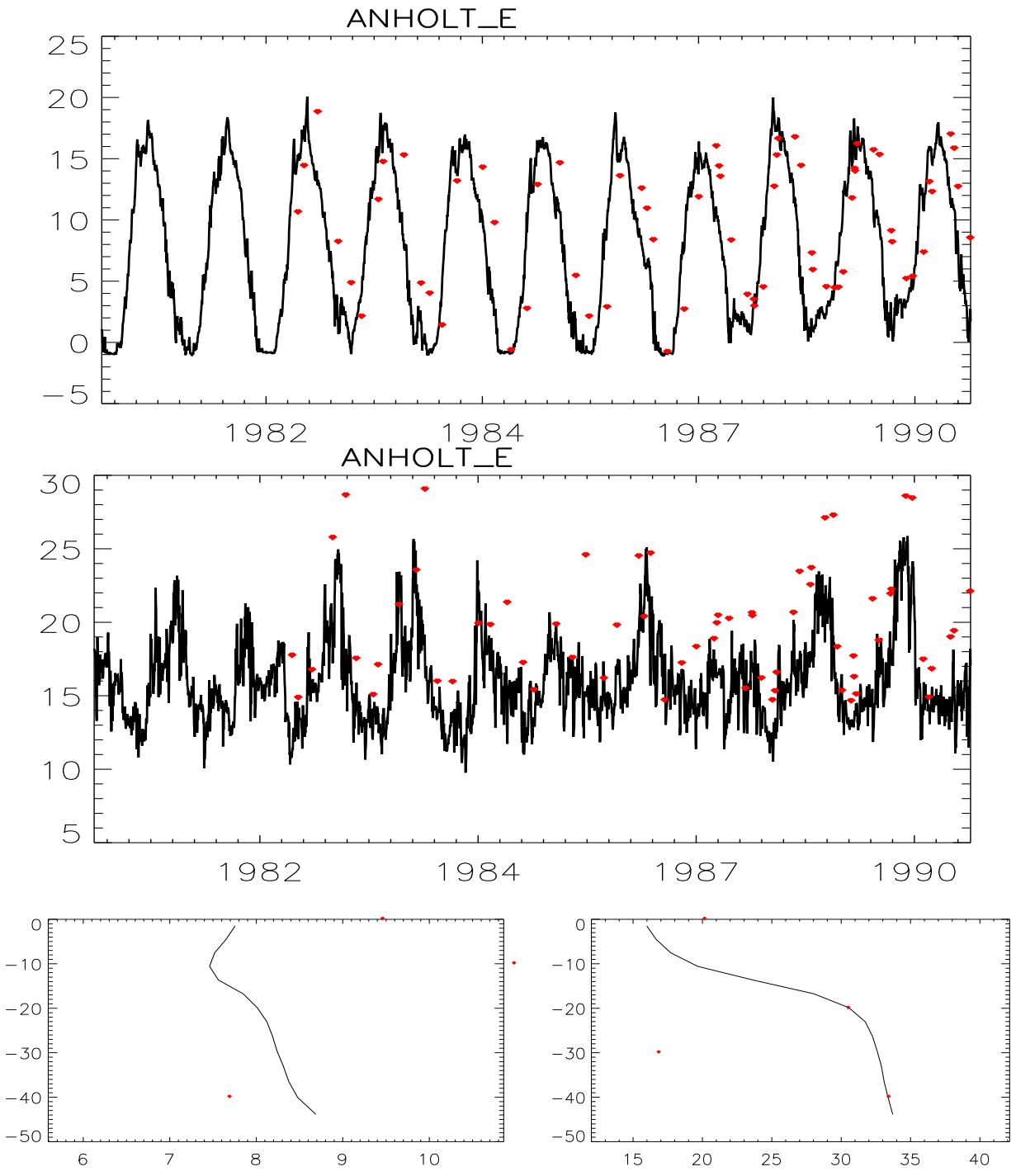

Figure 20: 1980-1990 Decade. Top two figures : Simulated SST & SSS (black), against measurement (red dots), Bottom figures: Simulated temperature and salinity profiles (black), against measurements (red dots). Temperature are measured in Celsius degrees and salinities in PSU.

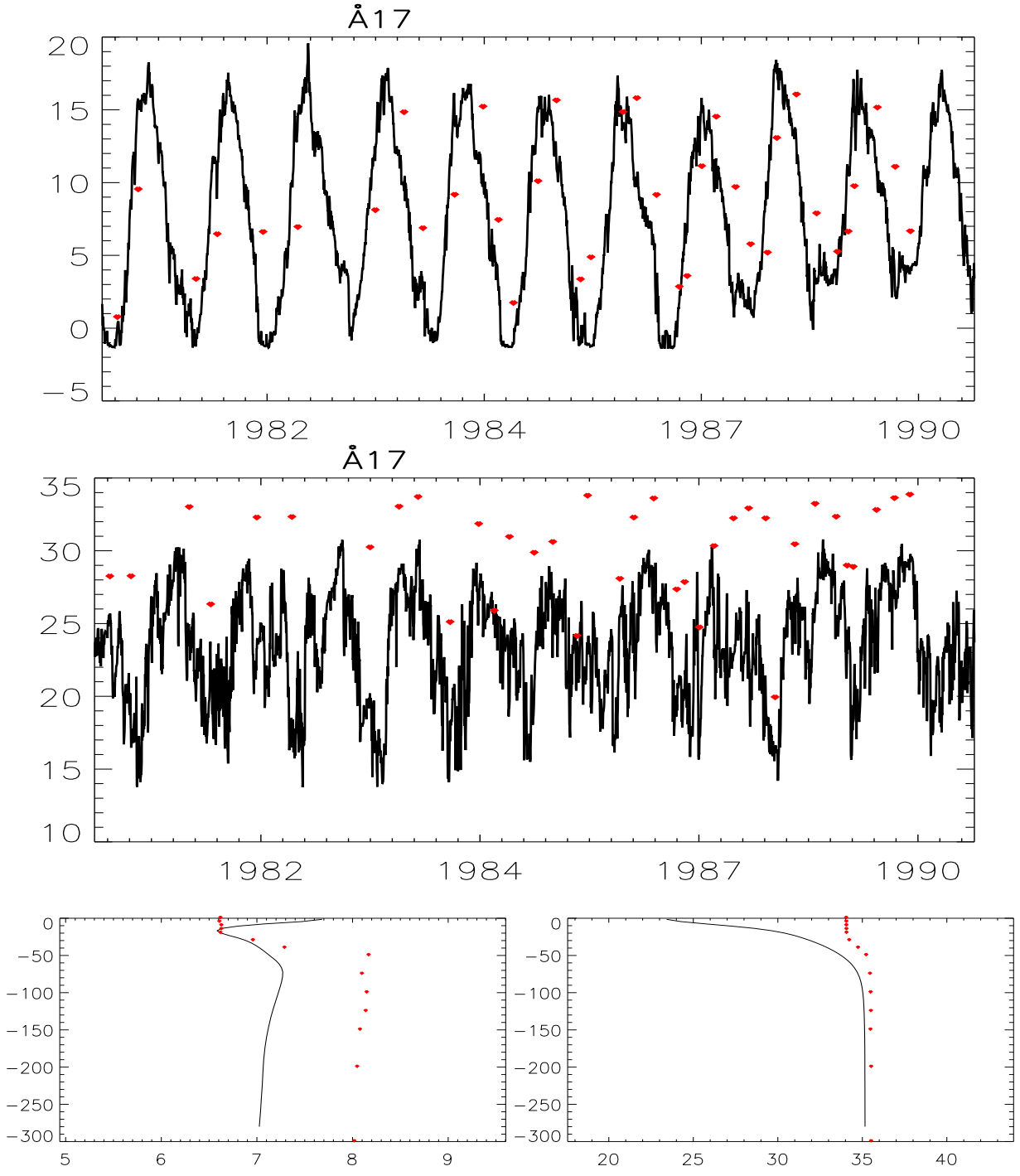

Figure 21: 1980-1990 Decade. Top two figures : Simulated SST & SSS (black), against measurement (red dots), Bottom figures: Simulated temperature and salinity profiles (black), against measurements (red dots). Temperature are measured in Celsius degrees and salinities in PSU.

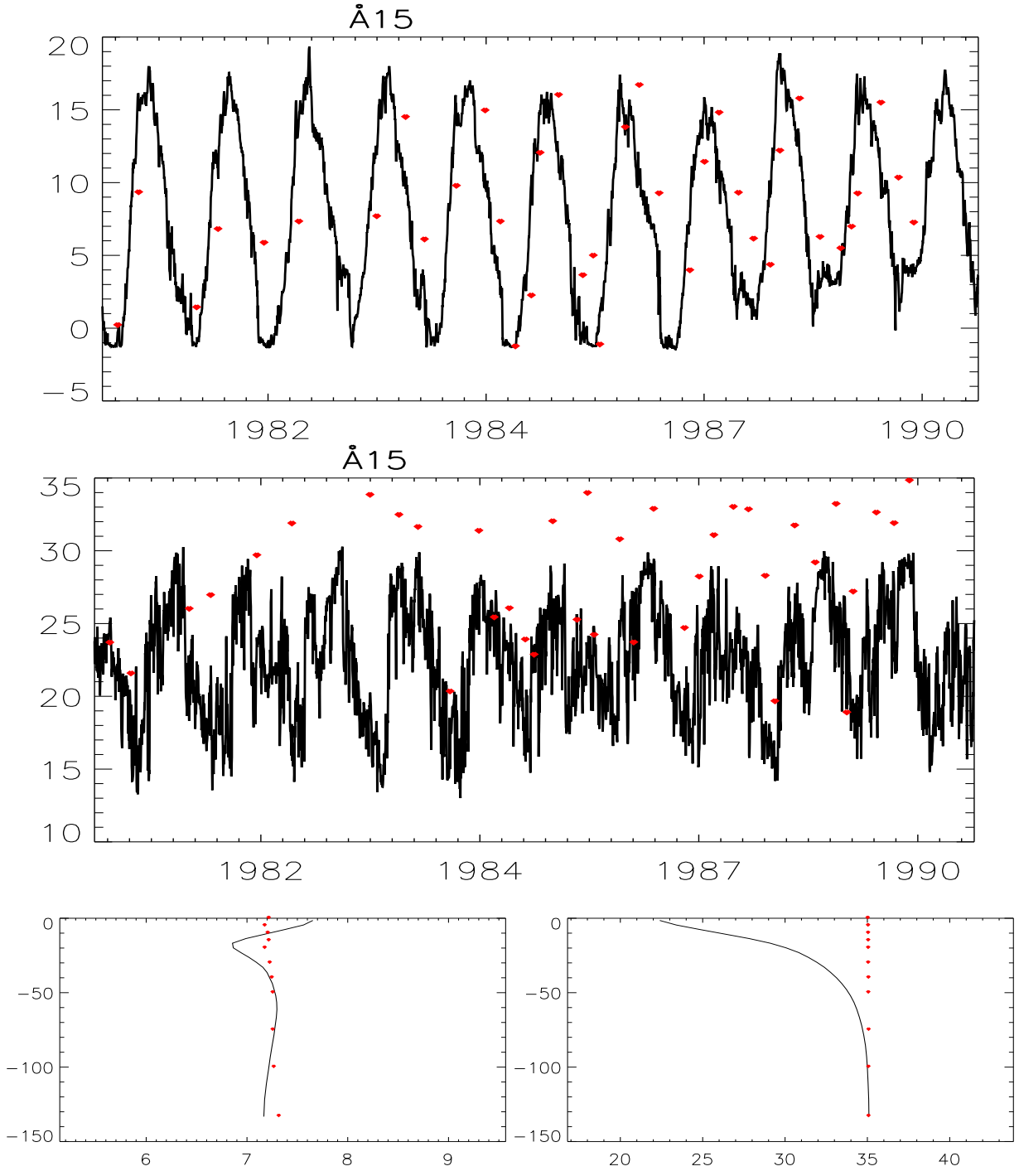

Figure 22: 1980-1990 Decade. Top two figures : Simulated SST & SSS (black), against measurement (red dots), Bottom figures: Simulated temperature and salinity profiles (black), against measurements (red dots). Temperature are measured in Celsius degrees and salinities in PSU.

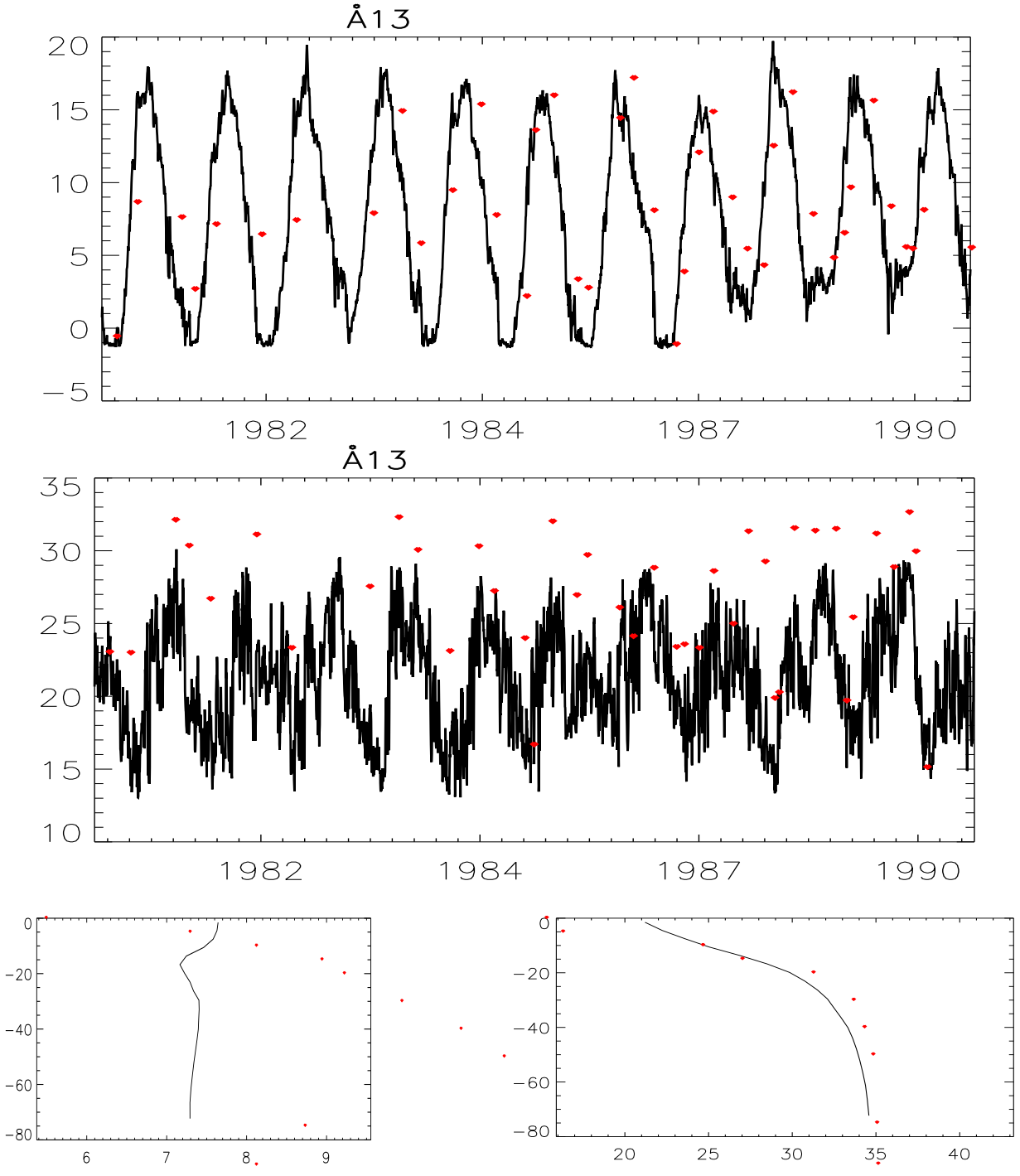

Figure 23: 1980-1990 Decade. Top two figures : Simulated SST & SSS (black), against measurement (red dots), Bottom figures: Simulated temperature and salinity profiles (black), against measurements (red dots). Temperature are measured in Celsius degrees and salinities in PSU.

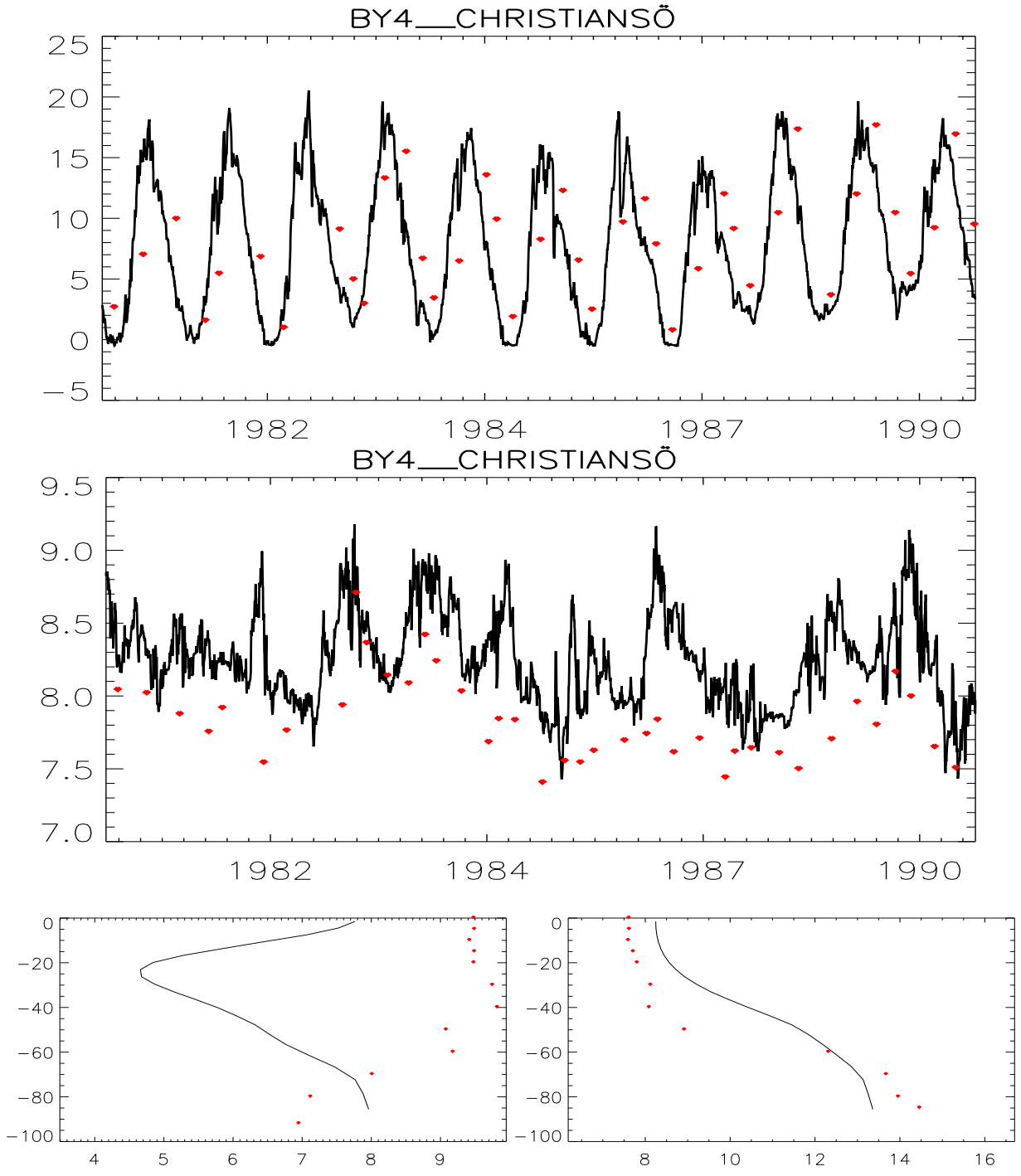

Figure 24: 1980-1990 Decade. Top two figures : Simulated SST & SSS (black), against measurement (red dots), Bottom figures: Simulated temperature and salinity profiles (black), against measurements (red dots). Temperature are measured in Celsius degrees and salinities in PSU.

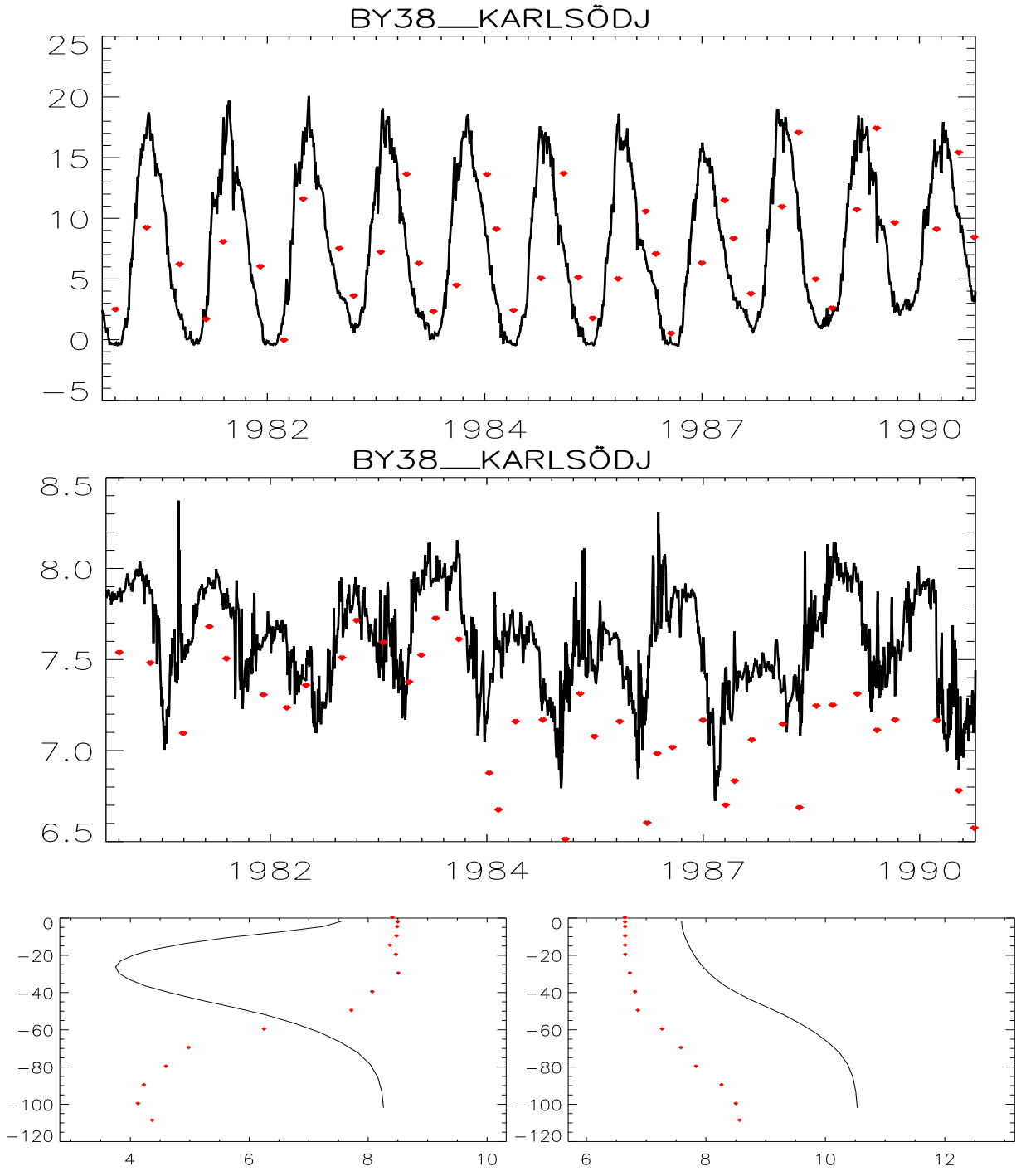

Figure 25: 1980-1990 Decade. Top two figures : Simulated SST & SSS (black), against measurement (red dots), Bottom figures: Simulated temperature and salinity profiles (black), against measurements (red dots). Temperature are measured in Celsius degrees and salinities in PSU.

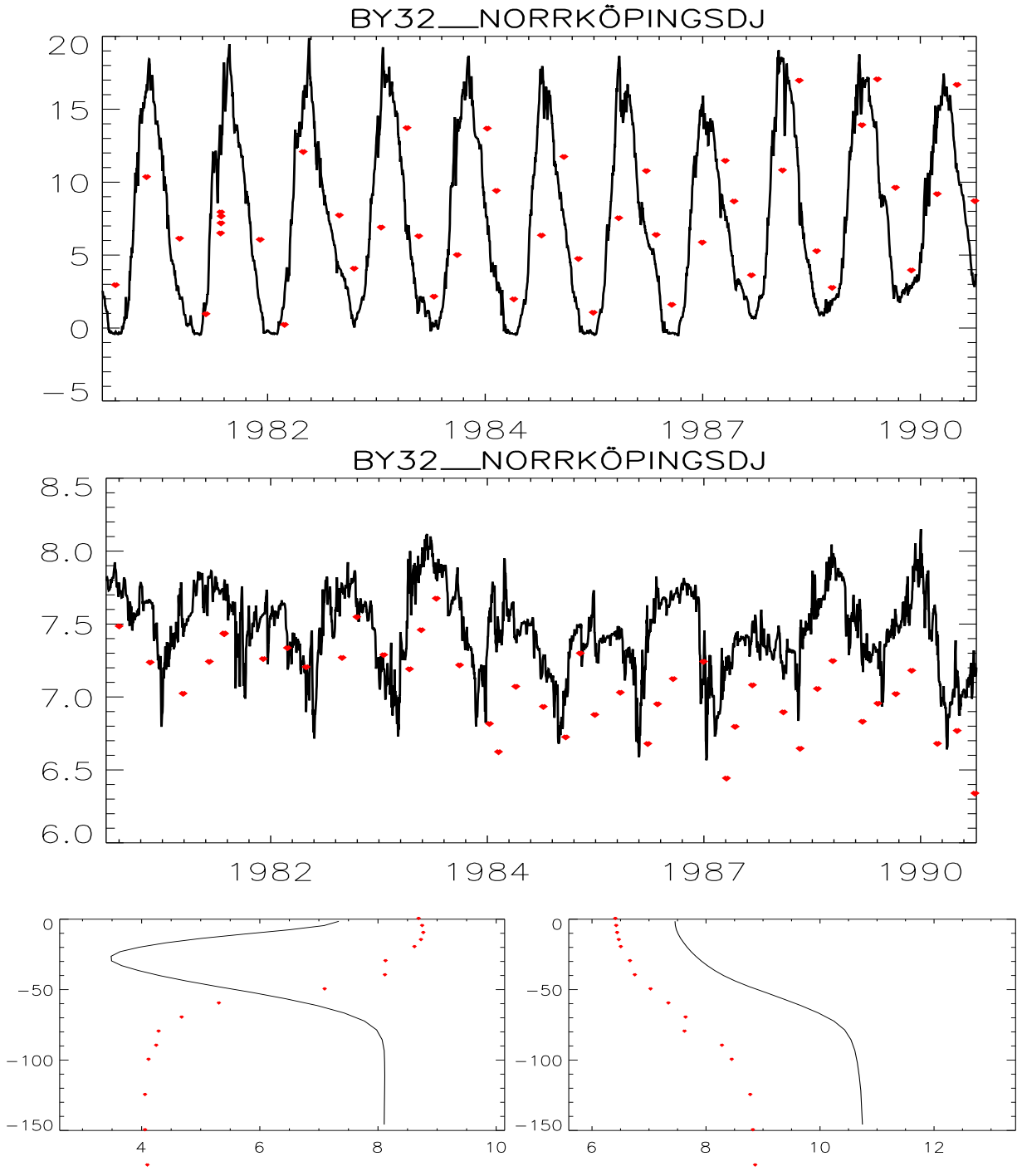

Figure 26: 1980-1990 Decade. Top two figures : Simulated SST & SSS (black), against measurement (red dots), Bottom figures: Simulated temperature and salinity profiles (black), against measurements (red dots). Temperature are measured in Celsius degrees and salinities in PSU.

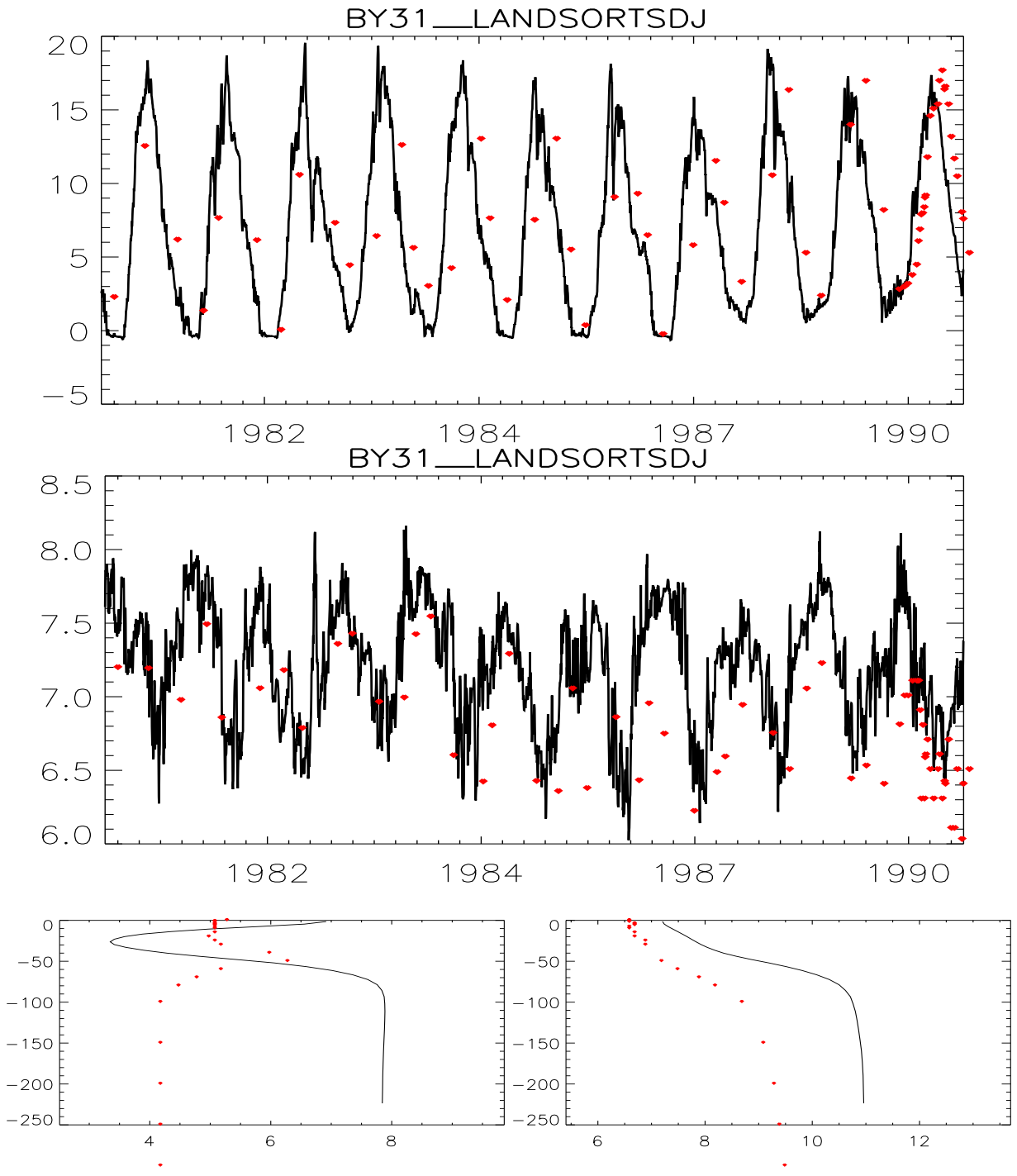

Figure 27: 1980-1990 Decade. Top two figures : Simulated SST & SSS (black), against measurement (red dots), Bottom figures: Simulated temperature and salinity profiles (black), against measurements (red dots). Temperature are measured in Celsius degrees and salinities in PSU.

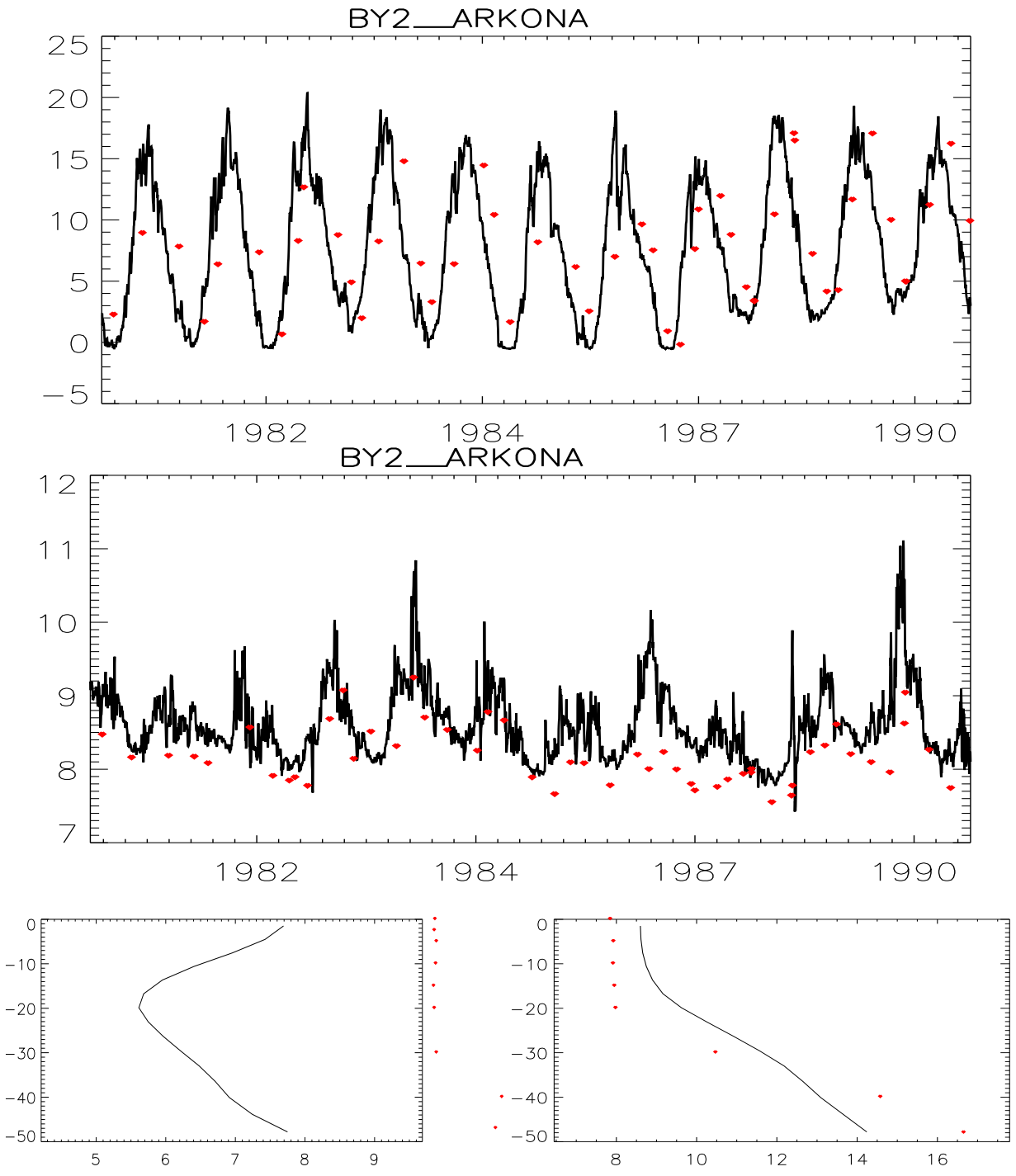

Figure 28: 1980-1990 Decade. Top two figures : Simulated SST & SSS (black), against measurement (red dots), Bottom figures: Simulated temperature and salinity profiles (black), against measurements (red dots). Temperature are measured in Celsius degrees and salinities in PSU.

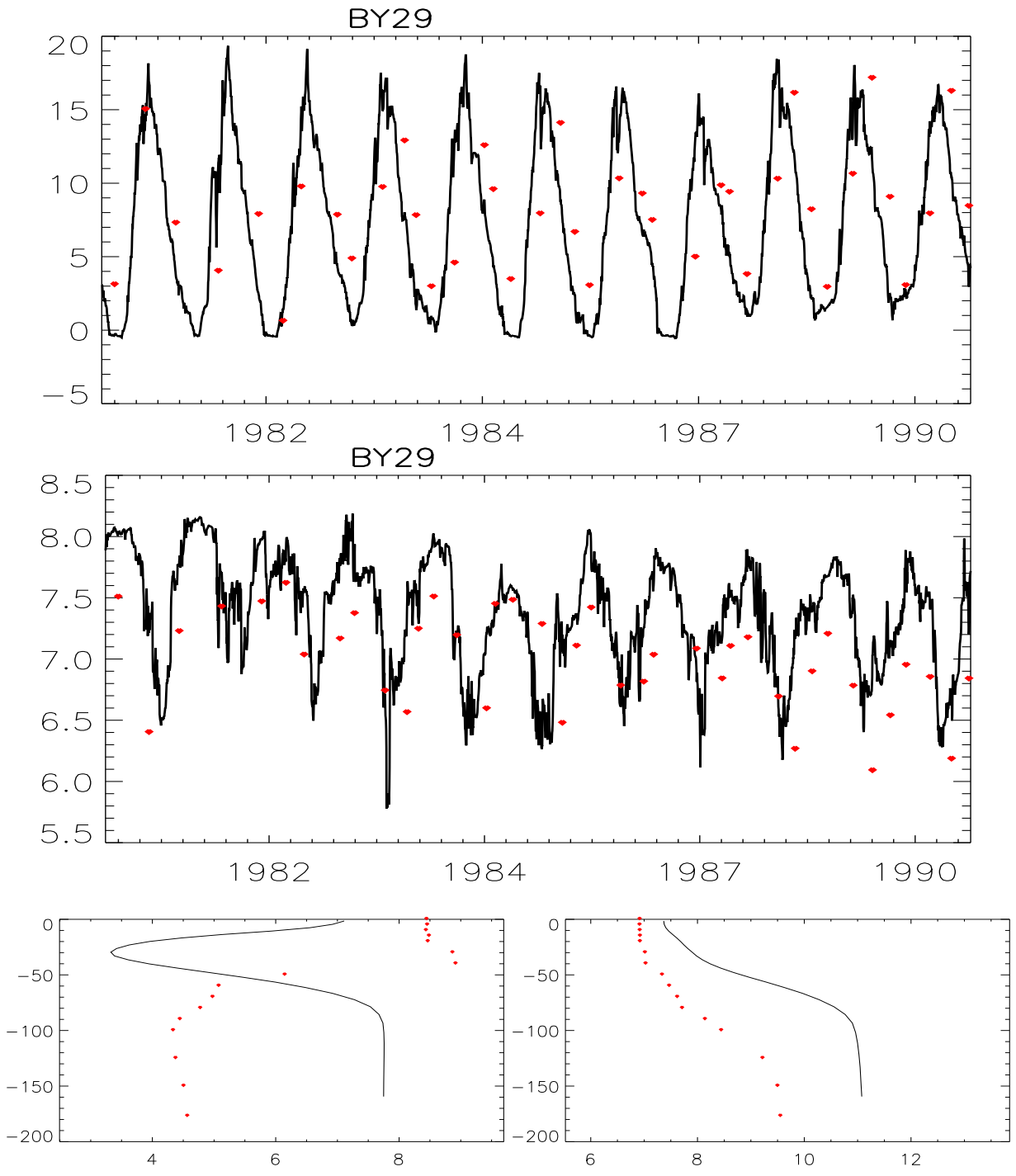

Figure 29: 1980-1990 Decade. Top two figures : Simulated SST & SSS (black), against measurement (red dots), Bottom figures: Simulated temperature and salinity profiles (black), against measurements (red dots). Temperature are measured in Celsius degrees and salinities in PSU.

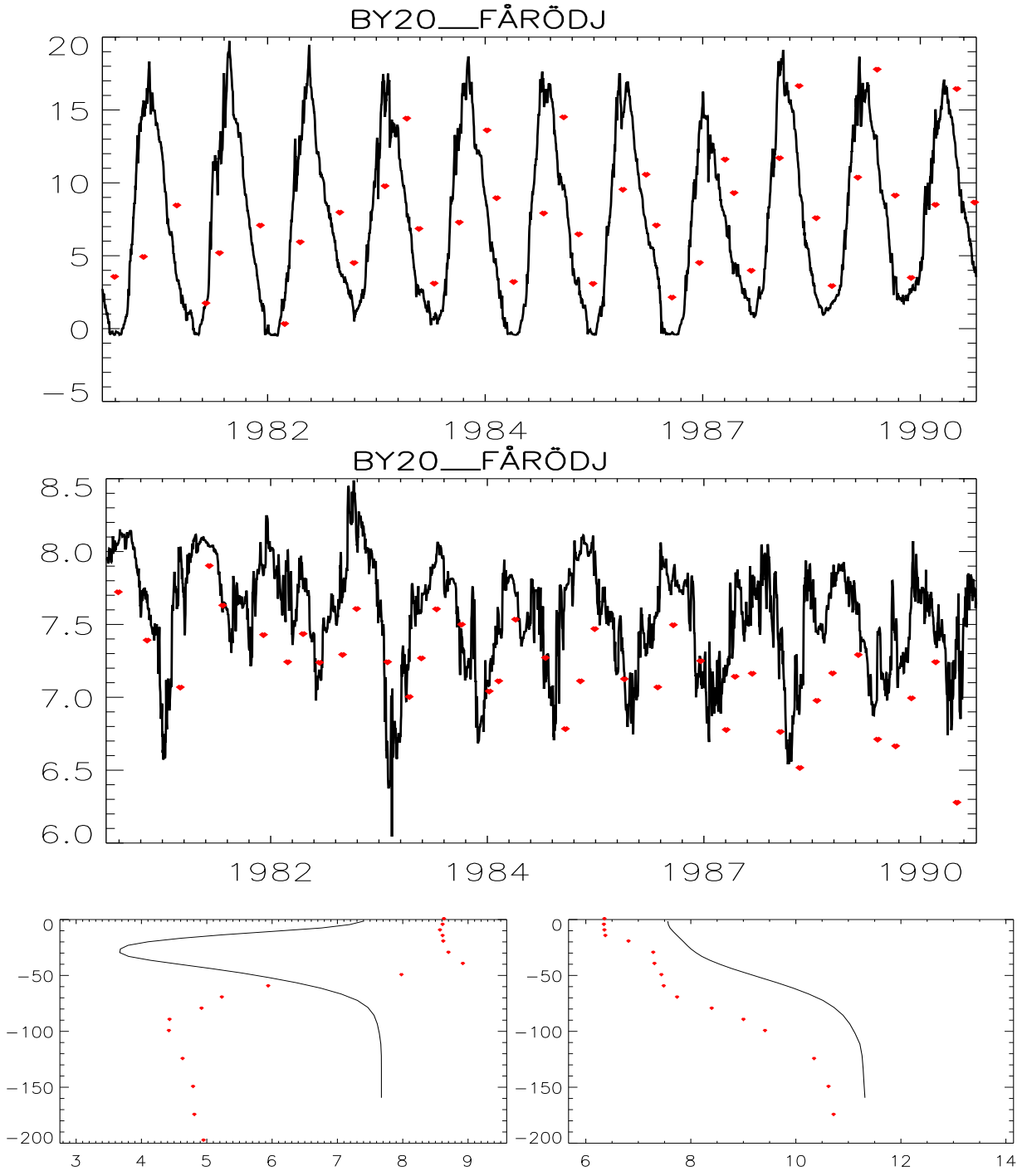

Figure 30: 1980-1990 Decade. Top two figures : Simulated SST & SSS (black), against measurement (red dots), Bottom figures: Simulated temperature and salinity profiles (black), against measurements (red dots). Temperature are measured in Celsius degrees and salinities in PSU.

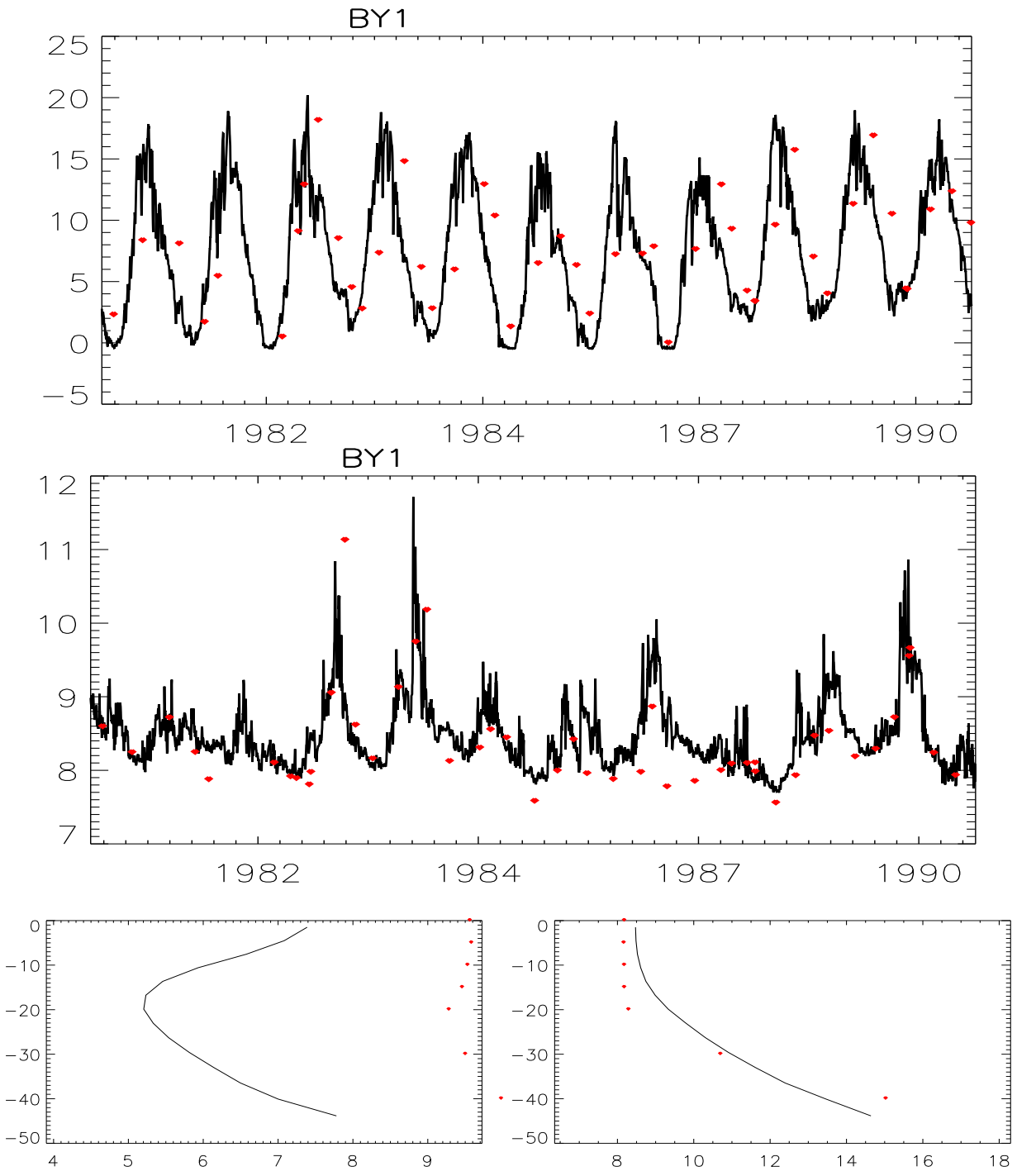

Figure 31: 1980-1990 Decade. Top two figures : Simulated SST & SSS (black), against measurement (red dots), Bottom figures: Simulated temperature and salinity profiles (black), against measurements (red dots). Temperature are measured in Celsius degrees and salinities in PSU.

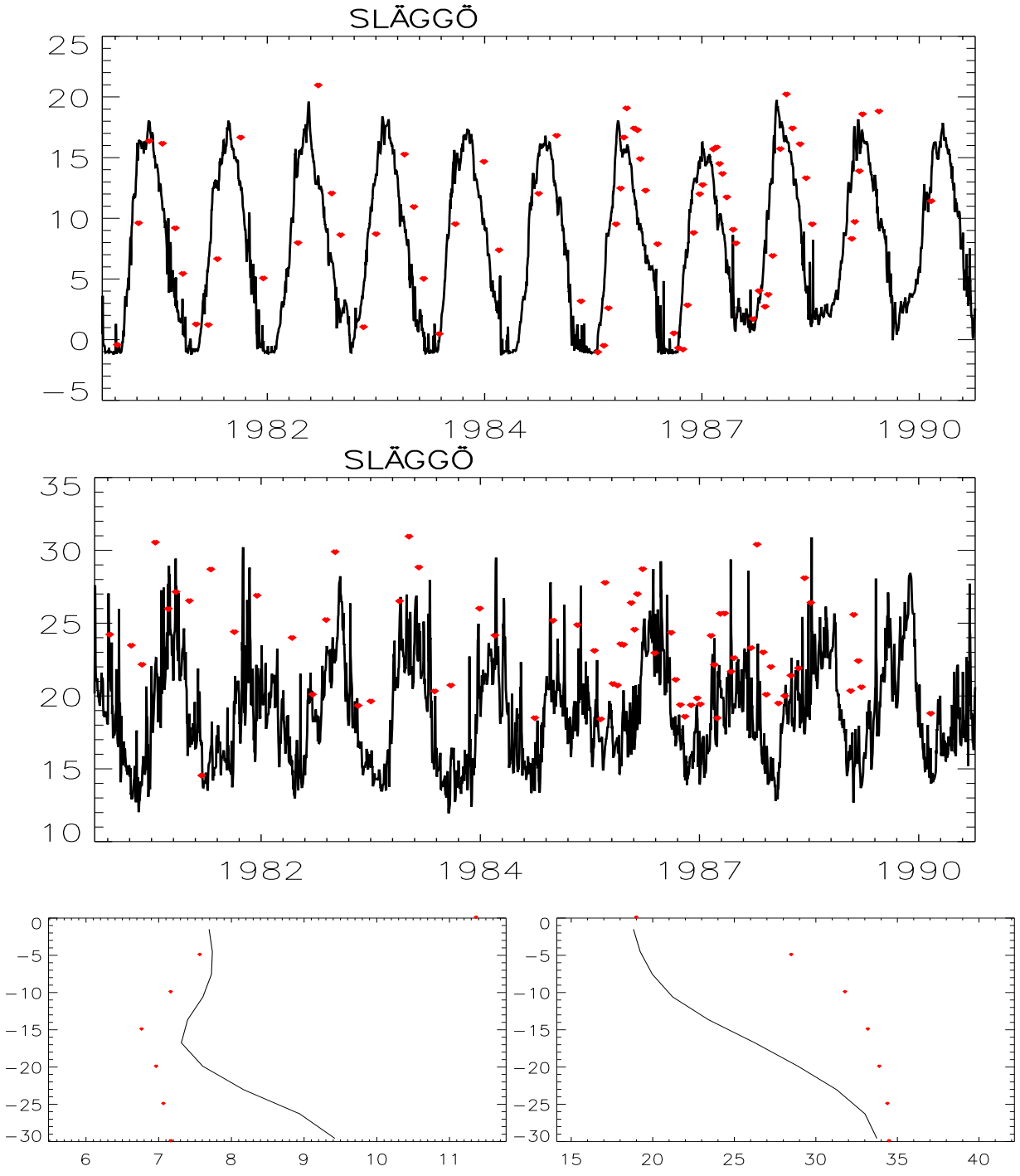

Figure 32: 1980-1990 Decade. Top two figures : Simulated SST & SSS (black), against measurement (red dots), Bottom figures: Simulated temperature and salinity profiles (black), against measurements (red dots). Temperature are measured in Celsius degrees and salinities in PSU.

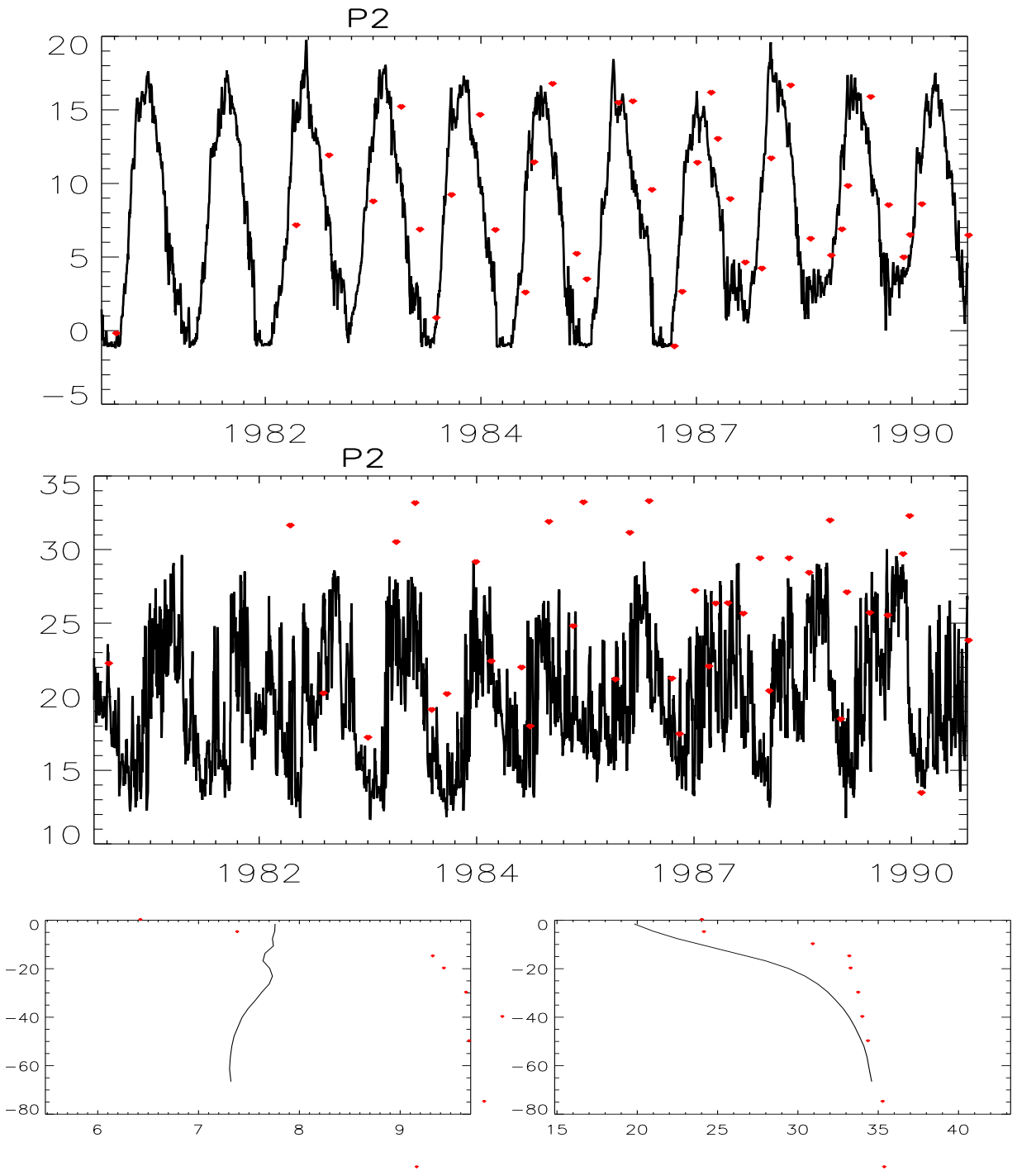

Figure 33: 1980-1990 Decade. Top two figures : Simulated SST & SSS (black), against measurement (red dots), Bottom figures: Simulated temperature and salinity profiles (black), against measurements (red dots). Temperature are measured in Celsius degrees and salinities in PSU.

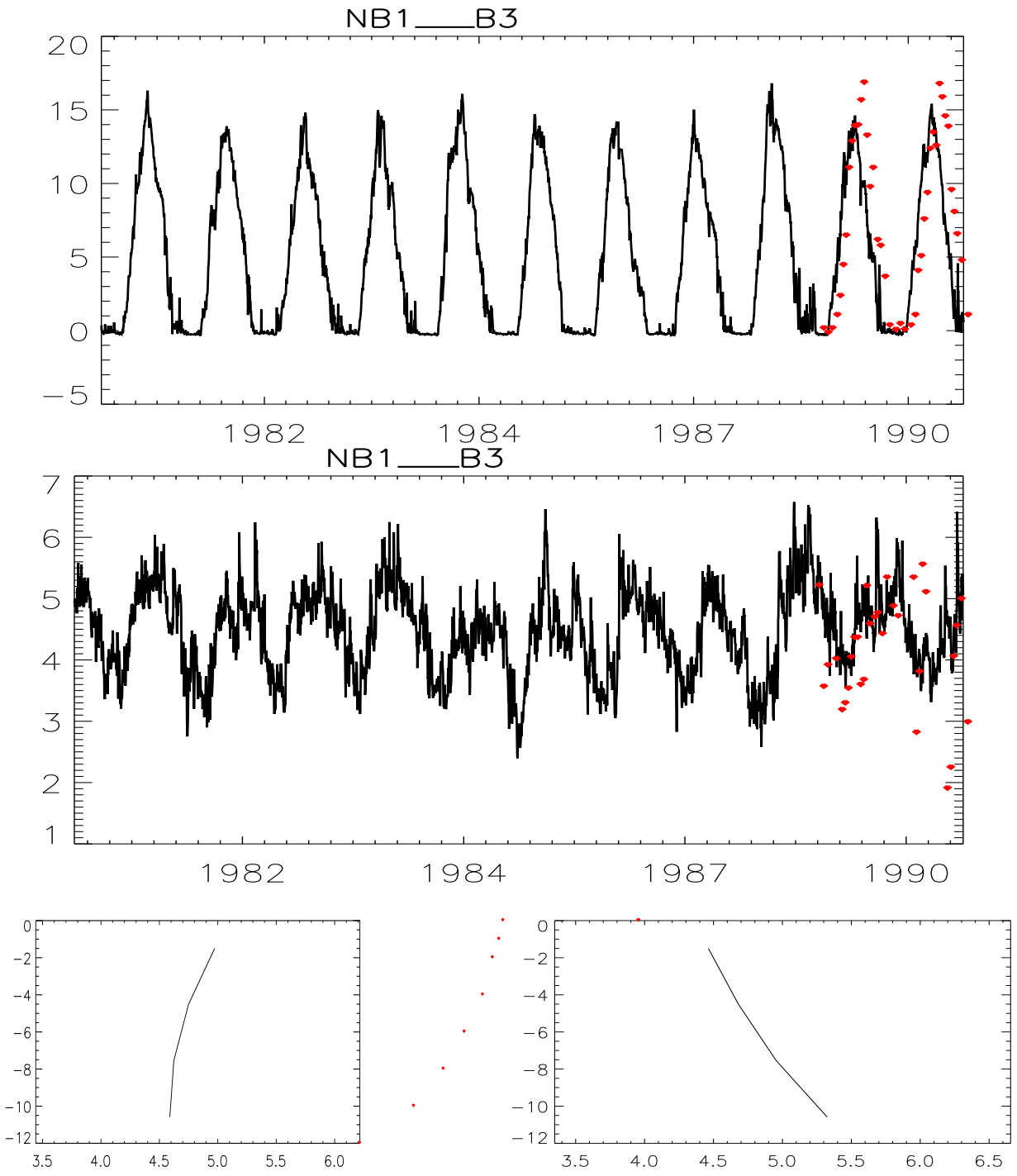

Figure 34: 1980-1990 Decade. Top two figures : Simulated SST & SSS (black), against measurement (red dots), Bottom figures: Simulated temperature and salinity profiles (black), against measurements (red dots). Temperature are measured in Celsius degrees and salinities in PSU.

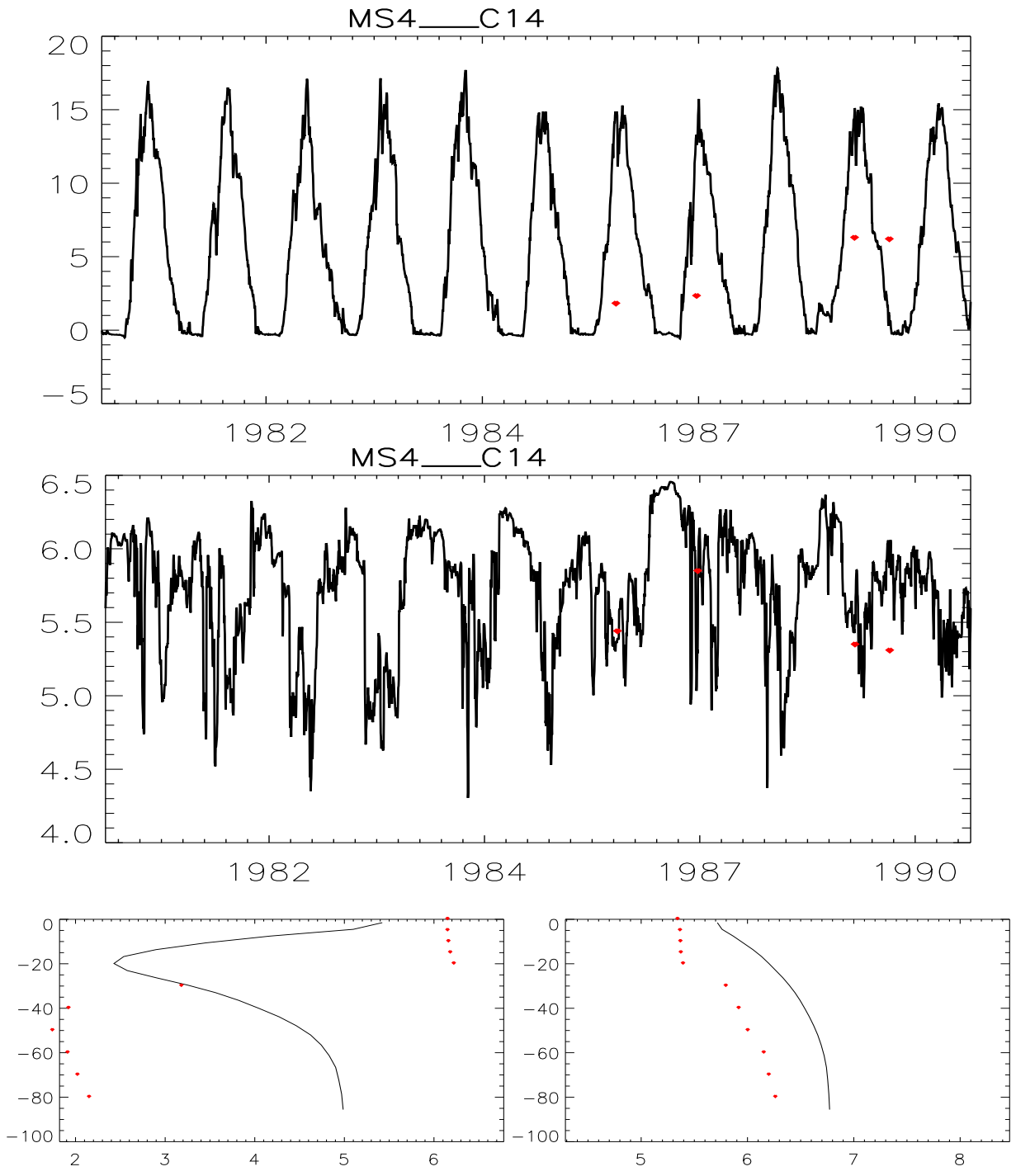

Figure 35: 1980-1990 Decade. Top two figures : Simulated SST & SSS (black), against measurement (red dots), Bottom figures: Simulated temperature and salinity profiles (black), against measurements (red dots). Temperature are measured in Celsius degrees and salinities in PSU.

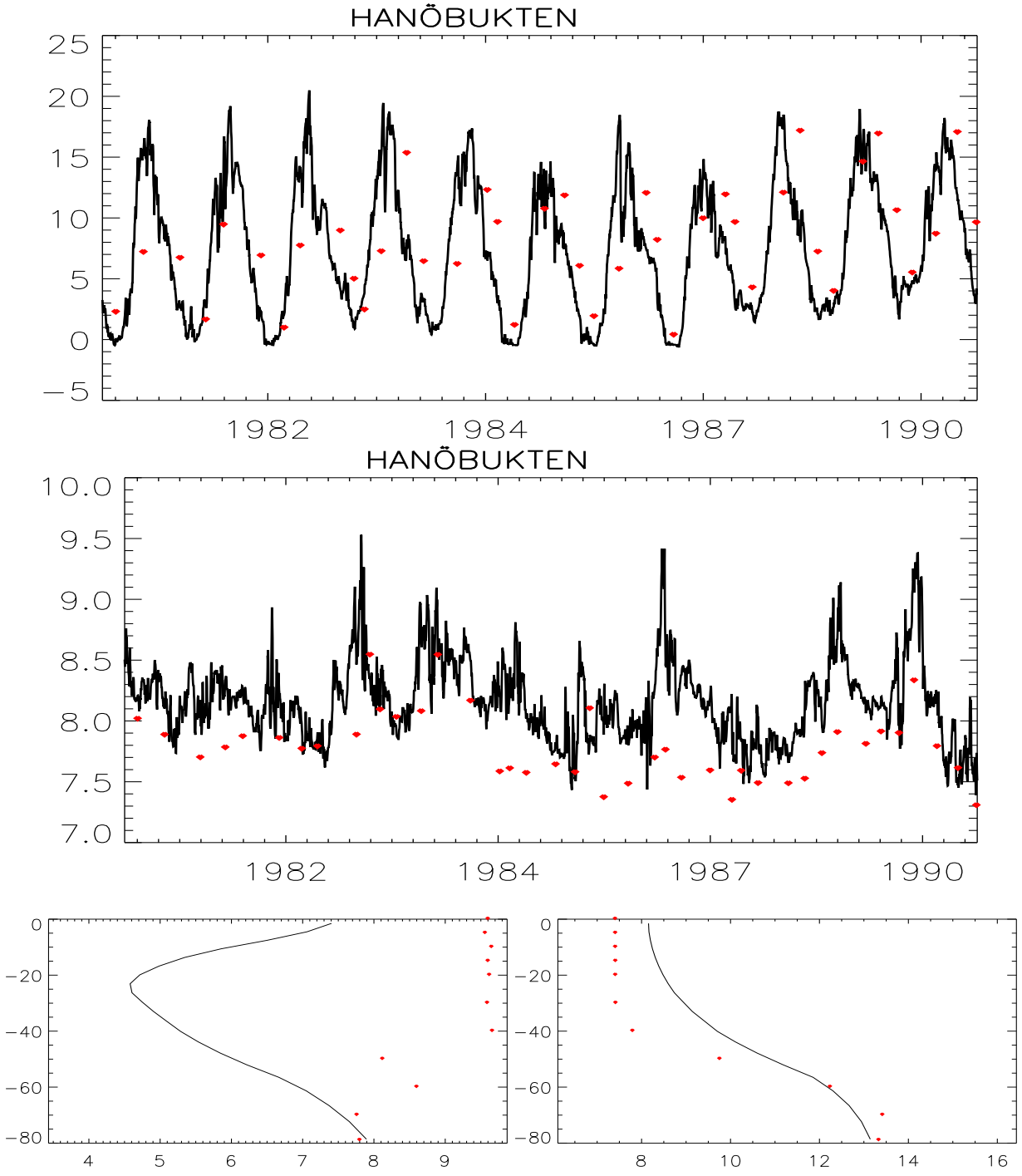

Figure 36: 1980-1990 Decade. Top two figures : Simulated SST & SSS (black), against measurement (red dots), Bottom figures: Simulated temperature and salinity profiles (black), against measurements (red dots). Temperature are measured in Celsius degrees and salinities in PSU.

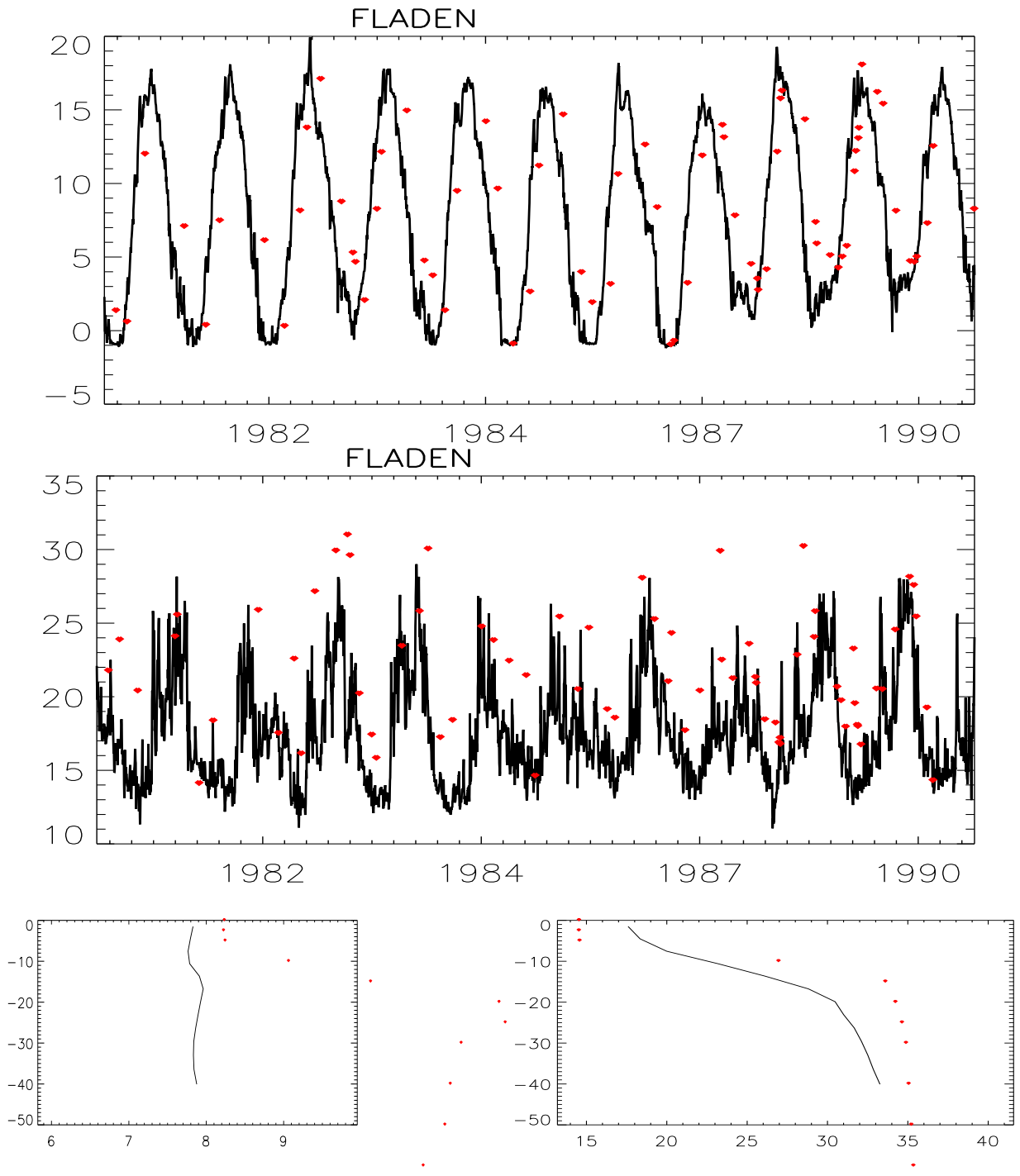

Figure 37: 1980-1990 Decade. Top two figures : Simulated SST & SSS (black), against measurement (red dots), Bottom figures: Simulated temperature and salinity profiles (black), against measurements (red dots). Temperature are measured in Celsius degrees and salinities in PSU.

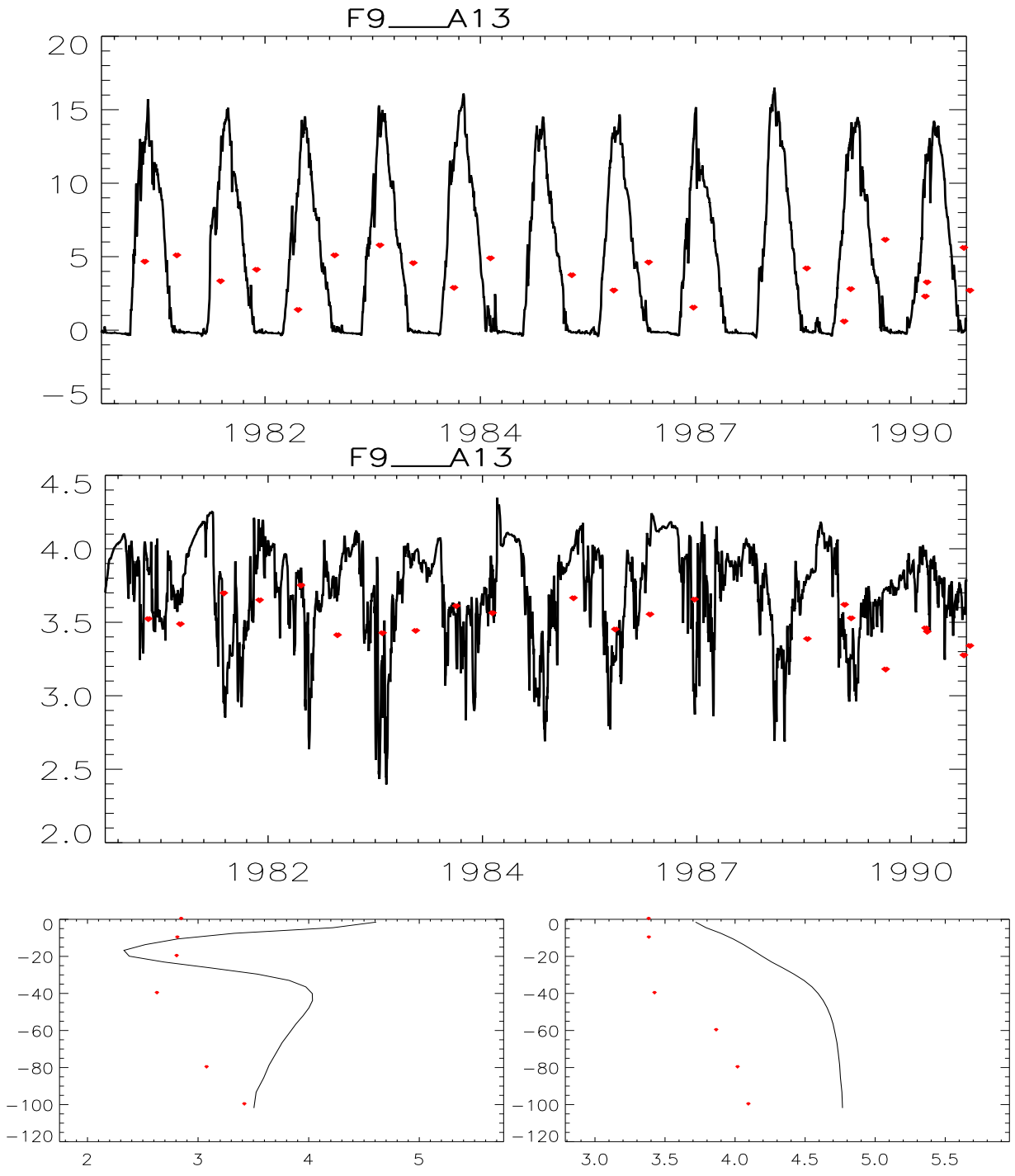

Figure 38: 1980-1990 Decade. Top two figures : Simulated SST & SSS (black), against measurement (red dots), Bottom figures: Simulated temperature and salinity profiles (black), against measurements (red dots). Temperature are measured in Celsius degrees and salinities in PSU.

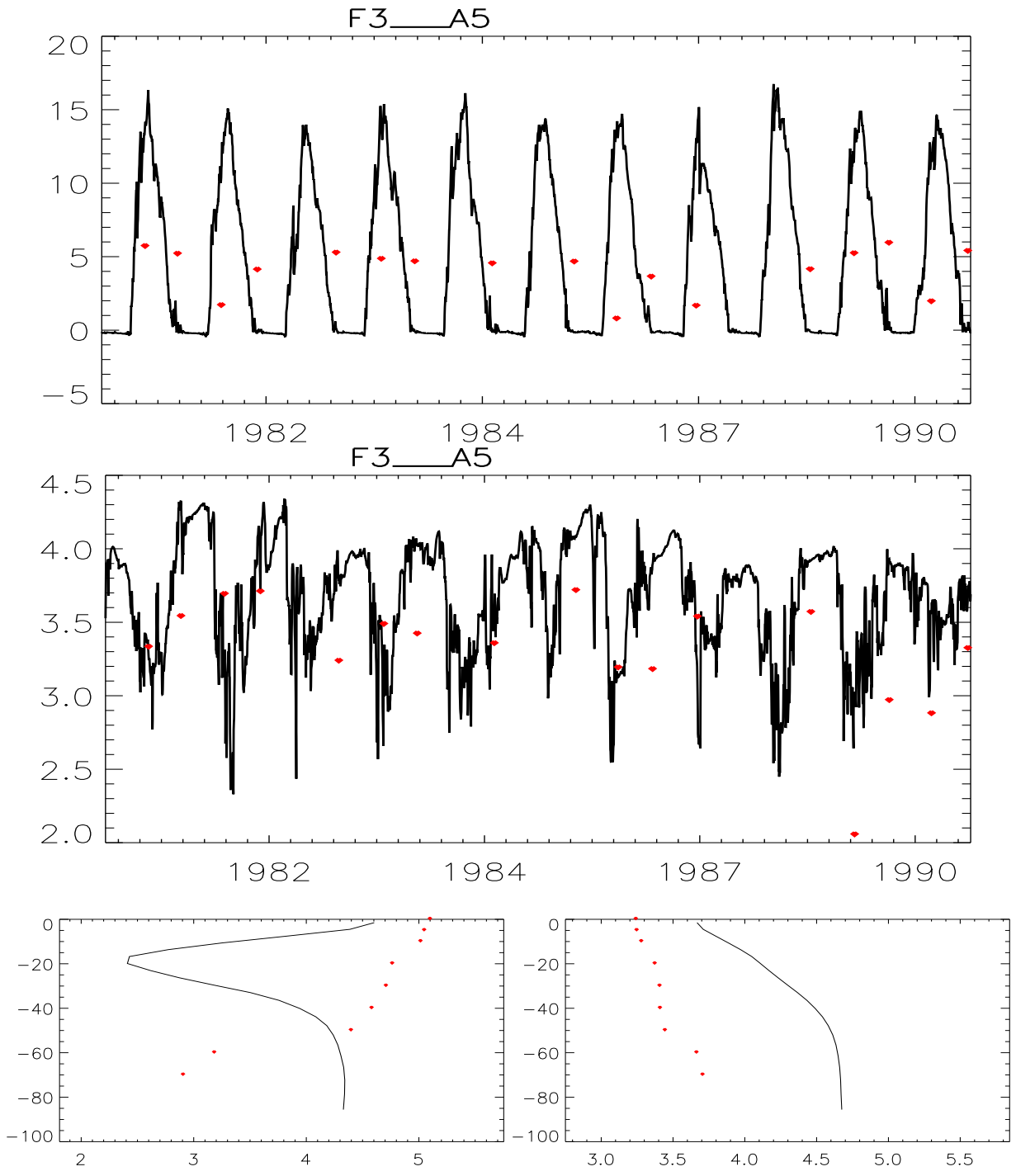

Figure 39: 1980-1990 Decade. Top two figures : Simulated SST & SSS (black), against measurement (red dots), Bottom figures: Simulated temperature and salinity profiles (black), against measurements (red dots). Temperature are measured in Celsius degrees and salinities in PSU.

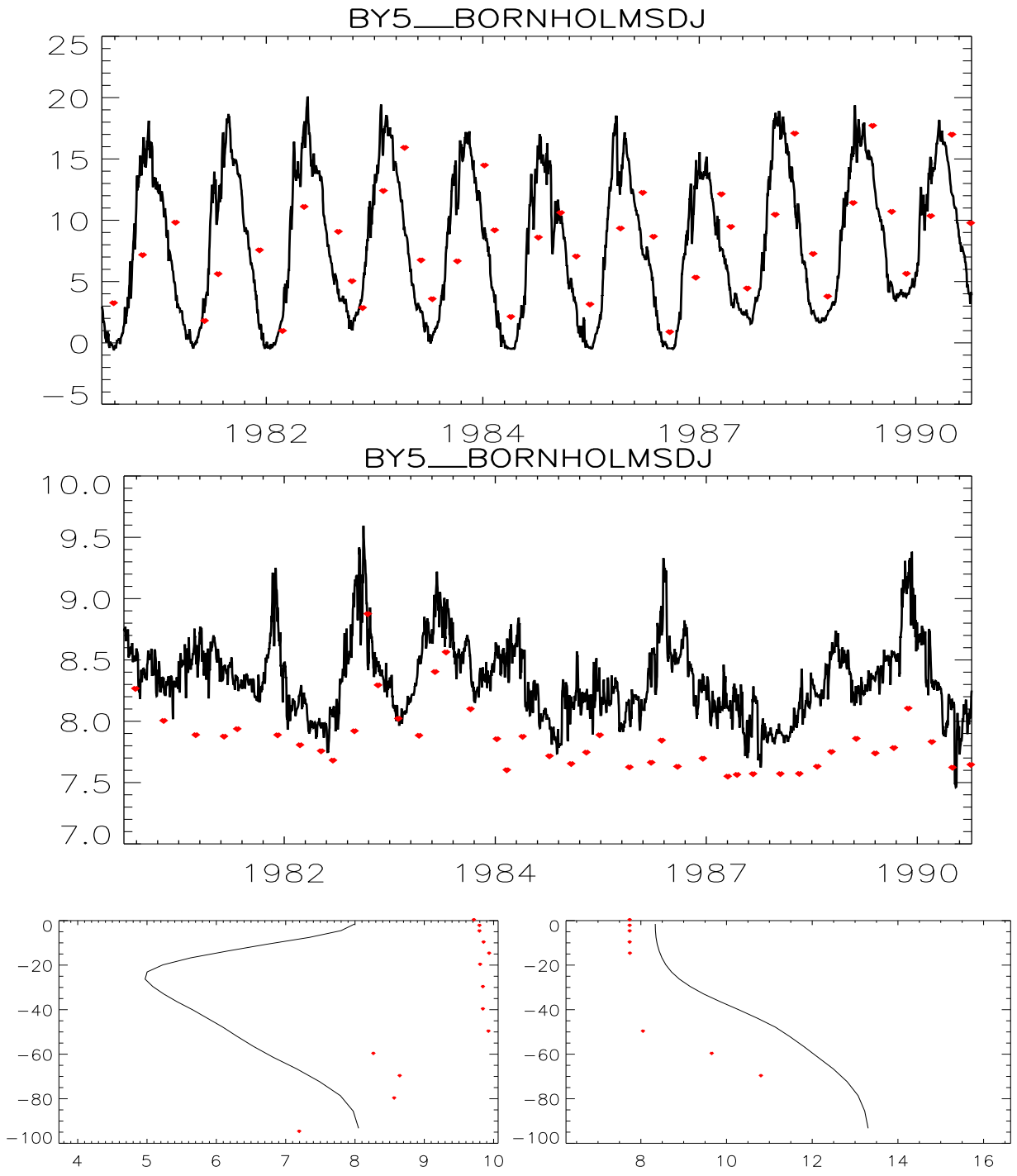

Figure 40: 1980-1990 Decade. Top two figures : Simulated SST & SSS (black), against measurement (red dots), Bottom figures: Simulated temperature and salinity profiles (black), against measurements (red dots). Temperature are measured in Celsius degrees and salinities in PSU.

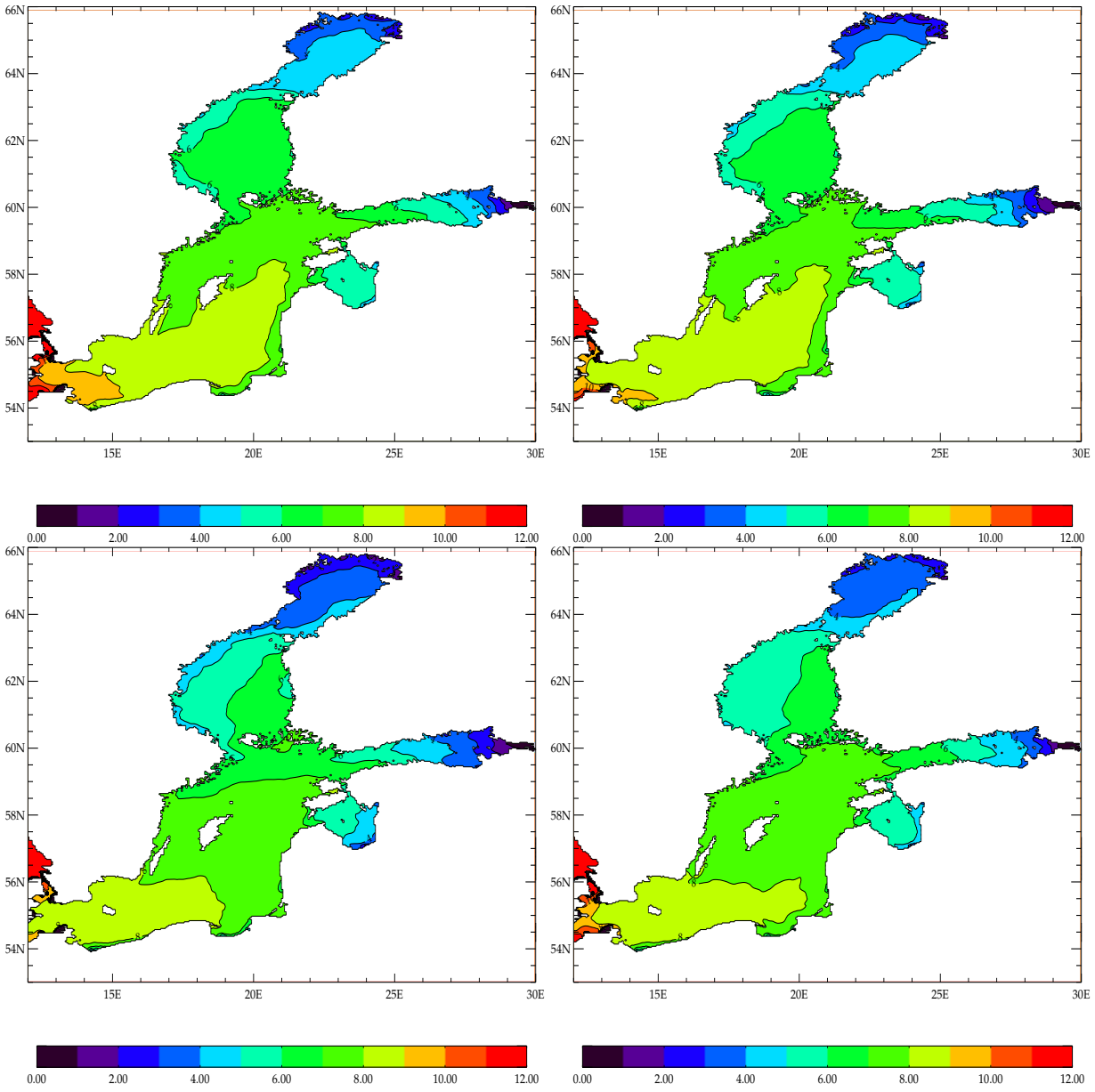

Figure 41: BaltiX climatological simulated surface salinity (in PSU) for January, April, July and November for the period 1980-1990. Baltic Sea Area

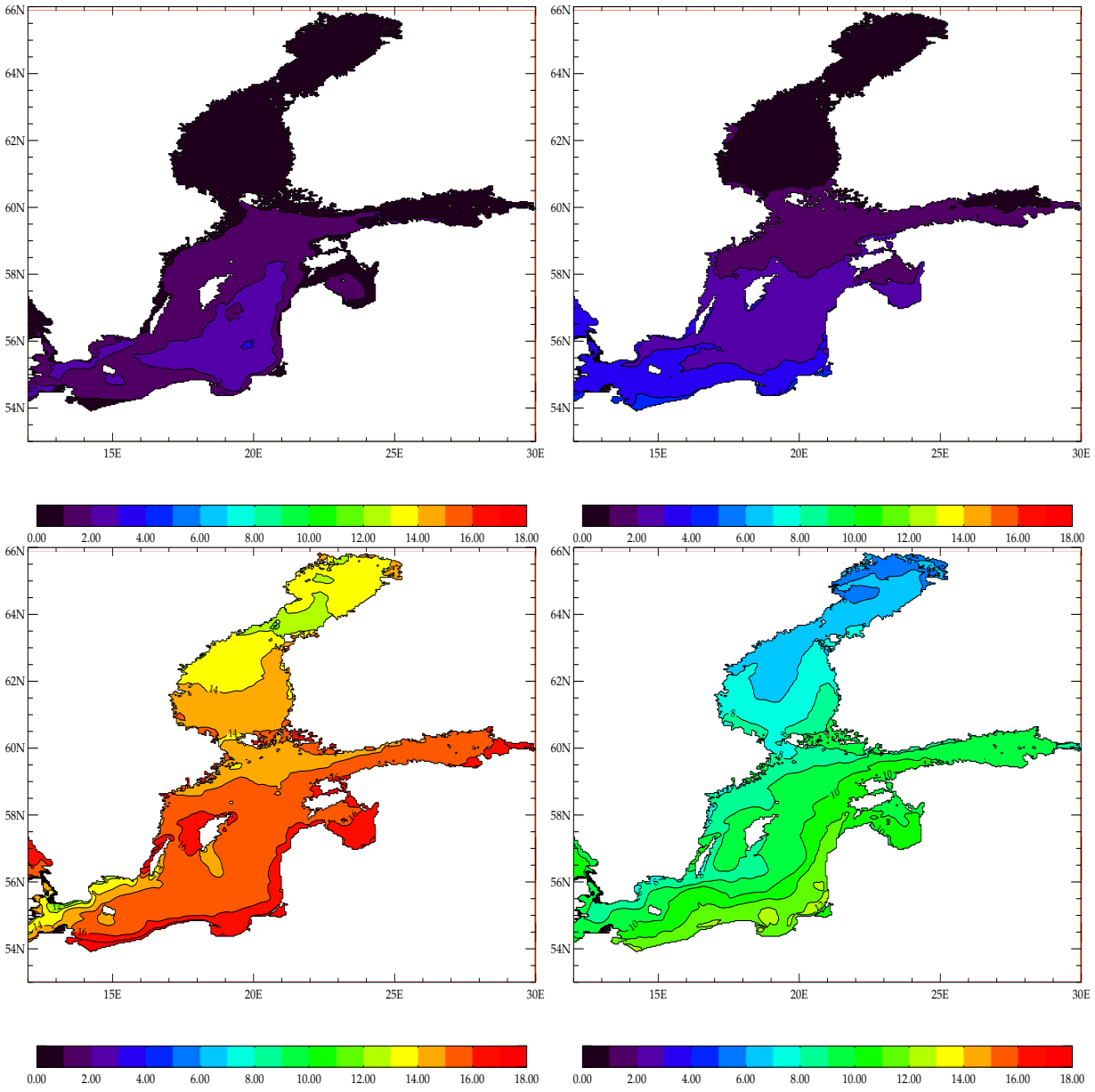

Figure 42: BaltiX climatological simulated surface temperature (in degrees) for January, April, July and November for the period 1980-1990. Baltic Sea Area

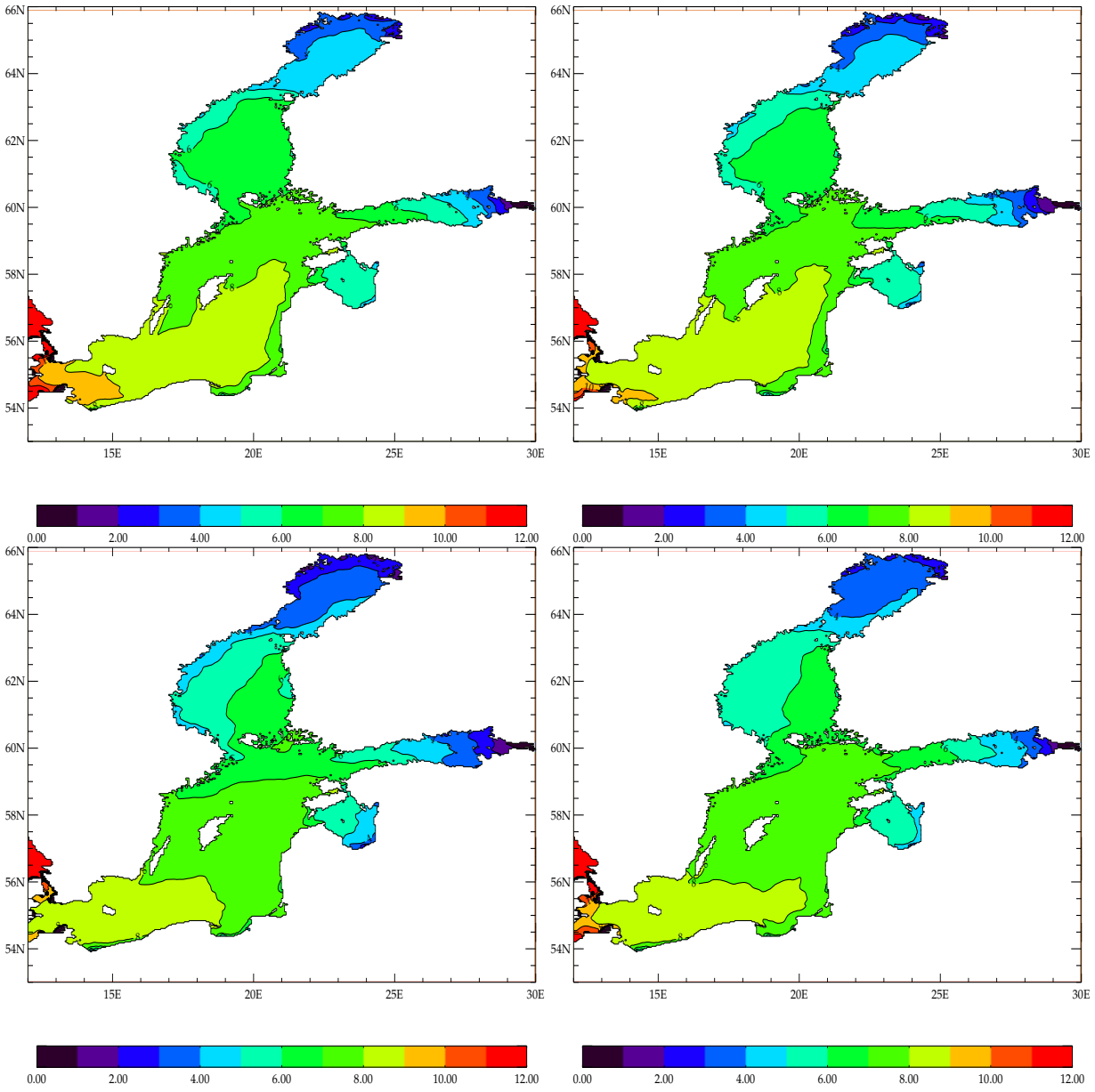

Figure 43: BaltiX climatological simulated surface salinity (in PSU) for January, April, July and November for the period 1980-1990. Baltic Sea Area

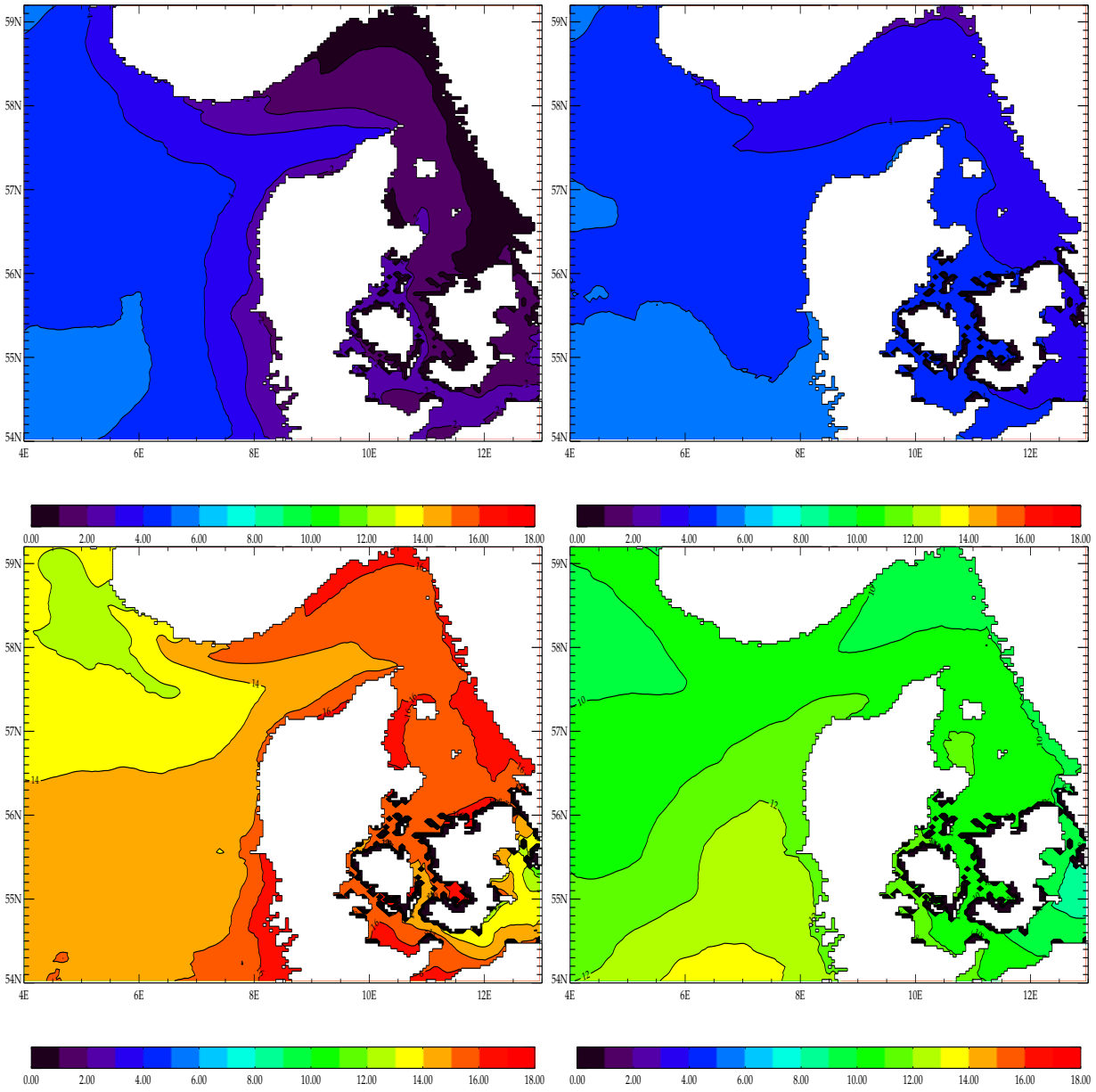

Figure 44: BaltiX climatological simulated surface temperature (in degrees) for January, April, July and November for the period 1980-1990. Kattegat/Skaggerak Area

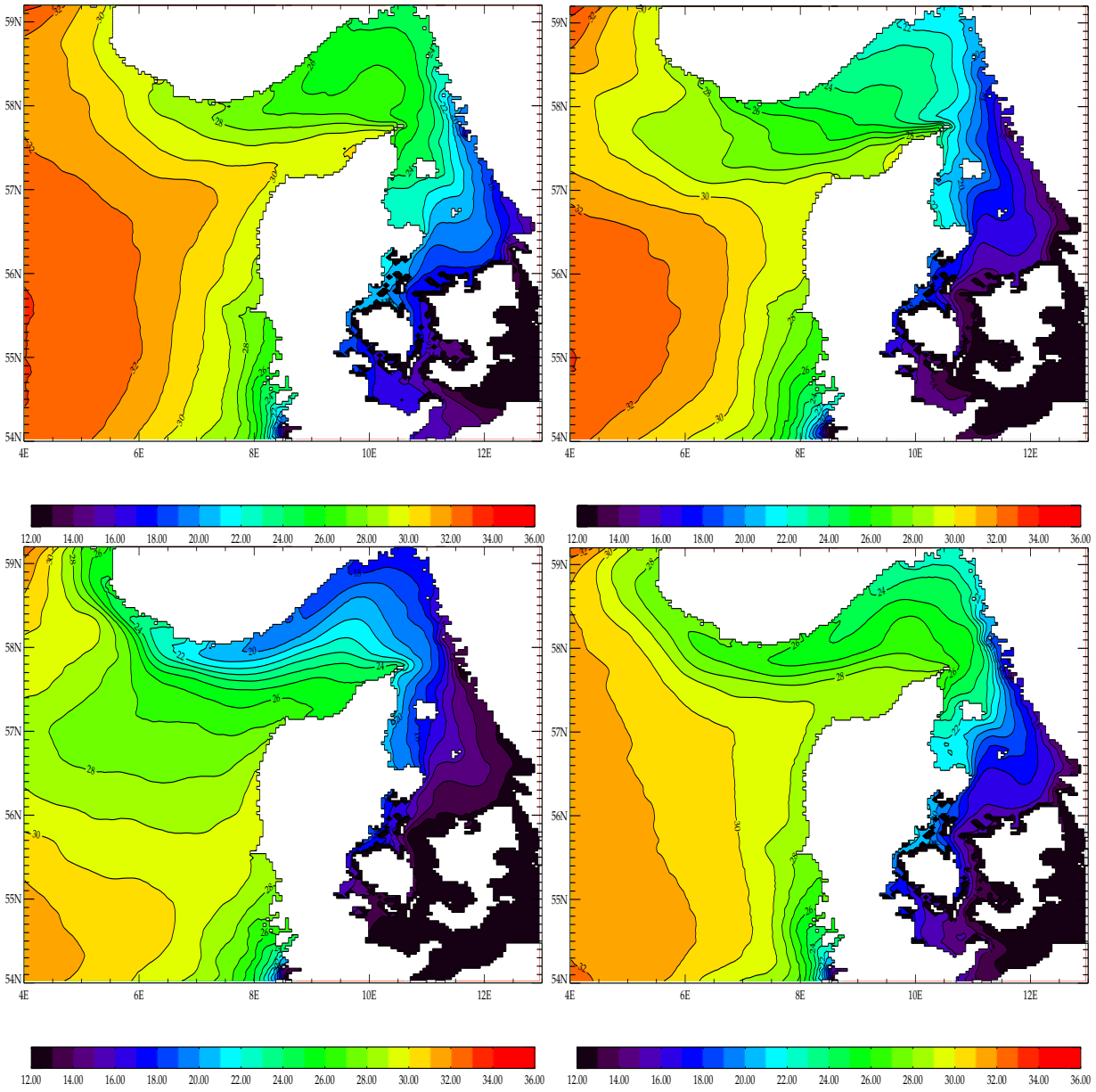

Figure 45: BaltiX climatological simulated surface salinity (in PSU) for January, April, July and November for the period 1980-1990. Kattegat/Skaggerak Area

4.3.3 Deep Baltic Salinity Trend

Figure 46 shows the Gotland Deep salinity for the time period 1961-2006. The model results are ploted for a typical BaltiX simulation, and based on observations. One can observe the deep salinity variability is well reproduced although a spin-up period is necessary for that variability to start. In order to reproduce that variability however, an opening of the Danish straights to an extent which is too high in comparison of the measured cross-sections is necessary. The configuration for the time being proves to have too much halocline ventilation as mentionned before. This issue is being adressed as this report is written. Apart from this model bias, one observes that the salinity jump due to the 2003 inflow is too low, although that of the 1993 inflow fits the observations. However, this bias is observed in other models, even in models including only the Baltic Sea [15], which highly suggests that this bias is related with the forcing dataset, and not a real bias of the ocean model indeed.

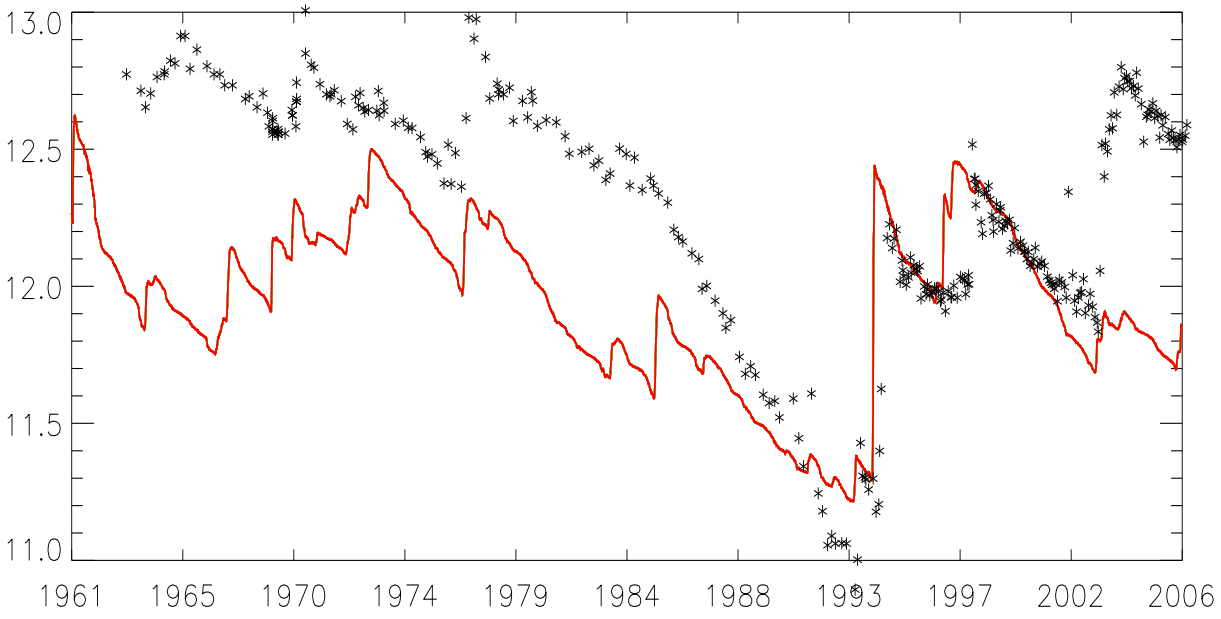

Figure 46: Gotland Deep salinity (in PSU) simulated by BaltiX (red line) against measurement (black diamonds) for the period 1961-2006

5 Coupling with LIM3 the framework of MyOcean: Validation and new developments

5.1 Model-Satellite SST comparison

The simulations are evaluated using satellite data provided by BSH. Figure 47 shows Nash-Sutcliffe Model Efficiency index (Nash, J. E. and J. V. Sutcliffe, 1970) of simulated and observed mean SST.

$$E = 1 - \frac{\sum_{t=1}^{T}(Q_o^t - Q_m^t)^2}{\sum_{t=1}^{T}(Q_o^t - \bar{Q}_o)^2} \quad (1)$$

where Q_o is observed (satellite) SST, Q_m is modelled SST, and t is grid point. Index (E) is classified according to range from excellent (E $>$ 0.65), very good (0.5 $<$ E $\leq$ 0.65), good (0.2 $<$ E $\leq$ 0.5), poor (0 $<$ E $\leq$ 0.2), and bad (E $\leq$0). The bar plot reports the frequency (in number of years) of classified index values of the each month. The model skill in 1992 and 2001 are particularly good with respect to the other years. The best skill is achieved all around the year except summer. It is because the accuracy of SST measured by Satellite during the Summer is uncertain because of water vapour and aerosol prevent to detect precise values.

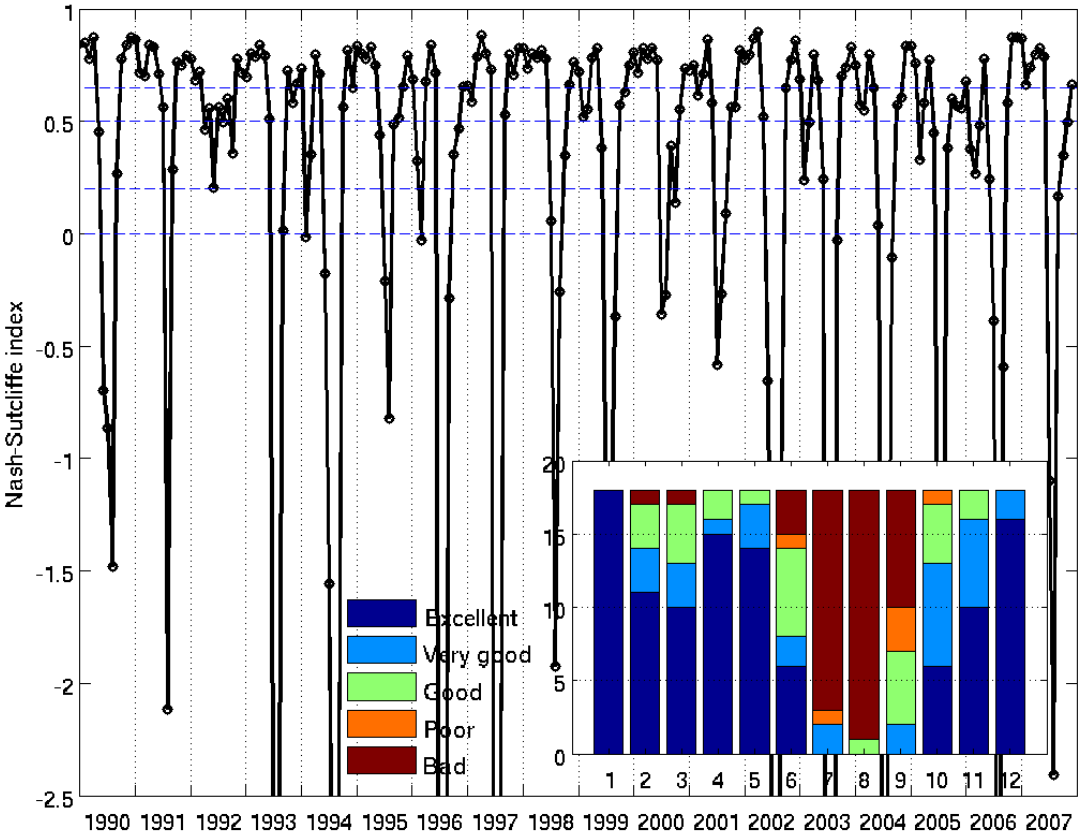

Figure 47: Nash-Sutcliffe Model Efficiency (E) index

Reference: Nash, J. E. and J. V. Sutcliffe (1970), River flow forecasting through conceptual models part I, A discussion of principles, Journal of Hydrology, 10 (3), 282-290.

5.2 Ice conditions in the Baltic Sea

Ice condition is one of the important controlling variable for thermodynamics and dynamics in the Baltic Sea circulation, and its inter-annual variation is critical. The maximum ice covered area varies between 52000 and 422000 km^2, which stands for 12 to 100 % of the total Baltic Sea area including Kattegatt and Skagerrak. The ice formation in the Baltic Sea starts along the coasts of the northern Bay of Bothnia and the inner Gulf of Finland in November. Thereafter the freezing spreads to the Quark, the open Bay of Bothnia and the coasts of Sea of Bothnia. The maximum ice cover is normally reached in March.

In mild winter, the Sea of Bothnia doesn't freeze at all and the Gulf of Finland only gets a partial ice cover. However, in severe winter, the ice extends to the Danish Sounds and the central Baltic Proper.

The melting of ice starts in April and proceeds from the south to the north. In the northern Baltic Proper the ice disappears in early April. By the beginning of May there is only ice left in the northern Bay of Bothnia, where also the last ice pieces melt away by the beginning of June.

5.3 Description of the LIM3 model

To carry out the MyOcean project for setting up the Baltic Sea operational model, we have implemented the model based on a non-linear free surface NEMO/OPA (www.nemo-ocean.eu) coupled to a comprehensive LIM3 (Vancoppenolle et. al., 2009) sea-ice model. This LIM3 model has a representation of both thermodynamic and dynamic processes. The thermodynamics calculate melting and freezing rates to achieve a local balance of heat and water fluxes. The dynamics calculate ice velocity by balancing forcing from wind stress, ocean drag and sea-surface tilt with internal ice stresses. LIM2 parameterises the storage of latent heat in brine (Fichefet and Morales Maqueda, 1997) using a heat reservoir, but LIM3 represents it explicitly using a vertically varying salinity profile. In addition, LIM3 resolves salinity variations in time using parameterizations of brine entrapment and drainage processes based on a simplification of the brine drainage model of Vancoppenolle et al.(2007). LIM3 also includes an explicit ice thickness distribution (5 ice categories) that enables to resolve 5 more intense growth and melt of thin ice, as well as the redistribution of thinner ice onto thicker ice due to ridging and rafting. For the dynamics, LIM3 uses the elastic viscous-plastic (EVP) formulation of Hunke and Dukowicz (1997). The momentum equation is solved using the C-grid formulation of Bouillon et al. (2009).

5.4 Experimental design for the hindcast

A hindcast simulation is performed with the NEMO-LIM3 driven by downscaled ERA40 reanalyzed surface forcing data with 25 km resolution and it covered the period of 1961-2007 (SMHI). The forcing consists of 3hourly wind, long wave, short wave radiation, air temperature, humidity, and precipitation.

Note that the sea ice salinity is assumed to be constant (0.001 psu) as defined in the namelist_ice bulk_sal. Melting ice albedo is defined in the namelist_ice rn_albice = 0.53, and this coefficient is the same as albedo of melting ice in the arctic and antarctic (Shine and Hendersson-Sellers, 1985). Albedo on the ocean assumed to be constant as albo = 0.066. The sea ice salinity is assumed to be constant (0.001 psu). Initial sea ice thickness is set to 0 m and initial snow ice thickness is set to 0 m. The BaltiX has a time step of 360 seconds and the sea ice models are called every 6 ocean time steps.

5.5 Results:Basin mean features

First a hindcasting has been performed successfully, so we briefly present the model output for understanding the general features of the Baltic Sea ice variability.

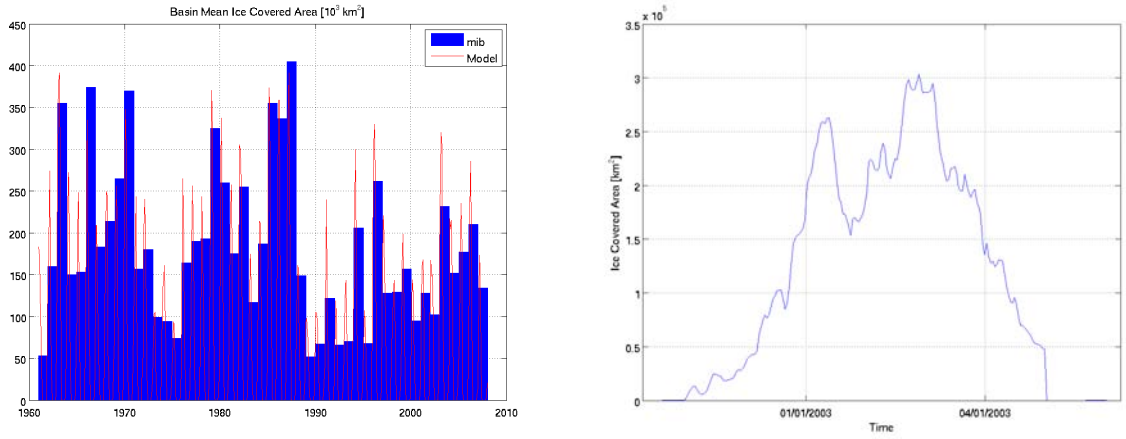

(a) Monthly ice cover area of model output and annual maximum ice measured data (mib)

(b) Daily (Oct.2002 to May 2003) ice covered area of model output

Figure 48: Monthly and daily (Oct.2002 to May 2003) basin mean sea-ice covered area.

Table 1: Comparison of ice model output and measured data (2002/2003).

	Kemi	Loviisa	Uto
First freezing date in model	01.11	01.12	01.12
First freezing date in data	04.11	28.11	01.01
Final disappearance date of ice in model	30.04	30.04	01.05
Final disappearance date of ice in data	18.05	29.04	14.04
Number of real ice days in model	181	151	121
Number of real ice days in data	195	152	75
The largest ice thickness in model (cm)	90	69	24
The largest ice thickness in data (cm)	232	54	21

Figure 48a shows inter-annual (from 1961 to 2007) variation of ice covered area (km^2) in the Baltic Sea with the comparison of the measured maximum ice covered area (mib) and model output. From this figure, we can find large inter-annual variation from mild to severe winter and the model reproduced ice extension in the Baltic Sea quite well. Figure 48b shows a time series of daily ice covered area variation from October 2002 to the end of May 2003 in the Baltic Sea. During that period ice was freezed gradually from the mid October and melted away quickly at the end of May.

From these figures, the pattern of modelled ice covered area variation (Figure 48a) is somewhat overestimated compare to ice chart data spatially and temporally.

Figures 50a, 50b, and 50c are plotted time series of the March ice thickness at Loviisa, Uto and Kemi, respectively. Bar plot represents measured data and line plot represents model output. These figures show the thickness of the model output is rather overestimated in the coastal area, but interannual variation patterns are well matched with the data.

According to the observed data, ice existed 195 days in Kemi in 2002/2003 winter, but 181 days in the model output. Table 1 shows the comparison of ice model output and measured data collected at 3 different locations during 2002/2003 winter.

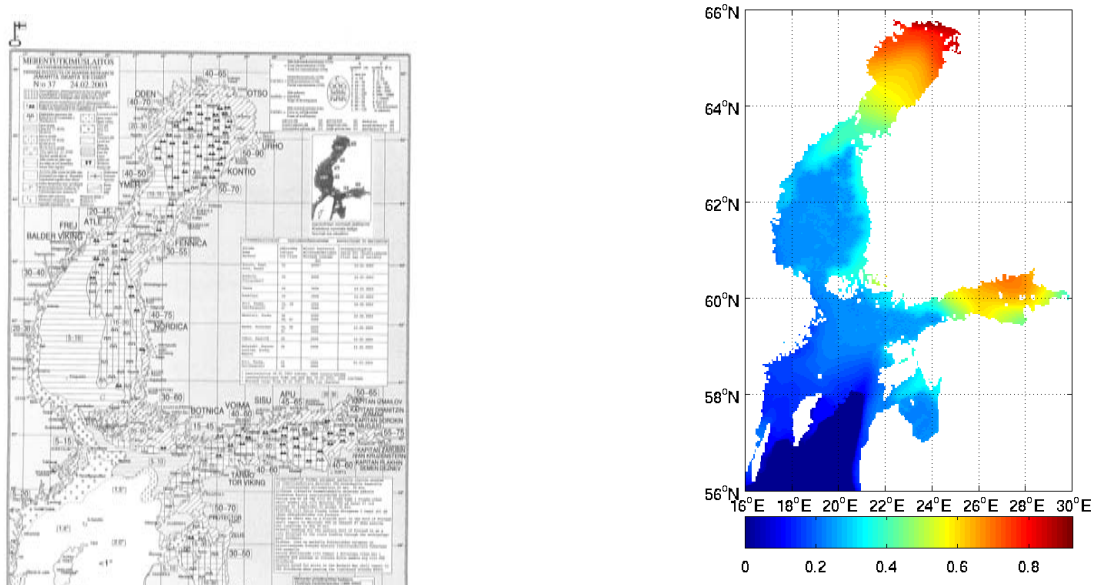

(a) Ice chart on 24th Feb. 2003

(b) Model ice thickness (m) on 24th Feb. 2003

Figure 49: Ice chart and model output on 24th Feb. 2003.

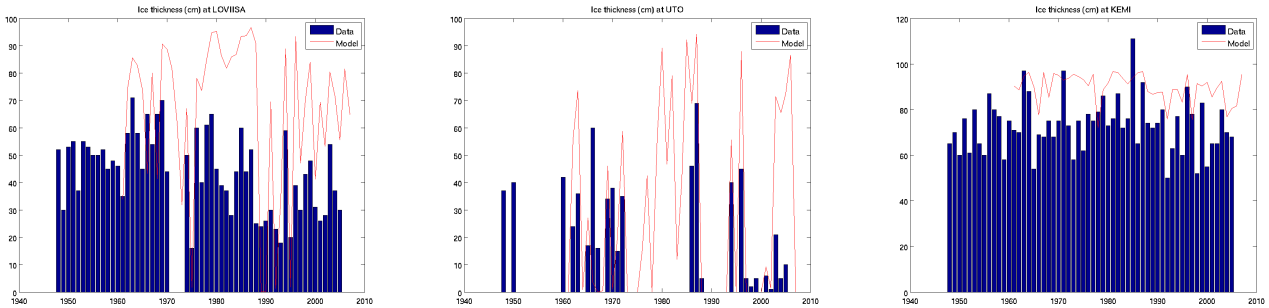

(a) LOVIISA

(b) UTO

(c) KEMI

Figure 50: Time series of sea ice thickness.

Table 2: Comparison of model parameters.

	HELMI	LIM3
Resolution	1 nm	2 nm
Hindcast forcing	NCEP/NCAR reanalysis	Downscaled ERA40 reanalysis (SMHI)
Ice category	5 undeformed and 2 deformed ice	5 ice + 1 for open water
thinnest category	not exceed 10 cm	not exceed 5 cm

5.6 Model to Model comparison

The HELMI is a multi category sea-ice model (Haapala, et al., 2005) and has been used for operational sea ice forecasting in the Baltic Sea. Here, we compare the NEMO/LIM3 model results to the HELMI reanalysis simulation focused on the ice season 2002/2003 which was regarded as severe than an average in the Baltic. The model physics and numerics are rather similar between HELMI and LIM3, but the differences are in the horizontal resolution and atmospheric forcing used. Table 2 shows the differences between HELMI and LIM3. Present set-up of the HELMI model predicts evolution of five undeformed and two deformed ice categories. Ice categories are "advected" in the thickness space without any limits, except that the thinnest category is not allowed to exceed 10 cm. Deformed ice is divided into separate categories of rafted and ridged ice types. The HELMI model is performed using the different configuration and different surface conditions. The main differences in the sea ice models lie in the formulation of the subgrid-scale ice thickness distribution, of the thermodynamic processes, of the sea ice salinity and of the sea ice rheology.

5.7 Model to observed data comparison

The observed and NEMO/LIM3 modelled evolution of ice concentration along the constant latitude (65 N) is shown in Figure 51. The western side is the coast of Sweden and the eastern side the coast of Finland. Apparent features are an advance of the ice extent from coast to central basin and frequent lead openings near the coast during an ice-covered period. Most of the leads are observed in western coast, which is very typical in the Bay of Bothnia. The modelled evolution of ice concentration reflects rather accurately the observed evolution and practically the model captures every observed lead opening situation. Figure 52 depicts an evolution of modelled ice thickness. As the western coast was experienced continuous divergence observed as leads, the eastern coast is correspondingly experiencing convergent motion which is observed as continuous accumulation of deformed ice.

In the following analysis, we limit our comparison of the modelled ice characteristics to those dates when the EM-measurements were made. The ice thickness and the intensity of ridging from the EM measurement on 23 February 2003 is shown in Figure 54a. The LIM3 modelled mean ice thickness (Figure 54b) is rather close to the EM thickness spatial distribution. However, the modelled mean ice thickness is more smooth and more thick along the coast line. The thickest ice is found in the northern Bay of Bothnia and the in the Gulf of Finland. The regions of the deformed ice correspond roughly to the regions of the high ridging intensity from the ice charts, but the model does not show this characteristic. Figure 54c shows the HELMI modelled ice thickness.

6 Conclusion

We have created a configuration for the Baltic and North Sea that provides consistent results. However, some concerns are still to be solved. The intensity of inflows seems to be too low which is consistent with a low correlation of SSH on the western coast of Sweden. This results into a salt de-

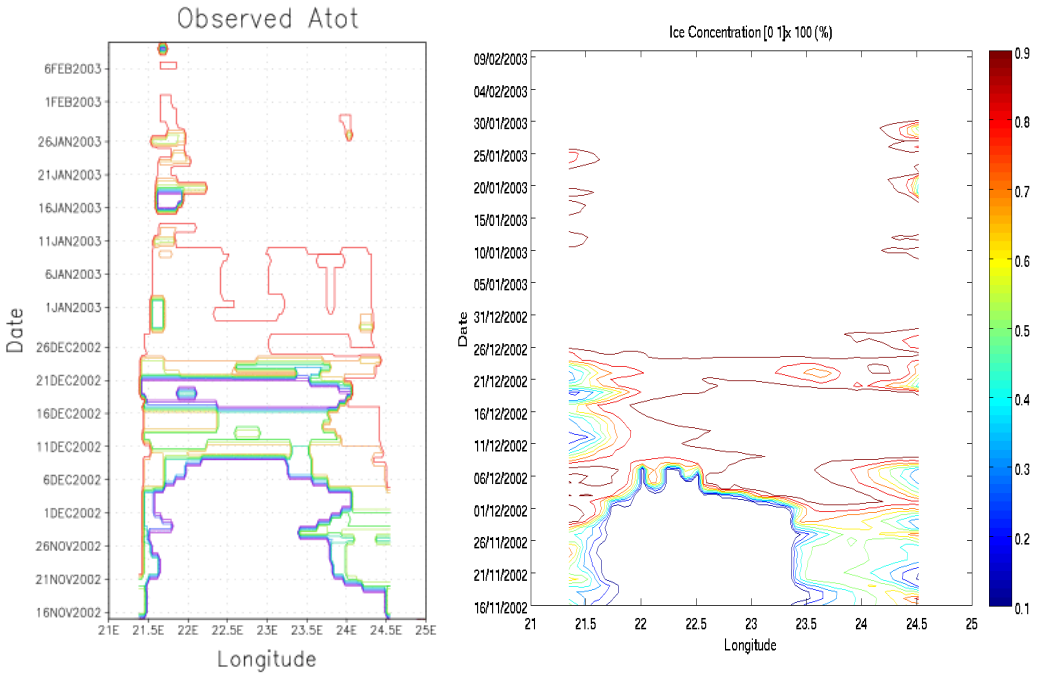

(a) Observed ice concentration (b) NEMO/LIM3 ice concentration

Figure 51: The observed and NEMO/LIM3 modelled evolution of ice concentration.

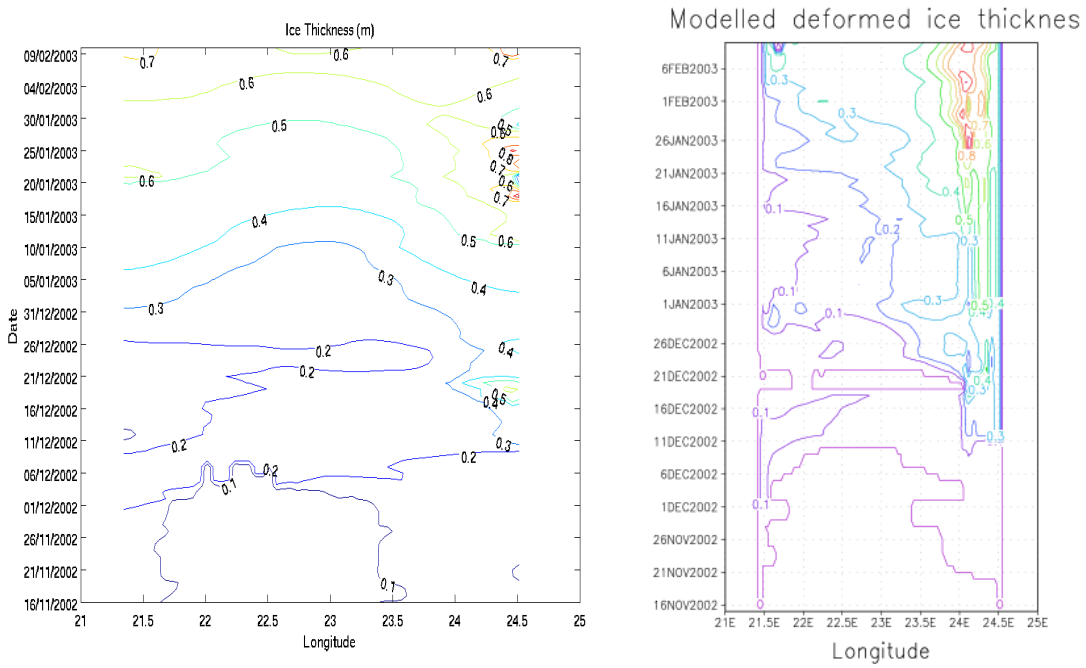

(a) NEMO/LIM3 ice thickness (b) HELMI ice thickness

Figure 52: Modelled ice thickness along the 65 N.

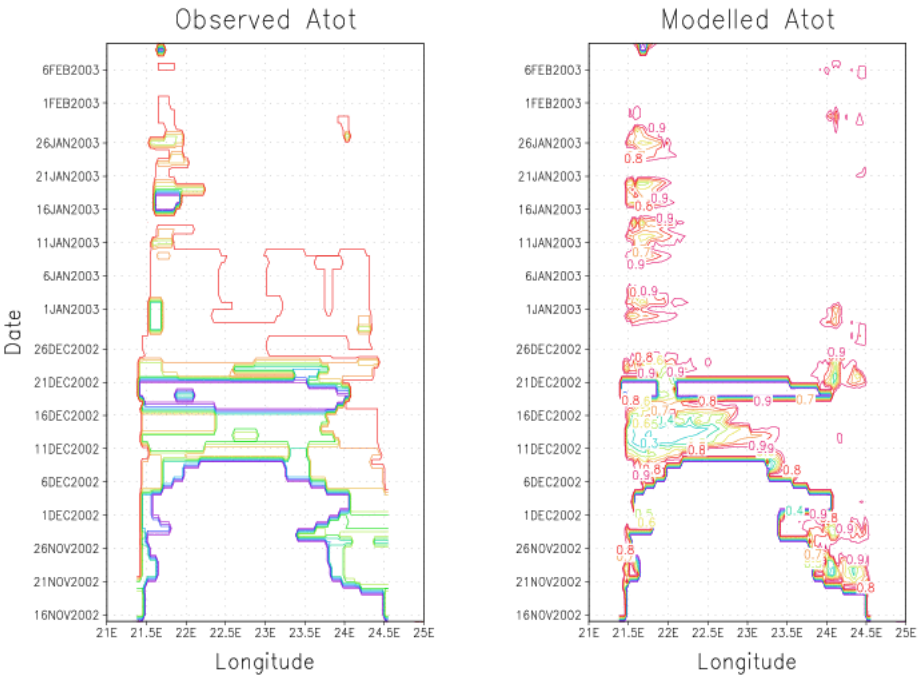

Figure 53: The observed and HELMI modelled ice concentration along the 65.

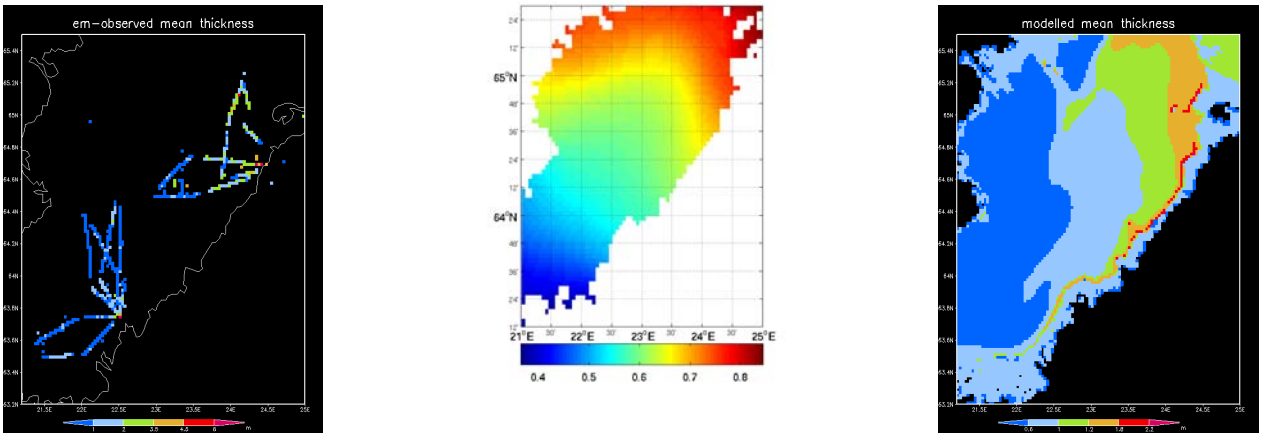

(a) EM measured ice thickness

(b) NEMO/LIM3

(c) HELMI

Figure 54: The observed and modelled ice thickness on 23th February 2003.

pletion of the deepest parts of the Baltic Sea, which can be however also explained by a high vertical mixing. Further tuning and experiments will be tried in order to solve this issue.
We have not plotted any temperature related results in this analysis as the main concern was to get a stable Baltic Sea salinity. This first report is however to be updated. In terms of sea ice dynamics, BaltiX reproduced the Baltic Sea ice temporal and spatial characteristics well. However, coastal ice is too thick and offshore ice is too thin. We will have particular look at the dynamics/thermodynamics of the model sea ice to tackle this issue. LIM3 is still under developing and we need further investigation and implementation of the LIM3 with the appropriate parameterization for the Baltic Sea condition. In particular, ice thickness categories and snow influence sea-ice dynamic. Snow cover is important on sea-ice mass and energy balance, so we will find a good values of snow physical parameters.

Acknoledgments

BaltiX devellopment was financed by MyOcean project FP7-SPACE-2007-1, and by the KASK project funded. The BaltiX computations were peformed on Ekman that is operated by the Centre for High Performance Computing (PDC) at the Royal Institute of Technology in Stockholm. This computing resource is funded by a grand from the Knut and Alice Wallenberg Foundation.

7 Appendix: A Technical Introduction to BaltiX

The philisophy behind BaltiX is that it tries to :

- Follow the devellopment of the NEMO ocean engine.
- Change the NEMO code as little as possible.
- Make an extensive use of the input files and CPP keys to define the configuration.
- Make it possible to easily identify where the NEMO code has been changed.
- Make the implementation of BaltiX into a new NEMO version as quick and easy as possible.

This means that everything has been made in order for BaltiX to remain a NEMO based configuration, and only a configuration

The following appendixes explain :

- The changes made into the code.
- The changes, choices or options made in the namelists (ocean and ice)
- The input files.

It is not possible to pursue the reading of this appendix without first having had an introduction to the NEMO structure, which can be made by reading the NEMO reference manual [14].

7.1 Preprocessing Keys (CPP Keys)

The set of CPP keys that is used is :***key_diafwb key_vvl key_bdy key_ldfsma key_lim3 key_trabbl key_zdfgls key_mpp_mpi key_baltix key_dynspg_ts***

- **key_diafwb** : Activation of diagnostics. Can be customised, can be costly if too many diagnostics used.

- **key_vvl** : Activation of the variable volume water column (i.e. : z^* coordinates).
- **key_bdy** : Activation of the open boundary condition module (The values specified for the OBCs are provided in Netcdf input files).
- **key_ldfsma** : Activation of Smagorinsky diffusion (the choice of the empirical coefficient is hard coded in the routine). This diffusion is not included in the reference version of NEMO. Therefore all the changes or additions related with this key are specific to BaltiX.
- **key_ldfslp** : Activation of the rotation of diffusion tensor.
- **key_lim3** : LIM3 is the ice model that is to be used (the physical choices are made in the ice namelist).
- **key_trabbl** : Activation of the bottom boundary layer parameterisation (the diffusive and advective aspects are chosen in the namelist).
- **key_zdfgls** : Activation of the General Length Scale vertical turbulence parameterisation. The choice of $k - \epsilon$ is made in the namelist.
- **key_mpp_mpi** : Activation of the MPI module of the code. The processor map is chosen in the namelist.
- **key_baltix** : All the code changes or additions related with the definition of BaltiX.
- **key_dynspg_ts** : The time splitting free-surface is chosen through this key.
- **key_iomput** : Activates the XML interface (produces outputs prescribed in the iodef.xml input file).

7.2 Code Changes And Additions

ALL the code changes are defined under two pre-processing keys (CPP keys), called ***key_baltix*** and ***key_ldfsma***. The first key is related to the definition of the configuration itself, and the second one to the use of the Smagorinsky diffusion, which is not implemented in NEMO for the time being.
This subsection goes through all the changes done in the NEMO code, based on the NEMO version that is used to build BaltiX when this document was written, that is the version 3.3.1 of the code.

7.2.1 Changes under *key_baltix*

Hereafter are listed and explained all the changes and additions made to the original code, related to the BaltiX configuration itself.

par_oce.F90

par_oce.F90 is a routine containing parameters that define the main features of the configuration, like for example the size of the horizontal or vertical domain. Depending on which configuration is used, a sub-routine containing the specific configuration related information

```
#elif defined key_baltix
   !!----------------------------------------------------------------------
   !!   'key_baltix'      :        Baltic + North Sea 2nm configuration
   !!----------------------------------------------------------------------
```

```
#              include "par_BALTIX_R2.h90"
#else
```

The **par_BALTIX_R2.h90** file that is included if key_baltix is activated contains the horizontal and vertical domain size parameters for the BaltiX configuration.

phycst.F90

phycst.F90 is a routine that contains an extensive list of physical parameters defined in the model, including the ice salinity. Although BaltiX uses the LIM3 ice model, for which the ice salinity is provided in the namelist, this salinity is also specified in this routine in case the LIM2 model is used. For consistency purpose, the following line is therefore added :

```
#if defined key_baltix
   REAL(wp), PUBLIC ::   sice    =   0._wp        !: reference salinity of
#else
   REAL(wp), PUBLIC ::   sice    =   6._wp        !: reference salinity of
#endif
```

diafwb.F90

diafwb.F90 is a routine which purpose is to compute salinity, volume and freshwater diagnostics. It was originally written for the ORCA2 configuration, and has been totally rewritten for BaltiX in order to compute various fluxes or mean values important for the configuration. One can cite the Baltic Sea outflow, the mean Baltic salinity, etc...

sbcblk_core.F90

This routine computes the ocean/atmosphere fluxes when the model is used in forced mode : fluxes of momentum, heat and humidity are computed based on a set of bulk formulaes. A validation work showed that this routine was the right choice for a costal/regional configuration and its formulation is very close or identical to that used in the RCO model [15].
However, a storm surge model called BZH has been added to the BaltiX package, and for which temperature and salinity are kept constant. BZH uses only wind-speed and atmospheric pressure data. As a coupling is made at the open boundary conditions between BZH and BaltiX, it is essential that both configurations use the same bulk formulaes and the same atmospheric forcing. For this purpose, the routine has been modified for the only case when BZH is used, and this modification has been made so that the heat and humidity fluxes are simply put to zero, regardless of the humidity and temperature forcing.

limistate.F90

limistate.F90 is a routine used to initialise the ice model thickness. By default, and if the model does not start from a restart file but from some initial condition files, this routine computes an initial ice thickness based on the upper layer heat content and the initial air temperature. This kind of initial condition, that can work for Arctic or Antarctic Ocean settings, is not well suited for the Baltic Sea, and creates an unrealistic ice cover and thickness. Therefore, unless a restart file is used, BaltiX is initialised with no sea ice, hence the following lines added to the routine.

```
#if defined key_baltix
```

```
                                                                    zidto(:,:)
#endif
```

7.2.2 Changes under *key_ldfsma*

The inclusion of the Smagorinsky diffusion has been made through the addition of a pre-processing key. Meanwhile, the structure of the code is not changed when compared with a normal Laplacian diffusion, except a routine (**ldfsma.F90**) has been added to compute the Smagorinsky diffusion at every time step.

step_oce.F90

This routine defines all the modules used in the code stepping.

```
#if defined key_ldfsma
   USE ldfsma
#endif
```

step.F90

A call is required from the stepping routine to update the Smagorinsky diffusion coefficient at every time step :

```
#if defined key_ldfsma
                              CALL ldf_sma( kstp )      ! Smagorinsky diffusi
#  endif
```

ldftra_oce.F90

```
#elif defined key_ldfsma
   REAL(wp), PUBLIC, ALLOCATABLE, SAVE, DIMENSION(:,:,:) ::   ahtt, ahtu, a
   REAL(wp), PUBLIC, ALLOCATABLE, SAVE, DIMENSION(:,:,:) ::   ahmi
```

Defines the 3D diffusion coefficients used for Smagorinsky diffusion at T, U, V & W points. **ahmi** is a background diffusion coefficient that is set to 0 for most of the domain, except along the open boundary conditions where it takes high values in order to be used as a sponge layer both for tracers and dynamics.

ldftra.F90

This routine initialises the diffusion coefficient. In this case, it is initialised to zero everywhere except close to the open boundaries as mentionned earlier.

```
#elif defined key_ldfsma
      CALL ldf_tra_sma( ll_print )      ! Smagorinsky diffusion, with a min
```

ldftra_substitute.h90 and ldfdyn_substitute.h90

These included files are used as data aliases. The parts included under the **key_ldfsma** do not change the structure but are just an addition just like for any 3D diffusion coefficient. They are included in the files **ldftra_oce.F90** and **ldfdyn_oce.F90** respectively.

8 Subversion Server

BaltiX V.1.1 based on NEMO 3.3.1 is available through svn for any user using the simple command :

```
svn co svn://gimle.nsc.liu.se/SVN_BALTIX_V1/tags/BALTIX_V1.1
password : baltix2012
```

References

[1] Adcroft, A., and J.-M. Campin (2004), Re-scaled height coordinates for accurate representation of free-surface flows in ocean circulation model, *Ocean Modelling*, *7*.

[2] Beckmann, A., and R. Döscher (1997), A method for improved representation of dense water spreading over topography in geopotential-coordinate models., *jpo*, pp. 581–591.

[3] Campin, J.-M., and H. Goosse (1999), A parameterization of density-driven downsloping flow for a coarse resolution ocean model in z-coordinates, *Tellus*, pp. 412–430.

[4] Egbert, G., A. Bennett, and M. Foreman (1994), Topex/poseidon tides estimated using a global inverse model, *J. of Geophys. Res.*, *99*, 24,821 – 24, 852, 1994.

[5] Egbert, G. D., and S. Y. Erofeeva (2002), Efficient inverse modeling of barotropic ocean tides, *Journal of Atmospheric and Oceanic Technology*, *19*(2), 183–204, doi:10.1175/1520-0426(2002)019¡0183:EIMOBO¿2.0.CO;2.

[6] Funkquist, L., and E. Kleine (2007), Hiromb - an introduction to hiromb, an operational baroclinic model for the baltic sea, *Tech. rep.*, SMHI.

[7] Gustafsson, B. G., and H. C. Andersson (2001), Modeling the exchange of the baltic sea from the meridional atmospheric pressure difference across the north sea, *J. Geophys. Res.*, *106*, 19,731–19,744.

[8] Hakansson, B. (2004), On water and salt exchange in a frictionally dominated: Connecting the baltic with the north sea, *Cont. Shelf. Res.*

[9] Hordoir, R., and H. E. M. Meier (2010), Freshwater fluxes in the baltic sea - a model study, *J. Geophys. Res.*, *doi:10.1029/2009JC005604*.

[10] J.Elken (1996), Deep water overflow, circulation and vertical exchange in the baltic proper, Estonian Marine Institute.

[11] Large, W. G., and S. Yeager (2004), Diurnal to decadal global forcing for ocean and sea-ice models : the data sets and flux climatologies, *Tech. rep.*, NCAR Technical Note, NCAR/TN-460+STR, CGD Division of the National Center for Atmospheric Research.

[12] Leclair, M., and G. Madec (2009), A conservative leapfrog time stepping method, *Ocean Modelling*, *doi:10.1016/j.ocemod.2009.06.006*.

[13] Levitus, S., and T. P. Boyer (1994), *World Ocean Atlas 1994*, vol. 5, Salinity, NOAA Atlas NESDIS, U.S. Gov. Print Off., Washington, D.C.

[14] Madec, G. (2010), Nemo ocean engine, version 3.3, *Tech. rep.*, IPSL, http://www.nemo-ocean.eu/.

[15] Meier, H. M., R. Döscher, A. Coward, J. Nycander, and K. Döös (1999), Rco - rossby centre regional ocean climate model : Model description and first results from the hindcast period 1992/1993, *Tech. rep.*, SMHI.

[16] Salomon, J.-C., M. Breton, and P. Guegueniat (1993), Residual flow in the straight of dover, *Oceanologica Acta*, pp. 449–455.

[17] Samuelsson, P., C. Jones, U. Willén, U. Ullerstig, S. Golvik, U. Hansson, C. Jansson, E. Kjellström, G. Nikulin, and K. Wyser (2011), The rossby centre regional climate model rca3: model description and performance, *Tellus*, *63A*, 4–23.

[18] Seifert, T., F. Tauber, and B. Kayser (2001), A high resolution spherical grid topography of the baltic sea - 2nd edition, in *Baltic Sea Science Congress, Stockholm*.

[19] Smagorinsky, J. (1963), General circulation experiments with primitive equations, 1. the basic experiment, *Mon. Weather Rev.*, *91*, 99–164.

[20] Vancoppenolle, M., T. Fichefet, H. Goosse, S. Bouillon, G. Madec, and M. A. M. Maqueda (2008), Simulating the mass balance and salinity of arctic and antarctic sea ice, *Ocean Modelling*.

Earlier issues published in RO

1 Lars Gidhagen, Lennart Funkquist and Ray Murthy (1986)
Calculations of horizontal exchange coefficients using Eulerian time series current meter data from the Baltic Sea.

2 Thomas Thompson (1986)
Ymer-80, satellites, arctic sea ice and weather.

3 Stig Carlberg et al (1986)
Program för miljökvalitetsövervakning - PMK.

4 Jan-Erik Lundqvist och Anders Omstedt (1987)
Isförhållandena i Sveriges södra och västra farvatten.

5 Stig Carlberg, Sven Engström, Stig Fonselius, Håkan Palmén, Eva-Gun Thelén, Lotta Fyrberg och Bengt Yhlen (1987)
Program för miljökvalitetsövervakning - PMK. Utsjöprogram under 1986.

6 Jorge C. Valderama (1987)
Results of a five year survey of the distribution of UREA in the Baltic sea.

7 Stig Carlberg, Sven Engström, Stig Fonselius, Håkan Palmén, Eva-Gun Thelén, Lotta Fyrberg, Bengt Yhlen och Danuta Zagradkin (1988).
Program för miljökvalitetsövervakning - PMK. Utsjöprogram under 1987

8 Bertil Håkansson (1988)
Ice reconnaissance and forecasts in Storfjorden, Svalbard.

9 Stig Carlberg, Sven Engström, Stig Fonse-lius, Håkan Palmén, Eva-Gun Thelén, Lotta Fyrberg, Bengt Yhlen, Danuta Zagradkin, Bo Juhlin och Jan Szaron (1989)
Program för miljökvalitetsövervakning - PMK. Utsjöprogram under 1988.

10 L. Fransson, B. Håkansson, A. Omstedt och L. Stehn (1989)
Sea ice properties studied from the ice-breaker Tor during BEPERS-88.

11 Stig Carlberg, Sven Engström, Stig Fonselius, Håkan Palmén, Lotta Fyrberg, Bengt Yhlen, Bo Juhlin och Jan Szaron (1990)
Program för miljökvalitetsövervakning - PMK. Utsjöprogram under 1989.

12 Anders Omstedt (1990)
Real-time modelling and forecasting of temperatures in the Baltic Sea.

13 Lars Andersson, Stig Carlberg, Elisabet Fogelqvist, Stig Fonselius, Håkan Palmén, Eva-Gun Thelén, Lotta Fyrberg, Bengt Yhlen och Danuta Zagradkin (1991) Program för miljökvalitetsövervakning – PMK. Utsjöprogram under 1989.

14 Lars Andersson, Stig Carlberg, Lars Edler, Elisabet Fogelqvist, Stig Fonselius, Lotta Fyrberg, Marie Larsson, Håkan Palmén, Björn Sjöberg, Danuta Zagradkin, och Bengt Yhlen (1992)
Haven runt Sverige 1991. Rapport från SMHI, Oceanografiska Laboratoriet, inklusive PMK - utsjöprogrammet. (The conditions of the seas around Sweden. Report from the activities in 1991, including PMK - The National Swedish Programme for Monitoring of Environmental Quality Open Sea Programme.)

15 Ray Murthy, Bertil Håkansson and Pekka Alenius (ed.) (1993)
The Gulf of Bothnia Year-1991 - Physical transport experiments.

16 Lars Andersson, Lars Edler and Björn Sjöberg (1993)
The conditions of the seas around Sweden. Report from activities in 1992.

17 Anders Omstedt, Leif Nyberg and Matti Leppäranta (1994)
A coupled ice-ocean model supporting winter navigation in the Baltic Sea.
Part 1. Ice dynamics and water levels.

18 Lennart Funkquist (1993)
An operational Baltic Sea circulation model. Part 1. Barotropic version.

19 Eleonor Marmefelt (1994)
Currents in the Gulf of Bothnia. During the Field Year of 1991.

20 Lars Andersson, Björn Sjöberg and Mikaell Krysell (1994)
The conditions of the seas around Sweden. Report from the activities in 1993.

21 Anders Omstedt and Leif Nyberg (1995)
A coupled ice-ocean model supporting winter navigation in the Baltic Sea. Part 2. Thermodynamics and meteorological coupling.

22 Lennart Funkquist and Eckhard Kleine (1995)
Application of the BSH model to Kattegat and Skagerrak.

23 Tarmo Köuts and Bertil Håkansson (1995)
Observations of water exchange, currents, sea levels and nutrients in the Gulf of Riga.

24 Urban Svensson (1998)
PROBE An Instruction Manual.

25 Maria Lundin (1999)
Time Series Analysis of SAR Sea Ice Backscatter Variability and its Dependence on Weather Conditions.

26 Markus Meier[1], Ralf Döscher[1], Andrew, C. Coward[2], Jonas Nycander[3] and Kristofer Döös[3] (1999). RCO – Rossby Centre regional Ocean climate model: model description (version 1.0) and first results from the hindcast period 1992/93.

[1] Rossby Centre, SMHI [2] James Rennell Division, Southampton Oceanography Centre, [3] Department of Meteorology, Stockholm University

27 H. E. Markus Meier (1999)
First results of multi-year simulations using a 3D Baltic Sea model.

28 H. E. Markus Meier (2000)
The use of the $k - \varepsilon$ turbulence model within the Rossby Centre regional ocean climate model: parameterization development and results.

29 Eleonor Marmefelt, Bertil Håkansson, Anders Christian Erichsen and Ian Sehested Hansen (2000)
Development of an Ecological Model System for the Kattegat and the Southern Baltic. Final Report to the Nordic Councils of Ministers.

30 H.E Markus Meier and Frank Kauker (2002).
Simulating Baltic Sea climate for the period 1902-1998 with the Rossby Centre coupled ice-ocean model.

31 Bertil Håkansson (2003)
Swedish National Report on Eutrophication Status in the Kattegat and the Skagerrak OSPAR ASSESSMENT 2002

32 Bengt Karlson & Lars Andersson (2003)
The Chattonella-bloom in year 2001 and effects of high freshwater input from river Göta Älv to the Kattegat-Skagerrak area

33 Philip Axe and Helma Lindow (2005)
Hydrographic Conditions Around Offshore Banks

34 Pia M Andersson, Lars S Andersson (2006)
Long term trends in the seas surrounding Sweden. Part one - Nutrients

35 Bengt Karlson, Ann-Sofi Rehnstam-Holm & Lars-Ove Loo (2007)
Temporal and spatial distribution of diarrhetic shellfish toxins in blue mussels, Mytilus edulis (L.), at the Swedish West Coast, NE Atlantic, years 1988-2005

36 Bertil Håkansson
Co-authors: Odd Lindahl, Rutger Rosenberg, Pilip Axe, Kari Eilola, Bengt Karlson (2007)
Swedish National Report on Eutrophication Status in the Kattegat and the Skagerrak OSPAR ASSESSMENT 2007

37 Lennart Funkquist and Eckhard Kleine (2007)
An introduction to HIROMB, an operational baroclinic model for the Baltic Sea

38 Philip Axe (2008)
Temporal and spatial monitoring of eutrophication variables in CEMP

39 Bengt Karlson, Philip Axe, Lennart Funkquist, Seppo Kaitala, Kai Sørensen (2009)
Infrastructure for marine monitoring and operational oceanography

40 Marie Johansen, Pia Andersson (2010)
Long term trends in the seas surrounding Sweden
Part two – Pelagic biology

41 Philip Axe, (2012)
Oceanographic Applications of Coastal Radar

42 Martin Hansson, Lars Andersson, Philip Axe (2011)
Areal Extent and Volume of Anoxia and Hypoxia in the Baltic Sea, 1960-2011

43 Philip Axe, Karin Wesslander, Johan Kronsell (2012)
Confidence rating for OSPAR COMP

44 Germo Väli, H.E. Markus Meier, Jüri Elken (2012)
Simulated variations of the Baltic Sea halocline during 1961-2007

45 Lars Axell (2012)
BSRA-15 A Baltic Sea Reanalysis 1999-2004 (ej publicerad)

46 Martin Hansson, Lars Andersson, Philip Axe, Jan Szaron (2013)
Oxygen Survey in the Baltic Sea 2012 - Extent of Anoxia and Hypoxia, 1960 -2012

ISSN 0283-1112

SMHI

Swedish Meteorological and Hydrological Institute
SE 601 76 NORRKÖPING
Phone +46 11-495 80 00 Telefax +46 11-495 80 01